Order Number 9025994

On the structural and acoustic design of guitar soundboards

Davis, Evan Brugh, Ph.D.

University of Washington, 1990

U·M·I
300 N. Zeeb Rd.
Ann Arbor, MI 48106

On the Structural and Acoustic Design of Guitar Soundboards

by

Evan Brugh Davis

A dissertation submitted in partial
fulfillment of the requirements
for the degree of

Doctor of Philosophy

University of Washington

1990

Approved by _____
(Chairperson of Supervisory Committee)

Program Authorized
to Offer Degree Mechanical Engineering

Date March 5, 1990

In presenting this dissertation in partial fulfillment of the requirements for the Doctoral degree at the University of Washington, I agree that the Library shall make its copies freely available for inspection. I further agree that extensive copying of this dissertation is allowable only for scholarly purposes, consistent with "fair use" as prescribed in the U.S. Copyright Law. Requests for copying or reproduction of this dissertation may be referred to University Microfilms, 300 North Zeeb Road, Ann Arbor, Michigan 48106, to whom the author has granted "the right to reproduce and sell (a) copies of the manuscript in microform and/cr (b) printed copies of the manuscript made from microform."

Signature Evan Byl Davis

Date March 5 1990

University of Washington

Abstract

ON THE STRUCTURAL AND ACOUSTIC DESIGN OF GUITAR SOUNDBOARDS

by Evan Brugh Davis

Chairperson of the Supervisory Committee:
Professor James Chalupnik
Department of Mechanical Engineering

An assumed mode model of a guitar soundboard has been built and experimentally verified. The frequency range of interest was from 55 to 880 Hertz, covering the frequency range of the fundamentals of the notes played on the guitar. The guitar soundboard is modeled as an orthotropic plate reinforced with tapered beams using the Rayleigh-Ritz technique. Sound power spectra are computed using the radiation impedance of an equivalent array of piston sources and the velocity distribution computed from the forced vibration analysis of the soundboard coupled to a backing cavity and soundhole. The prediction model is compared to an experimental guitar which was documented by recording mode shapes, Chladni patterns, at 25 steps in the assembly process. The material properties used in the prediction programs were determined experimentally. The major findings of the study were; 1) the bracing system dominates the

vibration pattern of the soundboard, 2) bracing patterns are required to improve the radiation efficiencies of the unbraced plates, 3) material property variations in the bracing materials can significantly influence the soundboard's dynamics and 4) plate materials and plate finishes have no significant impact on the radiated sound power spectrum in the modeled range.

Table of Contents

List of Figures

Acknowledgment

I would like to acknowledge the efforts of two individuals without whom this work would not have been possible, Darcel Sandland and Dr. Allen Sussman M.D. I live with a condition which effects my mind causing inappropriate emotional responses, muscular convulsive episodes, and sensory hallucinations. When this condition was developing and running unchecked and I had lost the ability to confront my condition rationally, Darcel Sandland kept me from allowing the depressive episodes to terminate in suicide. I will never be able to fully thank her for her sacrifices. It was Dr Allen Sussman who came to the conclusion that my problems were biological in nature and not psychological and found a medication which controls the bulk of my symptoms. Dr. Sussman is responsible for the initiation of this work when perplexed by my symptoms and noting the degradation of my condition he suggested "... if there is anything you wish to do, you should do it now.. " I applied to the University of Washington to start this work.

I would also like to single out two members of my committee for their efforts. Thanks to Professor James Chalupnik for his discussions on the experimental aspects of this project. Special thanks to Per Reinhall for his assistance and review of the computational model theory early in the project when changes are more easily incorporated.

Dedication

This work is dedicated to;

The memory of John C. Schelleng
upon whose work this study is based,

Carleen M. Hutchins
the First Lady of Violin Acoustics,

and
Linda Manzer
for her desire to learn,
her will to listen,
and her honest friendship.

1 Introduction to Guitar Design

How does a guitar soundboard produce sound? How do the construction details of the guitar soundboard affect the sound quality of the instrument? How does one work towards improving the guitar? These are the general problems which will be addressed in this dissertation. The primary goal of this work is to extend the ability to address the mechanical design of flat plate guitar soundboards.

A guitar for the purpose of this discussion is a string musical instrument played by plucking the strings with one hand and controlling speaking length of the string with the other. The instrument transforms the mechanical energy imparted to the string into radiated acoustic energy. The guitar tuning and stringing system determines the musical application of the instrument. The guitar tuning settled down to its modern form in the eighteenth century and is suitable for both instrumental and voice accompaniment applications. The guitar is musically notated an octave higher than it sounds; this fact can cause some confusion in relating musical score and frequency response information. The modern standard stringing calls for six single strings tuned E-A-D-G-B-E.

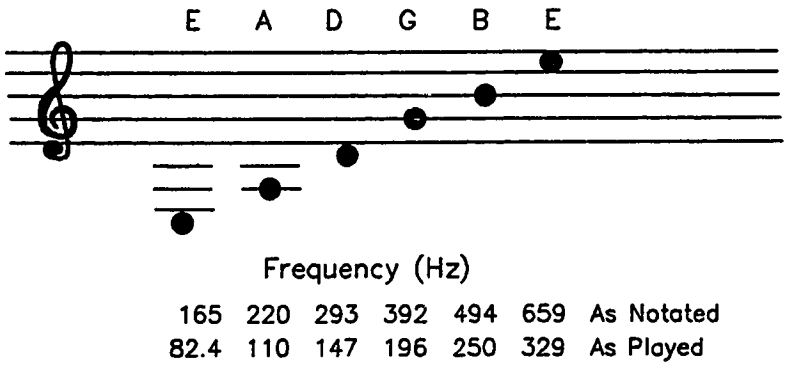

Figure 1.1 Standard Guitar Tuning

The guitars we play today are relatively new instruments. The inventor of the modern classical guitar was Antonino deTorres of Spain. His guitar building endeavors started in 1850 and continued on an irregular basis till his death in 1892. The modern classical guitar is built on his basic design with each builder adding their own variations. The use of steel strings on guitars has been experimented with since the 1790's. At the beginning of this century steel wires suitable for use as guitar strings became widely available. A number of guitar builders explored the design changes necessary to accommodate the increased tension of the steel string relative to the gut strings used previously. The classical fan bracing system was replaced by alternative bracing patterns, the most successful of which was the X-brace. Steel string X-braced guitars first appear around 1900 and by the 1930's dominated

popular music. The steel string flat top X-braced guitar design in its many variations remains the most popular steel string guitar design today.

In this work the possibilities of designing superior guitars by studying a simplified mechanical-acoustical model of the braced soundboard system will be explored. The model is limited to orthotropic flat plate soundboards with arbitrarily placed and tapered stiffening beams backed by a rigid cavity ported through the soundboard.

The definition of a superior instrument is deferred to the musical community of composers, musicians and audiences. A small body of knowledge is developing on turning subjective responses into acoustical criteria such as spectrum shapes. A guarded hypothesis on this subject will be proposed based on studies found in the literature. The definition of superior rests in the realm of the psychology of music and will not be addressed further.

Where should the study of the guitar take place? In this dissertation the studies will take place in the abstraction known as the acoustic power response spectra. The acoustic radiated power spectra is a common ground for both analytic and experimental studies.

A combination of analytical modeling and experimental studies have been undertaken to study the dynamics of the guitar soundboard and will be the primary subject of discussion. Vibration mode shapes and acoustic

power responses are the major data formats. The traditional classical guitar and X-braced steel string guitar will be introduced to the reader and the past efforts in their analysis reviewed. A mathematical model of a simplified soundboard model has been developed and numerical simulations conducted. The simulations will be verified using a number of check cases and a number of parameter studies have been preformed. An experimental program follows to understand the limits of the model's ability to predict guitar soundboard behavior.

1.1 The Classical Guitar

The classical guitar as it exists today is the invention of Antonino deTorres commonly referred to as simply Torres. The Torres guitar established the modern string scale length, the twelfth fret body joint and the modern guitar silhouette. The body shapes associated with guitars before deTorres were nearly rectangular with little difference between the upper and lower bout dimensions and the waist. The Torres guitars evolved into an enlarged lower bout and a well defined waist. Under the soundboard the changes were equally dramatic. The simple cross grain braces of the lute family were replaced by seven fan braces. These braces, possibly named for the radial lines of a ladies fan, run nearly parallel to the wood grain. The center for these radially diverging braces may lie at some point on the finger board of the instrument. Among the variations of the modern classical guitar there are

designs which have no single point of convergence for the radial pattern. In fact some builders use braces which are parallel to the wood grain of the soundboard.

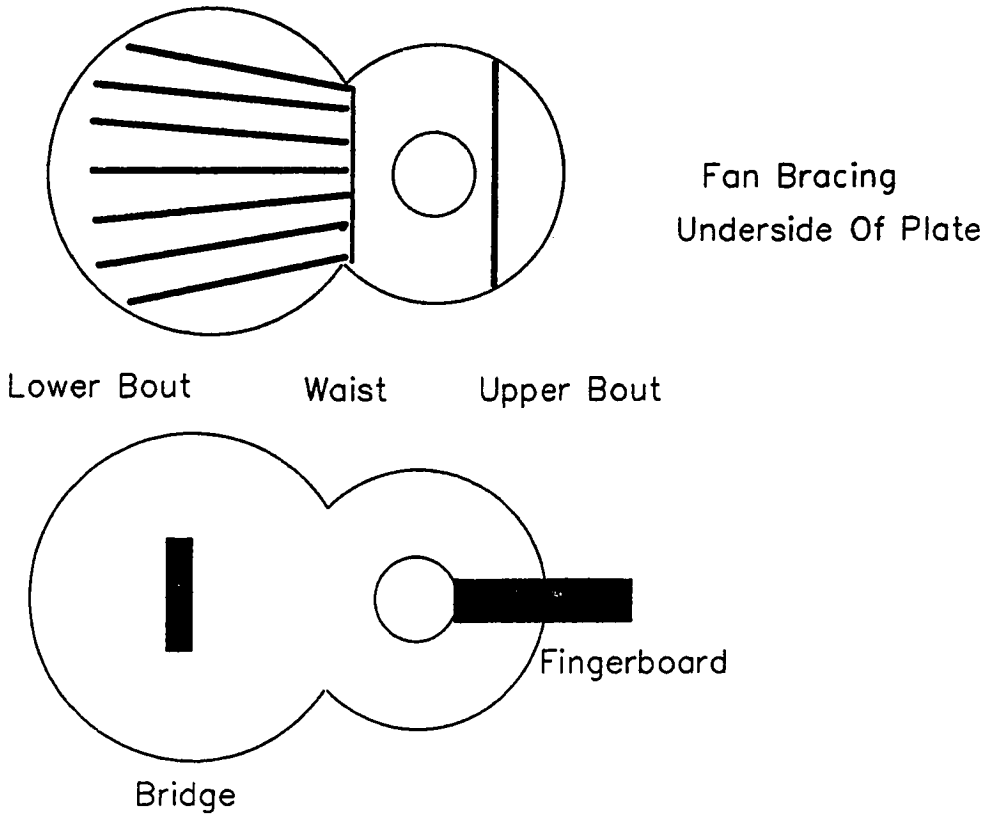

Figure 1.2 Torres Fan Bracing Pattern

The guitar must support the tension of the strings before any discussion of mode shapes and dynamics can be seriously considered. Resisting the force of the strings is a statics requirement. The modern nylon string requires 40 to 65 Newtons (9 to 15 lbs.) of tension to bring it up to pitch. For a complete set of six nylon strings the total tension load at the bridge is 320 Newtons (72 lbs.). This force is applied above the plane of the soundboard and appears to the top in the form of an applied static moment.

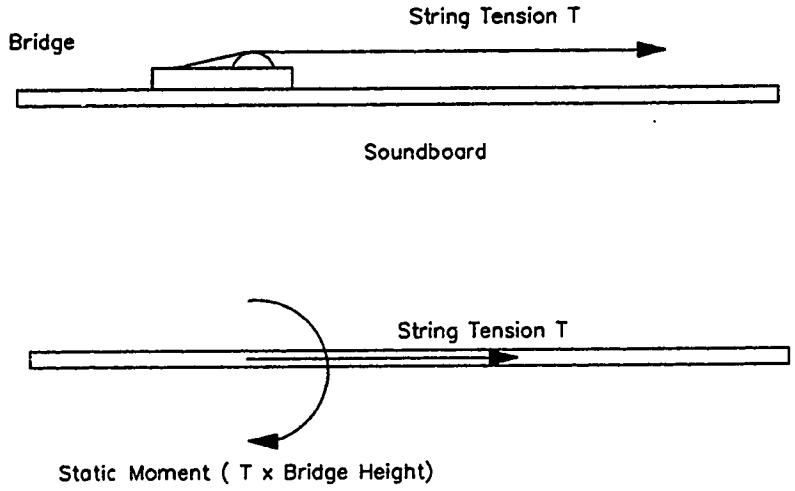

Figure 1.3 Static String Tension Generated Force System

The construction of the classical guitar including the neck, headstock and neck-body joint details are optimized to resist the string tension loads. The classical guitar is well matched to its strings and the fan

bracing pattern has defined a musically useful system for the last one hundred and forty years. Judging by the number of Torres-derived guitar designs which are being built and played today the Torres guitar is a successful platform, however no generally accepted ideal guitar has been declared by the musical world. In searching for the ideal guitar steel strings were experimented with and undoubtedly applied to the Torres design. The Torres fan bracing system could not withstand the increases in tension associated with steel strings and other designs were sought.

1.2 The Steel String Guitar

The modern steel strings used on guitars require 70 to 130 Newtons (16 to 30 lbs.) of tension to bring them up to pitch. The total tension force of the set of six strings being approximately 800 Newtons (180 lbs.). The static loads on the steel string guitar are two and one half times those imposed on a classical guitar. In order to solve the statics problem a number of solutions were proposed to adapt the basic Torres design to steel strings; steel reinforcing tubes were built into the body of the guitar, cello type tail piece assemblies were used to reduce the tension preload moment applied to the top and new bracing patterns were explored. The most successful of the new bracing systems was the X-brace. The invention of the X-brace is credited to a German emigrant to the United States by the name of C. F. Martin. Martin had apprenticed in Europe and carried into his work many methods still referred to as German. The X-brace was developed by C.

F. Martin in the 1850's but it was not incorporated into to the Martin steel string guitar until the 1920's and 30's and then by his son. A Larson guitar patent of 1904 clearly shows the use of a X-brace scheme for a steel string guitar[1]. The X-braced guitars which won the Martins their reputation as master builders were introduced in 1934.

---

1) Carl R. Hartman, Guitars and Mandolins in America, Hoffmann Estates, IL. Maurer & Co. 1984.

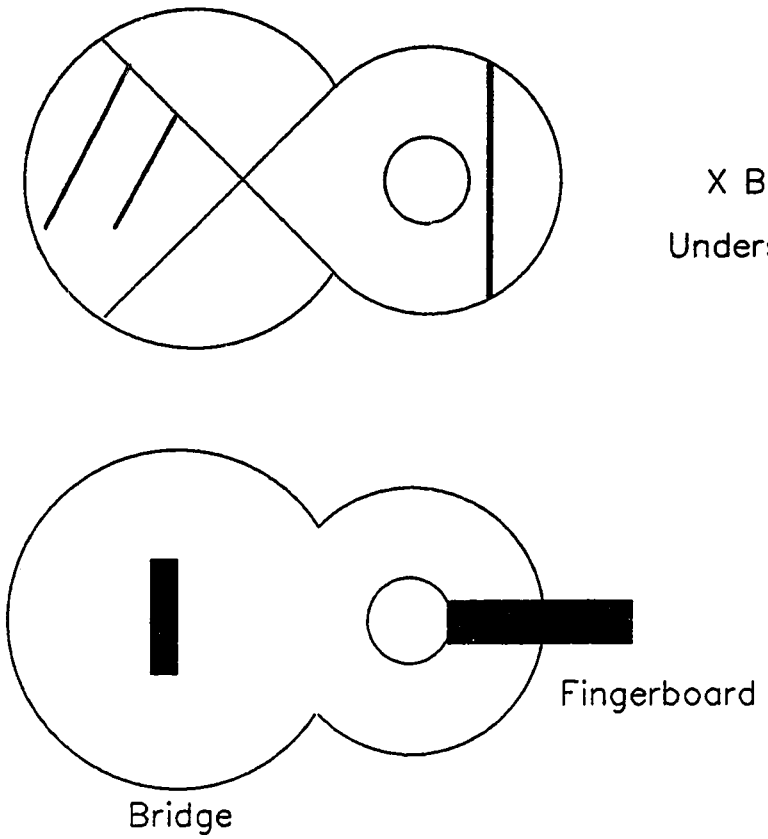

Figure 1.4 Steel String X Bracing Pattern

Since the introduction of the steel string guitar, the X-brace has been explored by many builders. The secondary braces are laid out for tone control and constitute the design freedom within the basic X pattern. Many different guitar body shapes have been adapted to the X-brace system from the Jumbo nineteen inch lower

bouts to small "travel" guitars with six inch lower bouts which are smaller than the pre-Torres guitar silhouettes.

1.3 Previous Analytic Studies

A number of subjects are reviewed to provide a platform on which to build the current work. The documented history of the study of violin acoustics can be said to predate the invention of the modern guitar. Appropriate parts of the violin research literature are integrated into the study of the guitar. The violin and guitar share the same basic physics and require similar measurements in their study. System analysis approaches for the guitar and violin produce the same equivalent circuit for the lower order modes. The models for the first two resonances differ only in the constants applied to the circuit. Determination of the mechanical properties of wood, an area of great discussion in the violin literature, is of direct value in the modeling of guitar soundboards. Modification of wood properties by the application of finishes has also been studied in conjunction with the violin and is directly transferable to the guitar soundboard.

1.3.1 Violin Research

The history of violin research is an old and interesting topic about which Carleen Hutchins has written an excellent survey article[2]. The modern history is however more important to this work. During the 1950's

---

2) Carleen M. Hutchins, "A History of Violin Research", J. Acoust. Soc. Am. 73(5) 1983.

a group of individuals (a violin maker, an electrical engineer and a chemist) formed an association which has become the center for the exchange of information on the analysis and construction of musical instruments. The association called itself the Catgut Acoustical Society and the early players were Carleen M. Hutchins, John C. Schelleng and Robert E. Fryxell. Of these three the work of John C. Schelleng is most important to the analysis of string musical instruments. In a 1963 paper he developed an equivalent circuit model of the violin and explored the relationships between the two lowest modes of the assembled instrument[3].

The Schelleng circuit was very general having a multitude of resonant side branches to represent the many modes of the top plate of the violin. He simplified the circuit to include only a single top plate mode and the Helmholtz mode of the air cavity. Material and geometric scaling rules for the top plate are included in the paper as well as system damping relationships. John Schelleng claimed no novelty in using an equivalent circuit approach to an acoustics problem and clearly stated that his analysis was a simplification. This humbleness is not found in papers which were published by others after him using similar approaches.

Another useful paper in the violin literature is a recent one by Kenneth Marshell on the measurement of

---

3) John C. Schelleng, "The Violin as a Circuit", J. Acoust. Soc. Am. 35(3) 1963.

the vibrational modes of a violin[4]. Modal analysis of a violin gives some general information on the interaction of the plates, ribs and neck assemblies. The importance of the modes of vibration of the neck on the body is evident in his figures. The nodal lines are seen to run off the top plate and along the ribs onto the back and return to the top of the instrument. The top plate is not acting as if it was subjected to simple boundary conditions at the plate rib interface. Beam-like twisting and bending modes of the complete instrument were also observed.

Acoustic radiation from bowed string instruments has been studied by Jansson (1986), Meyer (1972) and Weinreich (1980). Studies of the directivities of bowed instruments excited with sinusoidal drivers have been made. Acoustic reciprocity has also been used to study the directional properties of an instrument. Regardless of the technique used in the experimentation the questions of how to support the instrument, how to drive it and in what acoustic environment the measurement should take place must be addressed. Acoustic measurements always contain an element of compromise; it is in understanding those compromises that these papers are useful.

The material that has been borrowed from the study of the violin and applied to the guitar are the equivalent circuit concept of John Schelleng, the realization that

---

4) Kenneth D. Marshell, "Modal Analysis of a Violin", J. Acoust. Soc. Am. 77(2) 1985.

nodal lines on assembled instruments may lie along three dimensional surfaces (top-sides-back) and a number of experimental techniques.

1.3.2 Guitar Research

The previous studies on guitars have been primarily concerned with the classical, fan braced guitar. A number of studies have been conducted for the purpose of defining the quality of the guitar. These studies reflect the lack of an ideal instrument which could be used to establish design goals. The studies fall into two broad classifications; those by "black box" investigators and those by builders. The builders such as Dickens, Caldersmith, and Marty demonstrate a theoretical ability equal to that of the "black box" investigators such as Firth, Jansson, and Christensen. The "black box" investigators view the guitar externally and try to deduce its behavior from physical measurements and mathematical models. The builders are more capable of modifying the guitar structure and use this ability to explore new designs or the limits of simple mathematical models. Christensen has written a series of papers which outline the general path of guitar research over the last few years and will be used as a guide to this review of the literature.

The starting point for the review of the guitar studies is a simplified model of the plate and ported cavity system. The assumptions in these models are those of the earlier Schelleng equivalent circuit model of the violin. The circuits have been drawn using either an electrical analogy or a mechanical interpretation. The

mechanical interpretation lays a more direct foundation for the current study. Lumped circuit analyses have been presented by Dickens (1976), Firth (1977), Caldersmith (1978) and Christensen (1980). In these models two degrees of freedom are allowed, one representing the soundboard viewed as an equivalent piston and the other a port air mass also modeled as a rigid piston.

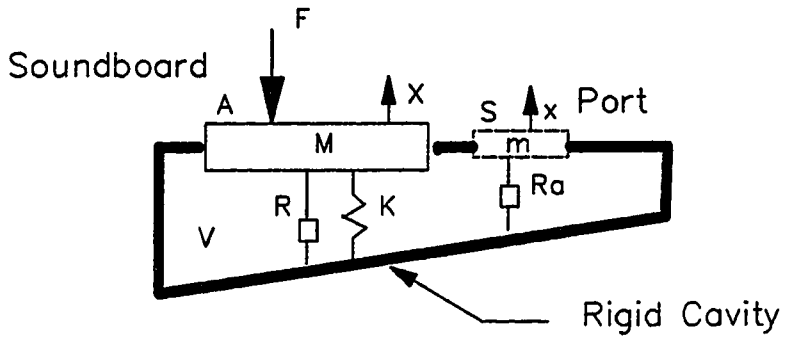

X = Plate Displacement x = Port Displacement

M = Plate Mass m = Port Mass

A = Plate Area S = Port Area

R = Plate Losses R_a = Port Losses

K = Plate Stiffness

V = Cavity Volume

F = Forcing Function

Figure 1.5 Lumped Element Guitar Model

The two degrees of freedom give rise to two resonances at approximately 100 and 200 Hertz. The equations of motion for the system can be developed from a simple force balance on each element.

1.1)

$$M\ddot{X} + R\dot{X} + KX = A\Delta P + F$$

$$m\ddot{x} + R_a\dot{x} = S\Delta P$$

If adiabatic compression of the air in the cavity is assumed and that the cavity is much smaller than a wavelength then the pressure in the cavity is related to the swept volume by;

1.2)

$$\Delta P = -\frac{\rho c^2}{V}(AX + Sx)$$

This equation can be used to eliminate the pressure term in the force balance equation and generate a two by two system matrix. If the equation for pressure is kept a three by three system matrix is created:

1.3)

$$\begin{bmatrix} K - \omega^2 M + i\omega R & -A & 0 \\ \frac{\rho c^2}{V}A & 1 & \frac{\rho c^2}{V}S \\ 0 & -S & -\omega^2 m + i\omega R_a \end{bmatrix} \begin{Bmatrix} X \\ \Delta P \\ x \end{Bmatrix} = \begin{Bmatrix} F \\ 0 \\ 0 \end{Bmatrix}$$

In this formulation harmonic time dependence has been assumed. The first row of the matrix is a force balance expression for the soundboard, the second row relates the volume displacement with the pressure in the cavity, and the third row is a force balance for the slug of air in the soundhole.

Various authors have taken these expressions and determined equivalent stiffness, mass and resistances for the circuit elements. The parameter selection is not unique. The area of the plate is a good example of the dilemma. The swept volume of the plate is needed for radiation calculations. Should the area of the plate be based on the geometric area with an average displacement or a smaller piston with the same maximum displacement? Both methods have been used. How should the port piston be modeled? The classical Helmholtz mass slug is used by most investigators. Dickens[5] built a guitar with half the body height of a conventional design and found that the inertance of the sound hole was strongly influenced by the proximity of the back plate. Dickens' work suggests that the simplified Helmholtz mass slug model is an adequate predictor for conventional guitar designs but may be in error for nonstandard configurations.

The simple lumped element model assumes that the wavelength of sound is far larger than the dimensions of the guitar. Under these conditions the guitar is

---

5) Fred T. Dickens, "Inertance of the Guitar Sound Hole", Catgut Acoust. Soc. Newsletter #29 1978.

modeled as a simple source. The simple radiation model neglects the acoustic loading on the sound hole due to the motion of the top plate. This loading is of concern because the action of the port is dominated by its radiation impedance. The interaction between the sound hole and the plate in terms of the separation distance between the two has been studied by Caldersmith[6]. In the simple source model acoustic pressure at a distance r from the source is related to the net volume displacement of the system as follows:

1.4)

$$P_a = \frac{\omega^2 \rho (AX + Sx)}{4\pi |r|}$$

Dickens (1978) extended the simple model by adding additional pistons to study the influence of the compliant back or sides. Caldersmith (1978) attempted to compute the equivalent mass and stiffness of a fan brace pattern by examining a rectangular plate with parallel ribs. Firth (1977) measured the displacement in the lower bout of a guitar to estimated the equivalent piston areas for his model.

The simple lumped element models explain the dynamics of the interaction between the ported cavity and soundboard. The location of the first two resonant frequencies and their radiation characteristics are predicted by these models. The first two resonances lie at

---

6) Graham Caldersmith, "Guitar as a Reflex Enclosure", J. Acoust. Soc. Am. 63(5) 1978.

approximately 100 and 200 Hertz. The playing range of the guitar includes notes with fundamentals up to a 880 Hertz.

Holographic interferometry has become a standard tool for examining guitar plates. The first guitar hologram was published by Jansson in 1971 has been followed up by Firth (1977), Caldersmith (1977), Richardson (1983), and most recently by Marty (1987). The holographic interferometry technique has been used to define a large number of resonance frequencies in the soundboard. Not all of these modes are good acoustic radiators. Approximately ten modes below eight hundred Hertz have been seen in most of the holographic studies. Some of these modes may have nodal lines running along the bridge and therefore cannot be effectually driven from forces applied at the bridge, however moment excitation may be very effective.

Christensen[7,8] conducted two complementary studies on recorded music and the physical spectra of guitars to estimated the number of strongly radiating modes. All the guitars were of the classical Torres design. In his initial studies he examined the accumulated energy content of the recorded guitar signal as a function of frequency. The major portion of the radiated energy was in the frequency range from 200 to 600 Hertz. In the second paper he used a simple oscillator model to

---

7) Ove Christensen, "The Response of Played Guitars at Middle Frequencies", Acustica 53 1983.

8) Ove Christensen, "An Oscillator Model for Analysis of Guitar Sound Pressure Response", Acustica 54 1984.

curve-fit the measured acoustic response spectra of a series of guitars with simple oscillator sources. Four to six harmonic oscillators were needed to fit the measured response functions from 100 to 800 Hertz.

The studies on classical guitar instrument quality have used short musical samples and listening juries to state their preferences. Boehm[9] and his coworkers had the listeners rate the instruments using metrics such as carrying power, brightness, timbre dispersion, fullness, dynamics and clearness. It has not been determined how these metrics can be translated into guitar structures or design criteria. Meyer[10] on the other hand augmented his listening tests with sinusoidal response curves of the played guitars and tried to correlate spectral features with listener preference. Meyer found that the best predictor of classical guitar quality was the third resonance at approximately 400 Hertz. The peak level of this resonance, its rise above the surrounding spectral levels and its bandwidth were all important. The next spectral feature which could be correlated with the perceived quality of the instrument were the average level of groups of one-third octave bands. The one-third octave correlations

---

9) Tomira Boehm, Kacper Miklaszewski, Friedrich Blutner, Eberhard Meinel,"Estimation of Guitar Sound Quality", Archiwum Akustyki (Archives of Acoustics) 11(3) 1986.

10) Jurgen Meyer, "Quality Aspects of Guitar Tone", in Function, Construction and Quality of the Guitar, edited by Erik V. Jansson, Stockholm, The Royal Swedish Academy of Music 1983.

were not as strong as the tonal correlations. The sound pressure levels in the one-third octave bands from 80 to 125 Hertz, 250 to 400 Hertz and 315 to 500 Hertz had approximately equal performance as predictor of guitar tone quality. The overall sound pressure level bands from 80 to 1000 Hertz followed the one-third octave band criteria as a single metric in the establishment of design criteria. The details of the first and second resonances played a small role in determining the sound quality of the instrument. The old rule of thumb that louder is better is not violated with these new findings and an idea of how the loudness should be distributed has been gained.

1.3.3 Wood Studies

The traditional material for guitar construction is wood. Traditionally spruces and cedars are used for the soundboards while rosewood, mahogany, koa, maple and fruit woods are used for backs and sides. Ebony and rosewood are the traditional woods of choice for fingerboards and bridges. In order to predict the dynamics of guitar soundboards an understanding of the properties of wood must be obtained.

The relationship between material strain and applied stresses is commonly used to characterize a material. These stress strain relationships for linear materials are known as Hooke's law. In the most general form of Hooke's Law 81 material constants are required. Symmetry in the stress and strain tensors reduce this number to 36 elastic constants. The matrix is symmetric which reduces the number of independent elastic constants to

21. If structural damping is to be modeled these material constants are complex numbers requiring the determination of 42 coefficients. Consider an idealized wood log as a cylinder of wood. The 21 material constants can be reduced to 9 in a cylindrical system if symmetry exists in the material. In this idealized log there is radial symmetry about the central axis. This symmetry allows a simpler version of Hooke's Law to be used to model the wood log.

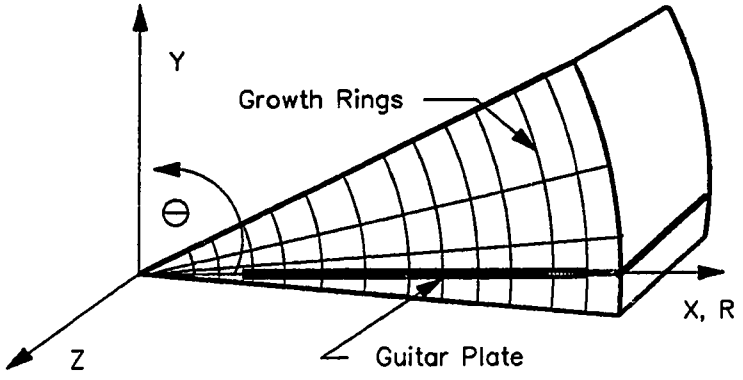

Figure 1.6 Guitar Plate Material Orientation

In the theory of elasticity the wood log is an orthotropic body with cylindrical anisotropy, a subject which has been addressed by Lekhnitskii[11]. Hooke's law in cylindrical coordinates;

---

11) S. G. Lekhnitskii, Anisotropic Plates, translated by S. W. Tsai and T. Cheron, New York: Gordon and Breach Science Publishers 1967.

1.5)

$$\epsilon_r = \frac{1}{E_r}\sigma_r - \frac{\nu_{\theta r}}{E_\theta}\sigma_\theta - \frac{\nu_{zr}}{E_z}\sigma_r \quad , \qquad \gamma_{\theta z} = \frac{1}{G_{\theta z}}\tau_{\theta z}$$

$$\epsilon_\theta = \frac{1}{E_\theta}\sigma_\theta - \frac{\nu_{r\theta}}{E_r}\sigma_r - \frac{\nu_{z\theta}}{E_z}\sigma_z \quad , \qquad \gamma_{rz} = \frac{1}{G_{rz}}\tau_{rz}$$

$$\epsilon_z = \frac{1}{E_z}\sigma_z - \frac{\nu_{rz}}{E_r}\sigma_r - \frac{\nu_{\theta z}}{E_\theta}\sigma_\theta \quad , \qquad \gamma_{r\theta} = \frac{1}{G_{r\theta}}\tau_{r\theta}$$

Where the material strains are;

ϵ_r = Radial Strain

ϵ_θ = Tangential Strain

ϵ_z = Axial Strain

γ = Shear Strain

and the material stresses are;

σ_r = Radial Stress

σ_θ = Tangential Stress

σ_z = Axial Stress

τ = Shear Stress

The engineering material properties are;

E = Modulus of Elasticity

G = Shear Modulus

ν = Poisson Ratio

The calculations of flat plate soundboard dynamics are based on a thin plate analysis in rectangular coordinates. The orthotropic material properties of the soundboard model are oriented along the principal directions of the cartesian coordinate system. Hooke's law using the cartesian material properties takes the form;

1.6)

$$\epsilon_x = \frac{1}{E_x}\sigma_x - \frac{\nu_{yx}}{E_y}\sigma_y - \frac{\nu_{zx}}{E_z}\sigma_z \quad , \qquad \gamma_{yz} = \frac{1}{G_{yz}}\tau_{yz}$$

$$\epsilon_y = \frac{1}{E_y}\sigma_y - \frac{\nu_{xy}}{E_x}\sigma_x - \frac{\nu_{zy}}{E_z}\sigma_z \quad , \qquad \gamma_{xz} = \frac{1}{G_{xz}}\tau_{xz}$$

$$\epsilon_z = \frac{1}{E_z}\sigma_z - \frac{\nu_{xz}}{E_x}\sigma_x - \frac{\nu_{yz}}{E_y}\sigma_y \quad , \qquad \gamma_{xy} = \frac{1}{G_{xy}}\tau_{xy}$$

A problem arises in mapping the natural cylindrical coordinate system for the log into the cartesian system for prediction and analysis. The stresses in one coordinate system can be expressed in terms of the other by a transformation between the two coordinate systems.

1.7)

$$\sigma_z = \sigma_z$$

$$\sigma_r = \sigma_x \cos^2\theta + \sigma_y \sin^2\theta + 2\tau_{xy}\sin\theta\cos\theta$$

$$\sigma_\theta = \sigma_x \sin^2\theta + \sigma_y \cos^2\theta - 2\tau_{xy}\sin\theta\cos\theta$$

$$\tau_{r\theta} = (\sigma_y - \sigma_x)\sin\theta\cos\theta + \tau_{xy}(\cos^2\theta - \sin^2\theta)$$

$$\tau_{rz} = \tau_{xz}\cos\theta - \tau_{yz}\sin\theta$$

$$\tau_{\theta z} = \tau_{yz}\cos\theta - \tau_{xz}\sin\theta$$

Guitar woods are cut radially "on the quarter" and the thickness of the plate is small compared to the radius of the log (see figure 1.6). With the thin radial cut geometry the elastic constants in both the rectangular and cylindrical coordinates must be identical in the limit as the plate thickness approaches zero. The literature on obtaining numerical values for the orthotropic elastic constants of woods rely very heavily on thin specimen data.

The recent papers of McIntyre and Woodhouse[12,13,14] explore in detail the theoretical and practical methods of obtaining wood properties using free-edged rectangular plate samples. In these papers very little data is collected. Caldersmith[15] and Haines[16] used simpler methods and collected larger databases. All the methods rely on setting a test sample into vibration at a resonance and measuring the resonant frequency and Q of

---

12) M. E. McIntyre, J. Woodhouse, "On Measuring Wood Properties, Part 1", J. Catgut Acoust. Soc. #42 1984.

13) M. E. McIntyre, J. Woodhouse, "On Measuring Wood Properties, Part 2", J. Catgut Acoust. Soc. #43 1985.

14) M. E. McIntyre, J. Woodhouse, "On Measuring Wood Properties, Part 3", J. Catgut Acoust. Soc. #45 1986.

15) G. W. Caldersmith, "Vibrations of Orthotropic Rectangular Plates", Acustica 56 1984.

16) Daniel W. Haines, "On Musical Instrument Wood", Catgut Acoust. Soc. Newsletter #31 1979.

the driven mode. The frequency and Q information is interpreted using a dynamic model for the system under test. The test sample is weighed and its geometry measured. This information along with the frequency domain information is then curve-fitted to generate the estimate of the material constants. McIntyre, Woodhouse and Caldersmith used thin rectangular plates with appropriate models. Haines used thin strips and applied beam theory.

Additional environmental conditions may effect the resonant qualities and material properties of wood. The externally controllable variables such as humidity and temperature can be eliminated in the laboratory measurements but may plague an instrument in use. Finishes, adhesives and wood surface preparation chemicals also modify the wood's apparent material properties. John Schelleng[17] performed a series of simple experiments to investigate the effects of finishes on musical instrument woods. The Schelleng model states the more flexible cross grain properties of the wood are the most affected by the addition of a finish. Traditional adhesives can have a strong influence on the damping properties of the assembled soundboard. The additional damping associated with the adhesive can be minimized by using the thinnest bond line which retains structural integrity. Adhesives should not be used as gap fillers if minimal damping is

---

17) John C. Schelleng, "Acoustical Effects of Violin Varnish", J. Acoust. Soc. Am. 44(5) 1968.

required. The damping properties of the adhesive are generally sensitive to the moisture content of the wood.

The data on woods is not exact and there can be a wide range of variation within a given species. The Haines data shows standard deviations in material modulus on the order of fifteen percent of the nominal value. The measurement accuracy for Young's modulus using the free plate sample test method was estimated by the authors to be ten percent or less. These uncertainties in modulus translate into a semitone uncertainty in resonant frequency predictions.

The strength of woods has not been addressed by those studying traditional instruments simply because traditional designs have empirically solved the problems associated with resisting the static the string tension forces. In new designs the statics problem may need to be resolved and therefore strength data is required. The early aircraft industry studied the strength, fatigue and creep of spruces. The construction industry collected data on common firs used in home building. The compiled data on spruce, fir and a few hardwoods can be used as a guide to estimating wood strengths[18]. The wood samples tested were not necessarily prepared with the same attention to grain orientation as musical instrument wood is and the wood quality may not have been acceptable for musical

---

18) U. S. Forest Service, Wood Handbook, Washington D.C.: Government Printing Office 1974.

instrument applications. A complete database for musical instrument woods including flexural modulus, damping properties, density, fatigue life, creep behavior, yield and ultimate strengths has yet to be complied.

1.3.4 The Plucked String

In the steady state "ring" of the string, after the initial transient has decayed, the forcing function driving the guitar top is a simple oscillating force. An overview of the plucked string as a forcing function is required to understand how a constant force model and a real string forcing function are related. In this analysis a simply supported ideal string model is used. The effects of moving boundary conditions and non-ideal behavior due to friction and bending stiffness has been discussed by Morse[19]. Let a string be displaced and released.

---

19) Philip M. Morse, Vibration and Sound. American Institute of Physics, New York: 1976. (Reprint of 1948 edition)

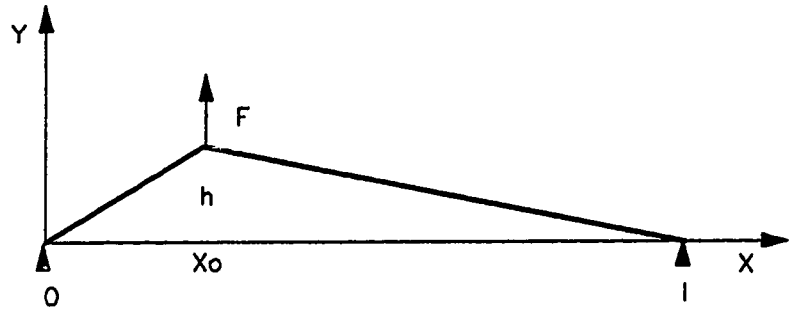

Figure 1.7 String Displacement Coordinates

The equation for the motion of the string as a function of the location and magnitude of the initial displacement is;

1.8)

$$y(x,t) = \frac{2h}{\pi^2}\left(\frac{x_0}{l}\right)\left(1-\frac{x_0}{l}\right)\sum_{n=1}^{\infty}\frac{1}{n^2}\sin\left(\frac{n\pi x_0}{l}\right)\sin\left(\frac{n\pi x}{l}\right)e^{i\omega t}$$

The initial displacement condition can be imposed with an applied force. A static force balance at the point of application of the force determines the initial displacement. Let T be the tension force in the string.

1.9)

$$F = T\left(\frac{h}{\sqrt{x_0^2+h^2}} + \frac{h}{\sqrt{(l-x_0)^2+h^2}}\right)$$

for small displacements,

$$F = T\left(\frac{h}{x_0} + \frac{h}{l-x_0}\right)$$

The constant force condition comes from the intuitive idea that the plucking system, a plectrum or finger nail, acts as cantilever beam. In this model the string is released when the string's restoring forces overcomes the beam's ability to resist deflection. The string deflection can be expressed in terms of the string tension and plucking point.

1.10)

$$h = x_0\left(\frac{F}{T}\right)\left(1+\left(\frac{x_0}{l}\right)+2\left(\frac{x_0}{l}\right)^2+4\left(\frac{x_0}{l}\right)^3 + \ldots + 2^{m-1}\left(\frac{x_0}{l}\right)^m\right)$$

for small displacements,

$$h = x_0\left(\frac{F}{T}\right)\left(1+\frac{x_0}{l}\right)$$

The force acting on the bridge of the guitar in this simple model is related to the slope of the deflection curve at the bridge. The deflection curve is differentiated to obtain the force expression. In the following equation the small displacement approximations have been used.

1.11)

$$F_{bridge} = F \left[\frac{x_0}{l}\left(1 - \frac{x_0}{l}\right)\right]^2 \sum_{n=1}^{\infty} \frac{2}{n\pi} \sin\left(\frac{n\pi x_0}{l}\right)$$

The ratio between distance from the support to the point of application of the force and the string length plays an important role in determining the relative levels of the forces generated at each harmonic. This ratio is constantly changing as the guitar is played. The absolute position of the application of the plucking force remains constant, the string length is varied by fretting. A simple approximation to the active string length as a function of fret number m is;

1.12)

$$l = l_{ref} \ (2^{-m/12})$$

The reference string length l_{ref} is that of the open, unfretted, string. The bridge force expression can be framed in terms of this new relationship by making the following substitution;

1.13)

$$\left(\frac{x_0}{l}\right) = \left(\frac{x_0}{l_{ref}}\right) (2^{m/12})$$

The plucked string force levels at the bridge are related to plucking displacement force and the location of the application of the force. A simple calculation shows that with this prediction of string forces the first few harmonics of the string can present approximately equal forces to the bridge. Given constant force response data the above equations can be applied to estimate the spectral balance of any plucking force magnitude and point of application.

Guitars are designed to react a certain guitar string tension range. Too heavy a string will result in structural failure of the instrument; strings which are too light will be unable to drive the soundboard. Data on commercially available nylon and steel string guitar sets has been collected by Hanson and Hood[20].

1.4 Historical Perspective of Current Work

The studies on the quality of guitars state that the best correlation with good classical guitar tone occurs when the third resonance of the system is at approximately 400 Hertz. The earlier work in guitar acoustics have explored the first two resonances of the guitar at approximately 100 and 200 Hertz. In order to estimate

---

20) Mark Hanson, Phil Hood, "The Ultimate String Test", Frets 9(2) issue #102 1987.

the performance of a guitar the dominant radiating frequency band from 80 to 800 Hertz must be modeled. The need to be able to predict the guitar dynamics in these higher order modes is addressed by examining the performance of the soundboard in this frequency range.

It is hypothesized that good classical guitar tone requires three well defined acoustic resonances at approximately 100, 200 and 400 hertz and that the relative peak levels and bandwidths of these resonances are important characteristics. The lower two of these resonances are required to define the instrument as a guitar to the listener and are relatively insensitive to deviations in tuning and bandwidth. The third resonance is the primary indicator of the quality of the instrument and has narrow limits in tuning and bandwidth.

This dissertation can be viewed as the next step in implementing the equivalent circuit of John Schelleng. The previous lumped element models were the low frequency approximation to the Schelleng circuit and the first step in modeling the guitar. The current model addresses the multi-resonant side branch circuit used to represent the top plate of the instrument and is coupled with the simple cavity model. Caldersmith has discussed a similar model to the one exercised here however he felt that the problem was unsolvable for nonuniform plate structures such as those found in guitars. The problem may be unsolvable in a closed form analytical sense however an approximate numerical solution is offered.

2 Structural-Acoustic Model

The structural-acoustic model is intended to represent the low to mid frequency behavior of a guitar top. The soundboard is modeled as a thin, orthotropic, simply supported plate of uniform thickness reinforced by a beam substructure. Three loading functions are modeled to drive the sound board, a cavity back pressure, a radiation pressure and a series of point forces representing the strings. Musical instruments are mathematically difficult systems to model therefore it is natural to accept approximate solutions for the dynamics of these systems. A linear mathematical model has been developed to estimate the dynamics of and acoustic radiation from typical guitar constructions in the 55 to 880 Hz range.

2.1 The Assumed Mode Technique

An assumed mode approach has been selected to reduce the continuous dynamic system of the guitar soundboard to an n-degree-of-freedom-system. The infinite series of mode shapes and resonant frequencies associated with the continuous system are replaced with a finite set of n mode shapes and resonant frequencies. The assumed modes method leads to a matrix formulation which will allow the building of guitar soundboard models by adding plate and beam component matrices.

The assumed modes technique requires a differential equation of motion or an energy expression for the dynamics of the system and an assumed solution. The assumed solution has the form of a finite series of n

known functions multiplied by n unknown coefficients. Increasing the number of degrees-of-freedom will generally increase the accuracy of the approximation. The accuracy of the estimation of a single mode will depend on the number of assumed mode shapes which can be used to reproduce the actual mode of the system. The displacement shapes of the low order modes are built up from a large family of assumed deflection shapes whereas, the higher order mode shapes are fit by summing only a few assumed mode shapes. In the case of the guitar soundboard approximately four modes were found in the frequency range of interest. One, four, nine and sixteen term assumed mode series were used to study the effects of mode series truncation. These studies lead to the determination of the number of modes to be used in the modeling studies. Nine assumed modes proved to be sufficient to model the lower order modes with minimal changes in the first five modes when sixteen assumed modes were used. Sixteen assumed modes are used in all the calculations presented in this work.

The assumed mode technique replaces the continuous equations of motion with a system of equations called Galerkin's equations. The nature of the assumed mode functions determines the method by which Galerkin's equations are derived. If the assumed functions meet the geometric boundary conditions and are differentiable to one-half the highest order of the differential equation then the Rayleigh-Ritz technique is used. Functions meeting these criteria are called admissible

functions. Admissible functions meet the weakest conditions for an assumed mode function. If the assumed functions, or a combination of them, meet the natural and geometric boundary conditions and are differentiable at least to the highest order of the differential operator the Galerkin technique can be applied. Functions meeting these criteria are called comparison functions. The assumed mode shapes used in the following models are comparison functions for the clamped plate cases and admissible functions for the simply supported cases. The Galerkin and Rayleigh-Ritz derivations outlined below follow those developed by Meirovitch[21].

The Galerkin method assumes the solution of a differential equation of motion in terms of a finite series of known functions and unknown coefficients. The assumed solution is substituted into the equation and an error results with any non-trivial selection of the unknown coefficients. The pathological case is if one has selected a set of eigen modes in which case the equation will be satisfied. To minimize the error and uniquely define the unknown coefficients a constraint equation is applied to the system of equations. The Galerkin method requires that the integral of the weighted error be set equal to zero. The weighting function used in this technique is one of the assumed mode functions. An eigenvalue problem is formulated in this process which leads to mass and stiffness matrices

---

21) Leonard Meirovitch. Analytical Methods in Vibrations. London: The Macmillion Company, 1967.

which will be used to predict system dynamics. The generic derivation will be given for the calculation of the stiffness and mass matrices and the details for the actual component operators presented in the following section.

Let L and M be linear, self-adjoint differential operators, L is associated with the stiffness of the system M with the mass distribution. The equation of motion can be expressed in operator notation as;

2.1)

$$L[w] + M[\ddot{w}] = 0$$

If harmonic time dependence is assumed then the time derivatives can be removed.

2.2)

$$L[w] - \omega^2 M[w] = 0$$

Consider an assumed solution with known functions and unknown coefficients.

2.3)

$$w_n = \sum_{j=1}^{N} a_j \cdot u_j(x,y)$$

Substituting the assumed mode series into the equation of motion, an error will result.

2.4)

$$\epsilon = L[w_n] - \Lambda_n M[w_n] \neq 0$$

where lambda is the eigenvalue associated with the n^{th} mode shape.

The integral of the weighted error is chosen such that it is equal to zero.

2.5)

$$\int_A u_i \{L[w_n] - \Lambda_n M[w_n]\} dA = 0$$

The differential operators are linear and self-adjoint therefore;

2.6)

$$\int_A u_i L\left[\sum_{j=1}^{n} a_j u_j\right] dA = \sum_{j=1}^{n} a_j \int_A u_i L[u_j] dA$$

$$\int_A u_i M\left[\sum_{j=1}^{n} a_j u_j\right] dA = \sum_{j=1}^{n} a_j \int_A u_i M[u_j] dA$$

The preceding expressions can be simplified by using the a short hand for the integral expressions.

2.7)

$$k_{i,j} = k_{j,i} = \int_A u_j L[u_i] dA$$

$$m_{i,j} = m_{j,i} = \int_A u_j M[u_i] dA$$

For each weighting function a series of equations are generated.

2.8)

$$\sum_{j=1}^{n}(k_{i,j}-\Lambda_n m_{i,j})a_j = 0$$

These are known as Galerkin's equations and form an eigenvalue problem. The eigenvalue problem solution yields the unknown coefficients associated with the fitting functions.

2.9)

$$[k_{i,j}]\{a_j\} = \Lambda_n[m_{i,j}]\{a_j\}$$

Each solution vector is associated with an eigenvalue which is proportional to the square root of the resonant frequency.

$$\omega_n = \sqrt{\Lambda_n}$$

There are N eigenvalue-eignenvector sets for the assumed mode series (see equation 2.3).

To arrive at Galerkin's equations using the Rayleigh-Ritz technique the ratio of the potential energy to the kinetic energy of the modeled system is minimized relative to the unknown coefficients of the assumed mode series. Rayleigh's quotient is defined as the ratio of the potential and kinetic energies for a given

assumed mode. Consider Rayleigh's quotient for the basic equation of motion for the general dynamic system.

2.2)

$$L[w]-\omega^2 M[w]=0$$

Rayleigh's quotient;

2.10)

$$R(w_n) = \frac{\int_A w_n L[w_n]dA}{\int_A w_n M[w_n]dA} = \frac{N(w_n)}{D(w_n)} = \Lambda_n$$

To determine the minimum of Rayleigh's quotient relative to the unknown series coefficients the partial derivatives of Rayleigh's quotient are computed and set equal to zero.

2.11)

$$\frac{\partial R(w_n)}{\partial a_j} = \frac{D(w_n)\frac{\partial N(w_n)}{\partial a_j} - N(w_n)\frac{\partial D(w_n)}{\partial a_j}}{D^2(w_n)} = 0$$

The above equation can be simplified using the Rayleigh quotient definition and the knowledge that the energy operators are positive definite functions.

2.12)

$$\frac{\partial N(w_n)}{\partial a_j} - \Lambda_n \frac{\partial D(w_n)}{\partial a_j} = 0$$

Using the shorthand notation of equation 2.7 the energy operators can be rewritten;

2.13)

$$N = \int_A \sum_{i=1}^{n} a_i u_i \mathrm{L}\left[\sum_{j=1}^{n} a_j u_j\right] dA = \sum_{i=1}^{n}\sum_{j=1}^{n} a_i a_j k_{i,j}$$

2.14)

$$D = \int_A \sum_{i=1}^{n} a_i u_i \mathrm{M}\left[\sum_{j=1}^{n} a_j u_j\right] dA = \sum_{i=1}^{n}\sum_{j=1}^{n} a_i a_j m_{i,j}$$

Evaluation of the partial derivatives yields;

2.15)

$$\frac{\partial N(w_n)}{\partial a_r} = \sum_{i=1}^{n}\sum_{j=1}^{n}\left(k_{i,j}\frac{\partial a_i}{\partial a_r}a_j + k_{i,j}\frac{\partial a_j}{\partial a_r}a_i\right)$$

2.16)

$$\frac{\partial N(w_n)}{\partial a_r} = \sum_{i=1}^{n}\sum_{j=1}^{n}(k_{i,j}\delta_{i,r}a_j + k_{i,j}\delta_{j,r}a_i)$$

2.17)

$$\frac{\partial N(w_n)}{\partial a_r} = 2\sum_{j=1}^{n} k_{j,r}a_j$$

The mass or kinetic energy related terms can be computed in a similar manner.

2.18)

$$\frac{\partial D(w_n)}{\partial a_r} = 2\sum_{j=1}^{n} m_{j,r}a_j$$

The partial derivatives can be used to determine the unknown series coefficients using equation (2.12). This procedure generates the Galerkin equations.

2.19)

$$\sum_{j=1}^{n}(k_{i,j}-\Lambda_n m_{i,j})a_j=\frac{\partial N(w_n)}{\partial a_j}-\Lambda_n\frac{\partial D(w_n)}{\partial a_j}=0$$

Regardless of the procedure used to derive them, the Galerkin equations are the key to the assumed mode approach. The ability to compute the stiffness and mass terms depends on the creation of appropriate assumed mode functions.

2.2 Assumed Mode Selection

In order to apply the assumed mode technique a mode shape function must be selected. The assumed mode shape must meet the natural and geometric boundary conditions of the model in the Galerkin method and only the geometric boundary conditions in the Rayleigh-Ritz method. A simply supported plate is desired imposing one geometric and one natural boundary condition, the displacement and moment at the edge of the plate must be set to zero. If a clamped plate model is desired the displacement and slope at the edge of the plate must be set to zero. The assumed mode functions must also posses a nontrivial fourth order derivative.

Let there be a function which describes the upper boundary of an axisymmetric plate.

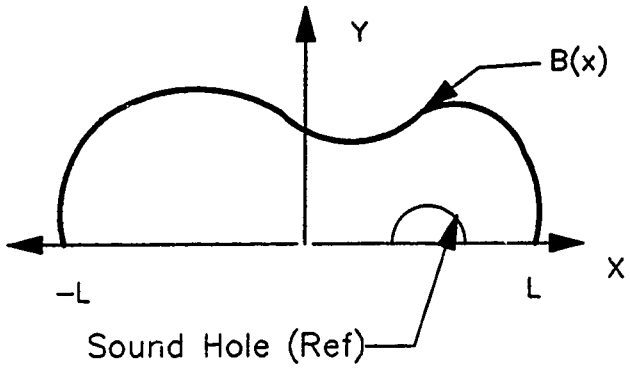

Figure 2.1 Plate Coordinate Definition

If the coordinate system is chosen such that the origin is in the geometric center of the plate, a suitable assumed displacement mode function has the form;

2.20)

$$w_i(x,y) = (B^2(x) - y^2)^{2\beta} \cdot \cos\left[\frac{n\pi x}{2L} + \frac{\pi(n-1)}{2}\right] \cdot \cos\left[\frac{m\pi y}{2B(x)} + \frac{\pi(m-1)}{2}\right]$$

$2L$ = Plate length

$B(x)$ = Boundary curve

n, m = Integers 1,2,3...

$\beta = 0$ Simple support

$= 1$ Clamped support

The assumed mode shape is built up of two functions, the first a bubble surface with zero displacement at the plate boundary and the second a mapping of the mode shapes of a simply supported rectangular plate. The mode shapes of the rectangular plate are mapped by adjusting the "width" of the rectangular plate in the second trigonometric term. The bubble term is used to satisfy the boundary conditions of a clamped plate.

The boundary conditions are satisfied for a Galerkin clamped plate or a Rayleigh-Ritz simply supported model depending on the value of the exponent beta. The expression has derivatives well beyond the four required. Each assumed mode has an associated pair of integers which define the number of nodal curves associated with each mode. The function requires that these nodal lines always lie inside the plate boundary.

To complete the assumed mode function an expression for the boundary curve must be established. An analytical expression for guitar shaped curves has been derived by Richard Childers[22] but was found to be awkward to use.

---

22) Richard L. Childers, "An Analytical Expression for the Shape of a Guitar". Catgut Acoustical Society News Letter # 41 1984.

Equation for guitar shaped plates;

$$y = \{\sqrt{(L/2)^2-(L/2-x^2)}\}\left\{C_1\sqrt{C_2^2+(x-x_0)^2}+y_0\right\}$$

For a Dreadnought type body; $0 > x > L$

$L = 50.8\ (cm)\ \ C_1 = 0.028\ (1/cm)\ \ C_2 = 4.166\ (cm)\ \ x_0 = 29.97\ (cm)\ \ y_0 = 0.45\ (cm)$

An alternative method was to employ a series approximation which could reproduce Childers' analytic guitar shape curves and be capable of fitting other boundary shapes.

Fourier and Polynomial series were attempted with little success. The Fourier and polynomial series tended to accumulate errors in the extremes of the fitted curve domain which generated large errors in the calculation of derivatives. The Chebyshev polynomial series eliminated this problem. A Chebyshev series approximation curve is a "bounded ripple" fit of the data which distributes the approximation error across the fitted domain. This "bounded ripple" property minimizes the numerical problems encountered in the calculation of the derivatives of the Fourier and Polynomial series in the extremes of the fitted ranges.

The general Chebyshev term is trigonometric but can also be expressed in terms of simple polynomials. The trigonometric form is;

2.21)

$$T_n(x) = \cos(n \cdot \cos^{-1}(x))$$

In polynomial form a recursive formula is used to generate the terms;

2.22)

$$T_{n+1}(x) = 2xT_n(x) - T_{n-1}(x)$$

$$T_0(x) = 1$$

$$T_1(x) = x$$

$$T_2(x) = 2x^2 - 1$$

$$T_3(x) = 4x^3 - 3x$$

Note that the polynomial terms are bounded in magnitude by one in the range minus one to one.

Using the Chebyshev polynomials the boundary curve for the outline of the guitar shaped plate has the form;

2.23)

$$B(x) = \sum_{n=1}^{N_{max}} c_n T_n(x)$$

The coefficients of the boundary series function are obtained using a least squares curve fitting procedure. Recursive formulas are used in the computation of the derivatives of the Chebyshev series terms. This allows the differentiation calculations to be completed by manipulating only the coefficients of the series.

2.3 Component Models

The component models used to develop the guitar soundboard system are an orthotropic plate model, a tapered beam model, a model of a ported air volume and a

radiation load model. These models are built in a systematic way to produce an approximation of the dynamic of a guitar soundboard. Each of these component models will be developed in detail. The general methods of the assumed mode approach will be applied to the specific differential operators used to model each element.

2.3.1 Plate Model

The model selected for the soundboard reflects current building practices. The plate model accommodates orthotropic material properties to model woods but requires a uniform thickness. The x coordinate axis is aligned with the grain direction of the wood. The cross grain direction is normal to this and denoted by the y axis. Rotation of the wood grain coordinate system independent of the geometric coordinate system is not allowed in the current model.

The equation of motion of a plate with orthotropic materials and uniform thickness is;

2.24)

$$D_x \frac{\partial^4 w}{\partial x^4} + 2D_{xy} \frac{\partial^4 w}{\partial x^2 \partial y^2} + D_y \frac{\partial^4 w}{\partial y^4} + \rho h \frac{\partial^2 w}{\partial t^2} = 0$$

D_x = bending stiffness along the grain

D_y = bending stiffness across the grain

D_{xy} = torsional stiffness

h = plate thickness

ρ = plate material density

In the operator notation introduced in equation 2.1 the stiffness and mass operators are;

2.25)

$$L_p[w] = D_x \frac{\partial^4 w}{\partial x^4} + 2D_{xy} \frac{\partial^4 w}{\partial x^2 \partial y^2} + D_y \frac{\partial^4 w}{\partial y^4}$$

2.26)

$$M_p[w] = \rho h w$$

The terms of the stiffness and mass matrices are determined by integrating the operators over the area of the plate using the assumed mode functions (equation 2.20) in equation 2.7.

2.27)

$$k^p_{i,j} = \int_{-L}^{L}\int_{-B(x)}^{B(x)} w_i\{ \; D_x\frac{\partial^4 w_j}{\partial x^4} + 2D_{xy}\frac{\partial^4 w_j}{\partial x^2\partial y^2} + D_y\frac{\partial^4 w_j}{\partial y^4} \; \} \; dydx$$

2.28)

$$m^p_{i,j} = \int_{-L}^{L}\int_{-B(x)}^{B(x)} w_i\rho h w_j dydx$$

The stiffness term in this formulation is material dependent. The stiffness term can be expressed as the sum of three integrals each depending on only a single material constant.

2.29)

$$k^p_{i,j} = k^{px}_{i,j} + k^{py}_{i,j} + k^{pc}_{i,j}$$

$$k^{px}_{i,j} = \int_{-L}^{L}\int_{-B(x)}^{B(x)} w_i D_x\frac{\partial^4 w_j}{\partial x^4}dydx$$

$$k^{py}_{i,j} = \int_{-L}^{L}\int_{-B(x)}^{B(x)} w_i D_y\frac{\partial^4 w_j}{\partial y^4}dydx$$

$$k^{pc}_{i,j} = \int_{-L}^{L}\int_{-B(x)}^{B(x)} 2w_i D_{xy}\frac{\partial^4 w_j}{\partial x^2\partial y^2}dydx$$

The four integrals, three stiffness and one mass, associated with the plate model are scaled by material properties and thickness. The numerical integrations required to evaluate the integrals are only calculated

once for each boundary curve. Material and thickness design studies can be preformed using simple scaling procedures.

2.30)

$$k^{px}_{i,j} = D_x \int_{-L}^{L} \int_{-B(x)}^{B(x)} w_i \frac{\partial^4 w_j}{\partial x^4} dy dx$$

$$k^{py}_{i,j} = D_y \int_{-L}^{L} \int_{-B(x)}^{B(x)} w_i \frac{\partial^4 w_j}{\partial y^4} dy dx$$

$$k^{pc}_{i,j} = D_{xy} \int_{-L}^{L} \int_{-B(x)}^{B(x)} 2 w_i \frac{\partial^4 w_j}{\partial x^2 \partial y^2} dy dx$$

2.31)

$$m^{p}_{i,j} = \rho h \int_{-L}^{L} \int_{-B(x)}^{B(x)} w_i w_j dy dx$$

The bending stiffness terms used in the plate equations can be expressed in terms of the more conventional variables of the theory of elasticity. The expression in terms of Young's Modulus, Shear Modulus and Poisson's ratio are as follows;

2.32)

$$D_x = \frac{E_x h^3}{12(1-\nu_x \nu_y)}$$

$$D_y = \frac{E_y h^3}{12(1-\nu_x \nu_y)}$$

$$D_{xy} = D_x \nu_y + \frac{2Gh^3}{12}$$

E = Young 's Modulus

G = Shear Modulus

ν = Poisson 's Ratio

The bending stiffness term may also be determined directly from experimental data. In a free plate test a family of resonant frequencies can be used to estimate the bending terms directly. The dominant part of the material data base used in this work is experimentally derived.

Material damping can be modeled using a complex bending stiffness.

2.33)

$$D = D(1 + i\eta)$$

η = Structural Damping Factor

The structural damping factor is estimated from test data.

Varnishes and other finishes are applied to the instrument wood for protection. These finishes act as unconstrained dampers and can modify the effective material properties of the soundboard woods. The cross grain bending stiffness is the parameter most sensitive to the application of a finish. The Ross-Kerwin-Unger unconstrained damper model is used to incorporate the effects of finishes on the woods[23].

2.34)

$$D_{finish} = D\left[1 + \frac{E}{D}\left(\frac{t}{h}\right)^3 + 3\left(1 + \frac{t}{h}\right)^2 \left\{\frac{\frac{E}{D}\frac{t}{h}}{1 + \frac{E}{D}\frac{t}{h}}\right\}\right]$$

E = Complex Young's Modulus for finish

t = Finish thickness

D = Complex Young's Modulus for wood

h = Wood thickness

---

23) Ahid D. Nashif, David I. G. Jones, John P. Henderson. Vibration Damping. New York: John Wiley & Sons, 1985.

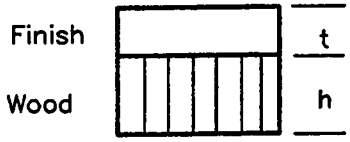

Figure 2.2 Unconstrained Layer Damper

The material properties for violin varnishes as determined by John Schelleng[24] form the data base for the finish model.

2.3.2 Beam Model

The legends of the "pre-war scalloped braces" and the claims of great improvement of the sound of the guitar with each new bracing scheme leads one to investigate the soundboard reinforcing system in detail.

In guitar construction great care is taken to ensure that bracing stock is from wood split along the grain lines. The brace is modeled using simple beam theory using the along-the-grain properties of the wood. The art of bracing is in the tapering of the brace as well is its position and orientation. The beam model reflects this design freedom. The beam has a fixed base width at the plate interface, the height and cross section shape are allowed to vary along the length of the brace. The brace runs along a straight line with the end points being anywhere on the plate surface.

---

24) John C. Schelleng, "Acoustical Effects of Violin Varnish" J. Acoust. Soc. Am. 44(5) 1968.

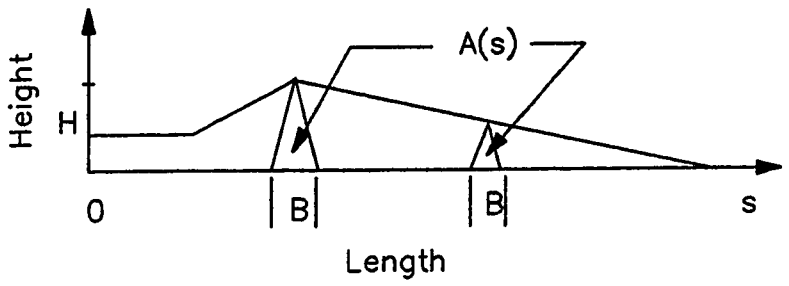

Figure 2.3 Beam Coordinate Geometry

The general expression for the equation of motion of the beam will be expressed in terms of beam coordinates initially and later converted to the plate coordinates. The equation of motion for a simple beam with varying cross section is;

2.35)

$$\frac{d^2}{ds^2}\left[EI(s)\frac{d^2w}{ds^2} \right] + \rho A(s)\frac{\partial^2 w}{\partial t^2} = 0$$

I = Moment of Inertia

A = Cross sectional area

s = Coordinate along the beam

Two moments of inertia are used in this work the first is a moment of inertia about the neutral axis of the beam and second is a moment of inertia about the plate beam interface. The moment about the neutral axis will be the minimum stiffness condition. The moment about the plate beam interface provides an upper limit on the stiffness of the beam system.

In the operator notation the stiffness and mass operators are;

2.36)

$$L_b[w] = \frac{d^2}{ds^2}\left[EI(s)\frac{d^2w}{ds^2} \right]$$

2.37)

$$M_b[w] = \rho A(s) w$$

The terms of the stiffness and mass matrices are determined by integrating the operators over the area of the plate using the assumed mode functions (equation 2.20) in equation 2.7. The displacement function can be expressed as a function of the plate coordinates or as a function of the axial position along the beam;

2.38)

$$k^b_{i,j} = \int_0^l w_i \frac{d^2}{ds^2}\left[EI(s)\frac{d^2w_j}{ds^2} \right] ds$$

2.39)

$$m^b_{i,j} = \int_0^l w_i \rho A(s) w_j ds$$

The expression for the stiffness term can be integrated by parts;

2.40)

$$k^b_{i,j} = \int_0^l EI(s)\frac{d^2w_i}{ds^2}\frac{d^2w_j}{ds^2}\,ds + w_i\left[\frac{d}{ds}\left(EI(s)\frac{d^2w_j}{ds^2}\right)\right]_0^l - \frac{dw_i}{ds}\left[EI(s)\frac{d^2w_j}{ds^2}\right]_0^l$$

The last two terms reflect the end conditions of the beam and require a more precise definition of the limits of integration. The only known boundary condition is at the boundary of the plate, let us assume all beams run from boundary to boundary for integration purposes. A beam may taper such that it has no height at the boundary. Using the edge to edge integration limit definition the first boundary term is identically zero. The second term would also be zero if either the beam were clamped or if the brace had zero thickness at the boundary. In guitar construction braces are either fared to zero height at the edge of the plate or locked into it to form a rigid termination. By neglecting the second boundary term we have violated nothing in the case of the tapered brace and stiffened the model for the locked brace which is appropriate.

The beam stiffness and mass expressions must be converted into forms which are in terms of the plate coordinate system. If a starting and end coordinate are identified for the beam the transformation is straight forward.

2.41)

$$x(s) = x_1 + (x_2 - x_1)\frac{s}{l}$$

$$y(s) = y_1 + (y_2 - y_1)\frac{s}{l}$$

$$l = \sqrt{(x_2 - x_1)^2 + (y_2 - y_1)^2}$$

Where the start and end points of the beam are; (x_1, y_1) and (x_2, y_2).

Applying the geometric transformation to the beam operators is done in stages. The derivatives along the beam are translated into the plate coordinate system using the chain rule for differentiation and the transformation relationships.

2.42)

$$w(s) = w(x, y)$$

2.43)

$$\frac{d^2w}{ds^2} = \frac{\partial^2 w}{\partial x^2}\left(\frac{dx}{ds}\right)^2 + 2\frac{\partial^2 w}{\partial x \partial y}\left(\frac{dx}{ds}\right)\left(\frac{dy}{ds}\right) + \frac{\partial^2 w}{\partial y^2}\left(\frac{dy}{ds}\right)^2$$

These transformed derivatives are then substituted into the beam operators.

2.44)

$$k^b_{i,j} = E\int_0^l I(s)\frac{d^2w_i}{ds^2}\frac{d^2w_j}{ds^2}ds$$

2.45)

$$m^b_{i,j} = \rho \int_0^l w_i A(s) w_j ds$$

The above set of equations can now be used to build beam mass and stiffness matrices in terms of the plate coordinates. The beam matrices can be added to the plate alone mass and stiffness matrices to produce braced plate models. The notation has been altered to extract the material dependent quantities from the preceding integrals.

2.46)

$$k_{i,j} = D_x k^{px}_{i,j} + D_y k^{py}_{i,j} + D_{xy} k^{pc}_{i,j} + \sum_{nb=1}^{braces} E_{nb} k^b_{i,j}$$

2.47)

$$m_{i,j} = \rho_p h m^p_{i,j} + \sum_{nb=1}^{braces} (\rho_{nb}) m^b_{i,j}$$

2.48)

$$[K]\{a\} - \omega^2[M]\{a\} = 0$$

At this point a braced plate in vacuo model has been derived. This is a standard eigenvalue problem.

2.3.3 Cavity and Port Models

The braced plate of the guitar soundboard is backed by a ported enclosure. The port cavity system adds two

degrees-of-freedom to the system. The port or sound-hole is modeled as a rigid piston and the cavity as a simple gas spring. These models are the first order or low frequency approximation to the system. The port cavity system has been shown to dominate the guitar system behavior in the 70-130 Hz frequency range. In this frequency range the low frequency models are appropriate for typical guitar constructions.

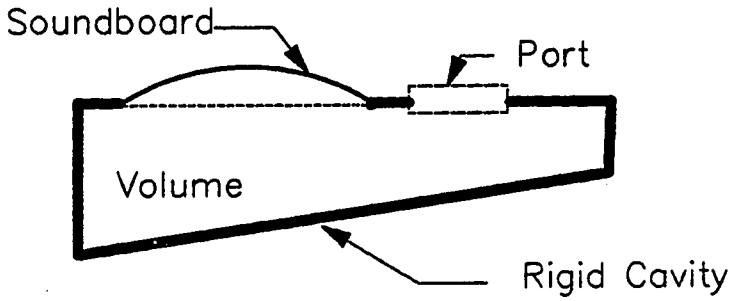

Figure 2.4 Cavity and Port Model

To model the port consider a thin tube of radius r with a depth on the order of the plate thickness seated in an infinite baffle. A lumped element mass and loss model can be constructed from the radiation impedance functions for a rigid piston. The small argument expansions and low frequency approximations have been applied to arrive at the following piston model.

2.49)

$$m_{port} = \pi r^2 \rho (h + 1.7r)$$

2.50)

$$r_{port} = \pi r^2 \rho c (kr)^2$$

In the piston port model the losses, r_{port}, are frequency dependent and the mass, m_{port}, is constant.

The cavity model is based on the adiabatic compression of a confined gas where the change in pressure in the cavity is proportional to the change of volume of the cavity. The constant of proportionality is inversely related to the cavity volume.

2.51)

$$\Delta P = -\frac{\rho c^2}{Vol} \Delta V$$

The change in volume of the cavity when bounded by the plate and port can be obtained by integrating the plate displacement functions.

2.52)

$$\Delta V = \int_{-L}^{L} \int_{-B(x)}^{B(x)} w(x,y) dy dx + \pi r^2 x$$

Where r is the radius of the soundhole and x is the acoustic displacement of the air slug modeling the soundhole.

The new degree-of-freedom can be added to the braced plate model by augmenting the basic structural matrix. Introducing a scaling constant,

2.53)

$$C_{box} = \frac{\rho c^2}{Vol}$$

The augmented system matrix has the form,

2.54)

$$\begin{bmatrix} k-\omega^2 m & -\int\int w dy dx & 0 \\ C_{box}\int\int w dy dx & 1 & C_{box}\pi r^2 \\ 0 & -\pi r^2 & -\omega^2 m_{port} + i\omega r_{port} \end{bmatrix} \begin{Bmatrix} a_j \\ \Delta P \\ x \end{Bmatrix} = \begin{Bmatrix} 0 \\ 0 \\ 0 \end{Bmatrix}$$

In the matrix equation the backing cavity is incorporated as additional constraint. The second row in the matrix is the cavity pressure equation in a form compatible with the sign convention of the plate model.

2.3.4 Radiation Models

Two levels of detail are used to model the acoustic back loading on the plate. A simple source radiation impedance model is used to calculate the basic system dynamics. The simple source model and the backing cavity model both present uniform pressures over the surface of the plate. The second model is for acoustic power radiation calculations and is a array model. The array model is used to estimate the radiation impedance of the system due to its own motion, as calculated with the simpler models.

The basic radiation loading function is that of a simple source with the area of the plate.

2.55)

$$P = \frac{i\omega \cdot \rho c}{\pi r_p^2}\left[\frac{(kr_p)^2}{1+(kr_p)^2} + i\frac{kr_p}{1+(kr_p)^2}\right] \cdot \Delta V = C_{rad} \cdot \Delta V$$

The cavity and radiation pressures can be added directly to give the net pressure acting on the plate. The matrix equation formulated for the cavity pressure can be generalized to accommodate both cavity and radiation pressure by changing the pressure scalar. This scalar is now frequency dependent.

2.56)

$$C_{box} \rightarrow C_{box} + C_{rad} = C_{net}$$

The pressure loads are assumed uniform across the plate which simplifies the calculations by making them non-iterative. This constant pressure assumption is valid when the acoustic wavelength of interest is large compared to the plate length. In the low frequency range of the guitar (below 400 Hz or wavelengths of 3/4 meters) this is a reasonable assumption. In the higher frequency ranges the fact the cavity will support acoustic modes and the radiation loading is non-uniform would require a more detailed model.

The second radiation model is that of a plane piston array. The piston array model generates the radiation impedances used to calculate total acoustic power radiated by the braced plate. The radiation impedances on a piston element is comprised of self radiation

impedance and a cross radiation impedance. The self impedance function can be found in most acoustic text books[25];

2.57)

$$Z_{pp} = \rho c \pi a^2 \left[1 - \frac{J_1(2ka)}{ka} + i \frac{H_1(2ka)}{ka} \right]$$

$J_1(2ka)$ = Bessel function

$H_1(2ka)$ = Struve function

a = piston radius

$k = \frac{\omega}{c}$ = wave number

The cross impedance term is due to the acoustic loading of one piston due the motion of another piston in the array. R. L. Pritchard[26] derived the cross impedance function for an array of identical pistons with arbitrary velocities. The cross impedance is computed using the formula;

---

25) Douglas D. Reynolds, Engineering Principles of Acoustics, Boston: Allyn and Bacon, Inc. 1981.

26) R. L. Pritchard, "Mutual Acoustic Impedance between Radiators in an Infinite Rigid Plane" J. Acoust. Soc. Am. 32(6) 1960.

2.58)

$$Z_{pq} = \rho c \pi a^2 \frac{(ka)^2}{2}\left[\frac{\sin(kd)}{kd} + i\frac{\cos(kd)}{kd}\right]\left\{\frac{v_p}{v_q}\right\}$$

d = distance between the centers of pistons p and q

v_p = velocity of piston p

v_q = velocity of piston q

This model has been derived for the case of identical pistons which are small compared to the radiated wavelength in an infinite baffle. The formula is valid for pistons whose centers are separated by distances equal to or greater than twice the piston radius. In the minimum separation case the pistons are tangent.

The acoustic power is computed using the impedance matrix and the displacements calculated from the structural equations. The displacements over the plate are converted into area-averaged piston velocities for each piston at the frequency of interest. The radiated power is then calculated by;

2.59)

$$Power = \begin{Bmatrix} v_1 \\ v_2 \\ .. \\ v_n \end{Bmatrix}^T \begin{bmatrix} Z_{11} & Z_{12} & \cdots & Z_{1n} \\ Z_{21} & Z_{22} & \cdots & Z_{2n} \\ \cdots & \cdots & \cdots & \cdots \\ Z_n 1 & \cdots & \cdots & Z_{nn} \end{bmatrix} \begin{Bmatrix} v_1 \\ v_2 \\ .. \\ v_n \end{Bmatrix}$$

Where;

$$v_p = \frac{i\omega}{\pi a^2} \int w dA_p$$

The piston size has been selected to match the size of the soundhole of the guitar, typically a four inch diameter. The piston size is small relative to the acoustic wavelength through out the modeling range. The modeling array using this size piston is typically a five by five element array.

2.3.5 Force Model

The driving force for the model is a simple constant force generator located at a point on the plate. The force locations are determined from body joint and string length information. The drive point locations are intended to represent the string bridge contact points. The forces are considered point loads and they will drive the soundboard-cavity-sound hole model.

2.60)

$$\text{Force} = F_{st} \cdot \delta(x - x_0)\delta(y - y_0)$$

The weighting functions must be applied to the point loads to convert them into the matrix formulation.

2.61)

$$f = \int_{-L}^{L} \int_{-B(x)}^{B(x)} w_i F_{st} \delta(x - x_0)\delta(y - y_0)\ dydx$$

$$= F_{st}\ \ w_i(x_0, y_0)$$

The complete system of equations has been developed to model the guitar soundboard and the computational modeling effort may begin.

2.4 Solution Methods

The solution methods have been selected to generate information which will be used to compare guitar soundboard designs. The nature of this work is to survey a large range of guitar designs therefore two basic output forms have been selected. The first is the determination of resonant frequencies and mode shapes for the undamped in vacuo braced plate system. The second form is the prediction of the radiated acoustic power of the guitar model under a constant force drive. These two output forms will indicate the sensitivity of construction variations on the mechanical and acoustical performance of the guitar.

2.4.1 Real Eigenvalue Problem

The real eigenvalue problem for the braced plate system is formulated in the earlier sections. A version of

the EISPACK[27] eigenvalue solving routines is used in the eigenvalue computations. The required integrals are computed numerically. The integrations were performed using a grid with evenly spaced points along the abscissas with an equal number of points evenly spaced between the limits of the boundary curve. A 25 point by 25 point computational grid was used in all calculations. Twelve by twelve computational grids were found to be the minimum size required to obtain good results. The beam integrals were also computed using a similar evenly spaced point approach. Each beam may have up to four sections or four slopes in the height of the beam. The beam has a constant cross section shape with a linearly varying height in each section. Beam integration points were chosen to have a spacing similar to that of the plate grid. A minimum of three points per section was required.

The overall mass and stiffness elements are computed by evaluating the integrals numerically and them scaling the integrals by the appropriate material constants.

2.62)

$$k_{i,j} = D_x k^{px}_{i,j} + D_y k^{py}_{i,j} + D_{xy} k^{pc}_{i,j} + \sum_{nb=1}^{braces} E_{nb} \sum_{s=1}^{4} k^{b}_{i,j,s}$$

---

27) T. B. Smith et. al. Matrix Eigensystem Routines EISPACK Guide, second edition vol 6 of Lecture Notes in Computer Science, New York: Springer-Verlag 1976.

2.63)

$$m_{i,j} = (\rho_p h) m^p_{i,j} + \sum_{nb=1}^{braces} \rho_{nb} \sum_{s=1}^{4} m^b_{i,j,s}$$

2.64)

$$[K]\{a\} - \omega^2 [M]\{a\} = 0$$

The eigenvalue problem has sixteen degrees-of-freedom with sixteen resonant frequencies. For typical guitar constructions only the lower four to six resonant frequencies lie in the frequency range of interest, 80 to 880 Hz.

2.4.2 Forced Response

The forced response problem is solved in 1/12 octave or semitone intervals from 55 to 880 Hz. To solve the system of equations a complex matrix inversion is required. A LINPACK[28] subroutine is used to solve the equations.

The structural model developed for the eigenvalue problem is augmented with the simple pressure models and forcing functions to compute the response.

---

28) J. J. Dongarra et. al. LINPACK Users Guide, Philadelphia: SIAM 1979.

2.65)

$$\begin{bmatrix} k-\omega^2 m & -\int\int w dy dx & 0 \\ C_{net}\int\int w dy dx & 1 & C_{net}\pi r^2 \\ 0 & -\pi r^2 & -\omega^2 m_{port} + i\omega r_{port} \end{bmatrix} \begin{Bmatrix} a_j \\ \Delta P \\ x \end{Bmatrix} = \begin{Bmatrix} f \\ 0 \\ 0 \end{Bmatrix}$$

The matrix pressure terms and port terms are frequency dependent requiring the inversion of this system matrix for each frequency of interest. Acoustic power is calculated from the displacement functions obtained using this procedure. The acoustic array impedance matrix is recalculated for each frequency.

3 Computer Model

The computer model is separated into three programs. These programs are named for their basic functions Model, Eigen and Spectra. Model defines the plate geometry and boundary conditions, the bracing pattern layout, the beam cross section shapes, the beam height tapers, and generates the material independent mass and stiffness integrals for the plate and associated beams. Eigen adds material properties to the mass and stiffness integrals computed in the Model program and solves the eigenvalue problem for the undamped braced plate in vacuo. Natural frequencies and mode shapes are plotted as output. The third program, Spectra, computes the forced response of the plate model with cavity and radiation pressures and plots the radiated acoustic power spectra. The guitar backing cavity size and drive point location(s) are defined in Spectra. All three programs communicate to each other via a number of data files.

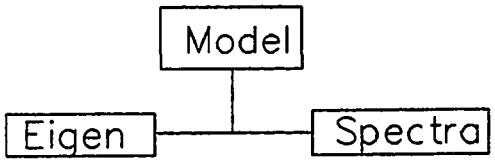

Figure 3.1 Program Overview

3.1 Program Logic and Data Flow

An overview of the programs and their interactive data flows will be presented in a straight line path. Re-entrant paths can be inferred by the input and output calling sequences. Before each major computation takes place a check is made to see if the file which would result from the computation already exists. If the file is found to exist it is read and the program advances to the next request for input.

To aid the reader, subroutine names will be in square brackets [subroutine] and file names will be in braces {filename.tag}. Questions which require input from the operator will terminate in a question mark. Program logic statements such as loop designations will be written in capital letters.

3.1.1 MODEL

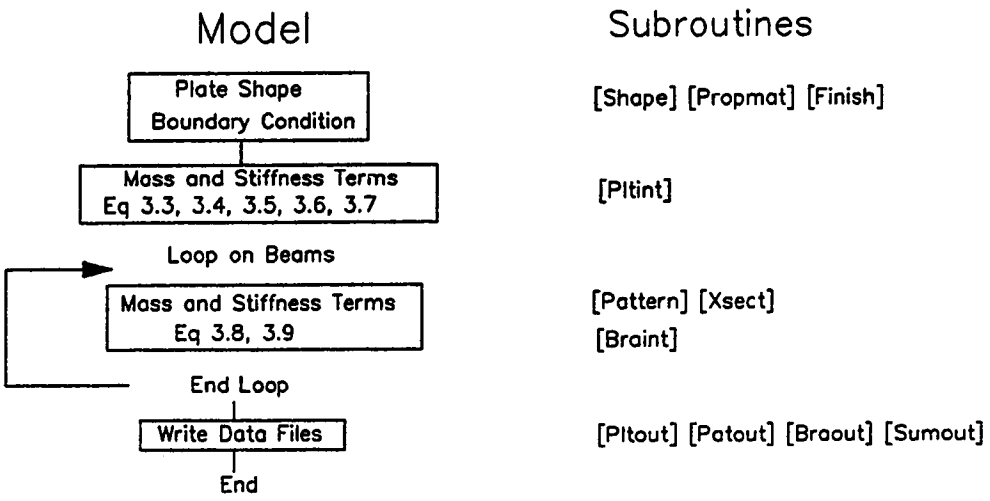

Figure 3.2 Model Flow Chart

[Main] controls the file handling and directs the overall program flow. The objective of the MODEL program is to define a braced plate geometry and then compute the mass and stiffness integral terms of equations 2.30 and 2.31 for the plate and equations 2.43, 2.44, and 2.45 for the tapered beam.

[Shape] defines the outline of the plate interactively. The geometry can be either one of the programmed options or a table of points. The outline options are circular, ellipsoidal or guitar shaped. The guitar shapes are those of Childers modified for use in the chosen coordinate system. The plate outline shapes, either analytical or tabular, are then fitted with a

Chebyshev polynomial series. A soundhole location and radius are entered. The coefficients of the Chebyshev polynomial series along with the sound hole information are written out to file (filename.cof) for future use.

[Main] Select a Plate thickness? A plate thickness is entered. It is useful to be able to compare plates in terms of a non-dimensional shape factor. For isentropic materials the natural frequency of a plate can be expressed in the general form;

3.1)

$$f = \frac{\Lambda^2 h}{2\pi(2L)^2}\sqrt{\frac{D}{\rho}}$$

f = Frequency (Hz)

h = Plate thickness

$2L$ = Plate length

D = Bending Modulus

ρ = Density

Λ^2 = Form factor

The constant Λ^2 is dependent on plate shape, plate boundary conditions and mode shape. By selecting a material, a thickness can be computed which will result in the frequency estimate being Λ^2, the geometric and material properties being selected so that;

3.2)

$$\frac{h}{2\pi(2L)^2}\sqrt{\frac{D}{\rho}} = 1$$

When the above expression is solved for thickness and that thickness is used in the determination of resonant frequencies the shape factor Λ^2 is produced.

[Main] What boundary conditions should be used? The options are clamped and simply supported, which are selected by choosing the β exponent.

2.20)

$$w_i(x,y) = (B^2(x)-y^2)^{2\beta} \cdot \cos\left[\frac{n\pi x}{2L}+\frac{\pi(n-1)}{2}\right]\cdot\cos\left[\frac{m\pi y}{2B(x)}+\frac{\pi(m-1)}{2}\right]$$

$2L$ = Plate length

$B(x)$ = Boundary curve

n,m = Integers 1,2,3...

β = 0 Simple support

= 1 Clamped support

All calculations executed in the current code are based on this general form of the deflection curve.

[Propmat] is the material data base. At this time it is used to assign a material type to the plate. The data base is presented in tabular form in the appendix.

[Finish] calculates the modified material properties due to the application of a finish. At this time it is being used to assign a finish type to the plate. Five options are available, no finish, a soft thick varnish, a soft thin varnish, a thick hard varnish and a thin hard varnish. Details of the varnish material constants and thicknesses are presented in the appendix.

[Pltint] calculates the plate mass, stiffness and net volume displacement integrals.

3.3)

$$k_{i,j}^{px} = \int_{-L}^{L}\int_{-B(x)}^{B(x)} w_i \frac{\partial^4 w_j}{\partial x^4} dy dx$$

3.4)

$$k_{i,j}^{py} = \int_{-L}^{L}\int_{-B(x)}^{B(x)} w_i \frac{\partial^4 w_j}{\partial y^4} dy dx$$

3.5)

$$k_{i,j}^{pc} = \int_{-L}^{L}\int_{-B(x)}^{B(x)} 2w_i \frac{\partial^4 w_j}{\partial x^2 \partial y^2} dy dx$$

3.6)

$$m_{i,j}^{p} = \int_{-L}^{L}\int_{-B(x)}^{B(x)} w_i w_j dy dx$$

3.7)

$$Vol_i = \int_{-L}^{L}\int_{-B(x)}^{B(x)} w_i dy dx$$

The derivatives of the deflection curve are evaluated using the chain rule for differentiation and take advantage of the fact that the derivatives of the boundary function can be computed using the recursion formula for the Chebyshev polynomial series[29].

[Pltout] writes out a data file (filename.plt) which includes a header which identifies a plate thickness, area, material, finish, the number of integration steps used to evaluate the integrals in the directions along-the-grain and across-the-grain and the number of assumed modes. The body of the file is the results of the calculations made in evaluating equations 3.3 to 3.7.

[Main] How many beam files do you wish to build? Up to ten beam files are currently allowed. Each beam file can describe up to four beams. The break down of the beam file system is to encourage the build up of bracing systems from simpler subsystems.

START LOOP ON BEAM FILES

START LOOP ON BEAMS

[Pattern] defines the beam geometry. Start and stop points along with a stock base width and height are entered to define the basic beam. The beam is then tapered by entering the percent height at a selected length along the beam from the start point. The length

---

29) William H. Press, Brian P. Flannery, Saul A. Teukolsky, William T. Vettering. Numerical Recipes The Art of Scientific Computing. New York : Cambridge University Press, 1968.

along the beam for the description of the taper also entered in percent. The tapers are linear. A material is assigned to each brace using the subroutine [Propmat].

[Xsect] A beam cross sectional shape is selected from three options rectangular, semi-elliptical or triangular. The neutral axis for bending of the beams is selected as either about the centroid of the section or about the plate beam interface.

[Patout] writes out a data file (filename.pat) which includes the geometry, cross section shape and material identification information collected in [Pattern], [Propmat] and [Xsect]. There are no computations associated with this file.

[Braint], calculates the beam mass, stiffness matrix terms. The mapping of the beam coordinates to plate coordinates has been described in the discussion of equations 2.42 and 2.43 and will not be repeated here. The material independent integrals follow from equations 2.44 and 2.45;

3.8)

$$k^b_{i,j} = \int_0^l I(s)\frac{d^2w_i}{ds^2}\frac{d^2w_j}{ds^2}ds$$

3.9)

$$m^b_{i,j} = \int_0^l w_i A(s) w_j ds$$

[Braout] writes out a data file (filename.bra) which has the same filename as the associated brace geometry definition file (filename.pat). The body of the file is the results of the calculations expressed in equations 3.8 to 3.9.

END LOOP ON BEAMS

END LOOP ON BEAM FILES

[Sumout] writes out a model summary file listing itself (filename.sum), the boundary coefficient file (filename.cof) the plate file (filename.plt) and the number of bracing files and then the bracing files in pairs (filename.pat), (filename.bra). The sum file provides a short hand way of bookkeeping complete models.

3.1.2 EIGEN

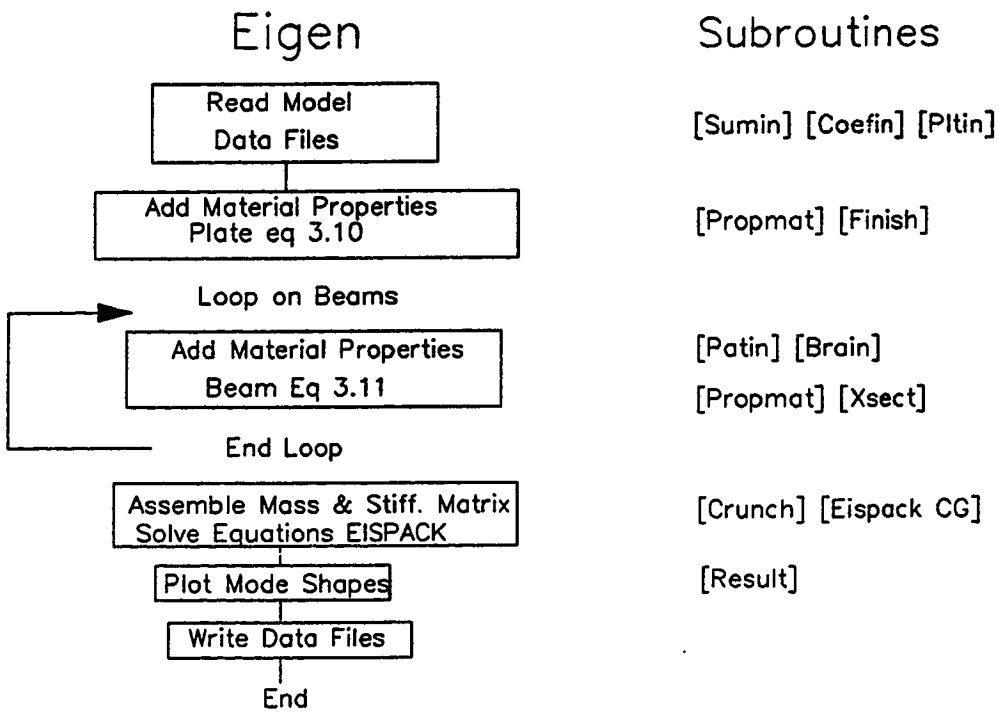

Figure 3.3 Eigen Flow Chart

[Main] controls the file handling and directs the overall program flow. The objective of the EIGEN program is to assemble a braced plate model for eigenvalue solution of natural frequencies and mode shapes from the material data base and the mass and stiffness integral terms of computed in MODEL. The addition of the material properties to the MODEL files converts the

plate equations 3.3 to 3.6 into their parent forms equations 2.30 and 2.31. The tapered beam equations 3.8 and 3.9 are returned to the equations 2.44, and 2.45. The stiffness and mass matrices can be combined as discussed earlier to form a standard eigenvalue problem (equations 2.46, 2.47, 2.28).

[Sumin] reads the summary file written by MODEL. The summary file includes a list of files; itself (filename.sum), the boundary coefficient file (filename.cof) the plate file (filename.plt) and the number of bracing files and then the bracing files in pairs (filename.pat), (filename.bra). The sum file provides a short hand way of bookkeeping complete models.

[Coefin] The coefficients of the Chebyshev polynomial series along with the soundhole information are read out of file (filename.cof). This information will be used to plot mode shapes.

[Pltin] reads the data file (filename.plt) which was written by MODEL. This file includes plate thickness, area, material, finish, the number of integration steps and the number of assumed modes information. The body of the file is the results of the calculations made in evaluating equations 3.3 to 3.7.

[Propmat] is the material data base. At this time it is used to take the material type assigned to the plate in the MODEL program and recover the material properties needed for the eigenvalue calculations.

[Finish] calculates the modified material properties due to the application of a finish. The calculation has been discussed in terms of unconstrained layer damper theory (equation 2.34) and the material properties are listed in the appendix.

[Main] begin assembly of system dynamics matrix with the plate elements.

3.10)

$$k_{i,j} = D_x k^{px}_{i,j} + D_y k^{py}_{i,j} + D_{xy} k^{pc}_{i,j}$$

$$m_{i,j} = \rho_p h m^{p}_{i,j}$$

LOOP ON BEAM FILES

[Patin] reads the data file (filename.pat) written by MODEL which includes the geometry, cross section shape and material identification information collected in [Pattern], [Propmat] and [Xsect].

[Brain] reads a data file called (filename.bra) which has the same filename as the associated brace geometry definition file (filename.pat). The body of the file is the results of the calculations performed in MODEL.

LOOP ON BEAMS

[Propmat] is the material data base. The beam material properties assigned by a type designation in the MODEL program are recovered.

[Xsect] The beam cross sectional shape properties are recovered from the selection code.

3.11)

$$k_{i,j} = k_{i,j} + D_x \cdot (I_{cof}) \cdot (BH^3) \cdot k^b_{i,j}$$

$$m_{i,j} = m_{i,j} + \rho \cdot A_{cof} \cdot (BH) \cdot m^b_{i,j}$$

I_{cof} = Inertia Scaling factor

A_{cof} = Area Scaling factor

D_x = Bending Modulus along the grain

ρ = Density

B = Base width of Beam stock

H = Height of Beam stock

The scaling factors are used to account for the various cross sectional shapes and the location of the neutral axis of bending.

END LOOP ON BEAMS

END LOOP ON BEAM FILES

[Crunch] takes the mass and stiffness matrices and sets up a standard eigenvalue problem for solution with an Eispack[30] subroutine.

[Result] reformats the eigenvalue solution. The solution set is ordered by increasing eigenvalue and natural frequencies are calculated from the eigenvalues. A table of participation factors of the assumed modes and

---

30) B. T. Smith, et al. Matrix Eigensystem Routines EISPACK Guide. 2nd ed., vol 6 of Lecture Notes in Computer Science, New York: Springer-Verlag 1976.

printer plots of the mode shapes are the primary output. The modal output data is written to a file for future use and analysis (filename.res).

3.1.3 SPECTRA

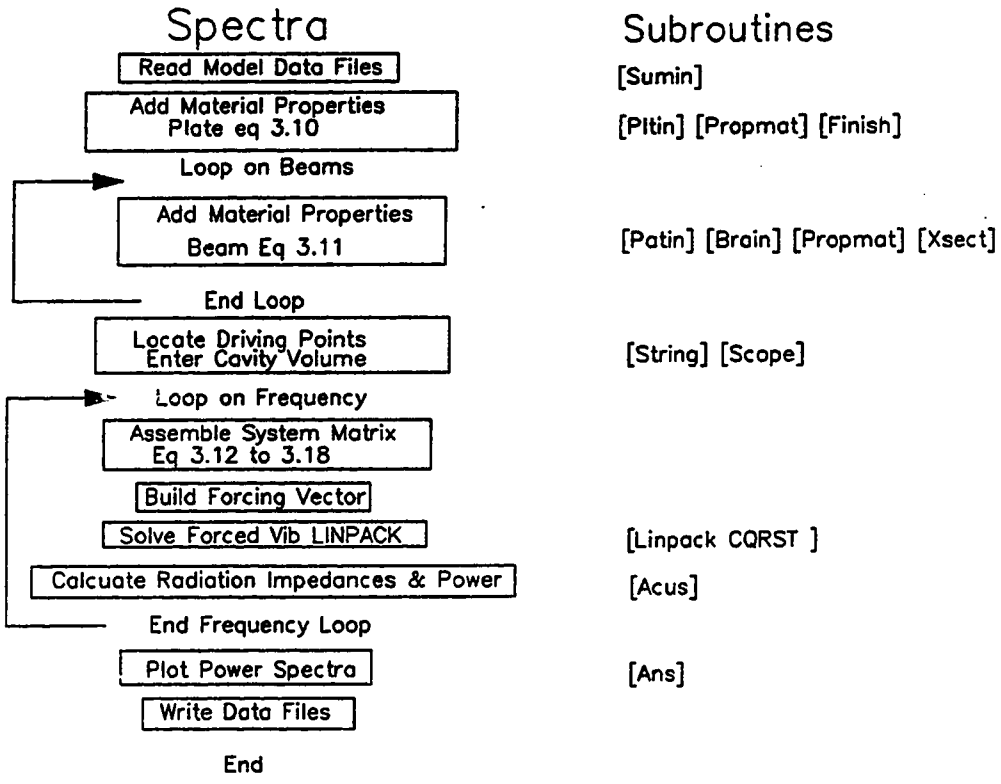

Figure 3.4 Spectra Flow Chart

[Main] controls the file handling and directs the overall program flow. The objective of the SPECTRA program is to assemble a braced plate model with acoustic and cavity pressure loadings for forced response estimates of the radiated sound power. The braced plate mass and stiffness matrices are assembled in the same manner

they were in EIGEN with the extension that complex material properties are used in SPECTRA to account for material damping. The frequency dependent forced vibration system has been derived in Chapter 2 leading to equation 2.65. SPECTRA solves equation 2.65 for the displacements and then applies equations 2.57 to 2.59 to calculate the radiated power. The radiated power is calculated from the radiation impedance and velocities of a piston array representing the surface of the soundboard. The stiffness and mass matrices are augmented by the pressure loading terms and the rigid piston soundhole model. The system is forced by a set of one or more constant force point sources. The resulting system of equations forms a complex matrix inversion problem. This complex matrix inversion is accomplished using a Linpack subroutine[31].

[Sumin] reads the summary file written by MODEL. The summary file includes a list of files; itself (filename.sum), the boundary coefficient file (filename.cof) the plate file (filename.plt) and the number of bracing files and then the bracing files in pairs (filename.pat), (filename.bra).

[String] addresses the location and number of drive points. The drive points are located using standard string length scales and body joint locations. The neck of the guitar joins the body at either the twelfth or fourteenth fret. The axial locations of the drive

---

31) J. J. Dongarra, C. B. Moler, J. R. Bunch, G.W. Stewart Linpack Users' Guide. Philadelphia: SIAM, 1979.

points are determined once a body joint and a scale length are specified. To determine the vertical separation between the strings a nut width is entered which fixes the string to string spacing at the bridge. This information has been gathered from several sources and reflects current building practices.

[Scope] is an input routine to gather new information such as the volume of the backing cavity and the frequency range over which calculations are to take place.

[Coefin] The coefficients of the Chebyshev polynomial series along with the sound hole information are read out of file {filename.cof}. This information is used to calculate the participation factor for the forcing function and the velocity distribution in the acoustic array.

[Pltin] reads the data file {filename.plt} which was written by MODEL. This file includes plate thickness, area, material, finish, the number of integration steps and the number of assumed modes information. The body of the file is the results of the calculations made in evaluating equations 3.3 to 3.7.

[Propmat (complex)] is the material data base. Complex material properties are introduced to model material damping. The material type assigned to the plate in the MODEL program is used to recover the material properties needed for the forced response calculations.

[Finish (complex)] calculates the modified complex material properties due to the application of a finish. The calculation has been discussed in terms of unconstrained layer damper theory.

[Main] assembles the system stiffness and mass matrices beginning with the plate elements. This procedure is identical to that used in EIGEN see equation 3.10.

LOOP ON BEAM FILES

[Patin] reads the data file {filename.pat} written by MODEL which includes the geometry, cross section shape and material identification information collected in [Pattern], [Propmat] and [Xsect].

[Brain] reads a data file called {filename.bra} which has the same filename as the associated brace geometry definition file {filename.pat}. The body of the file is the results of the calculations performed in MODEL.

LOOP ON BEAMS

[Propmat (complex)] is the complex material data base. Properties are assigned to each beam.

[Main] start the assembly of the frequency independent parts of the mass matrix and stiffness matrix. This is a parallel construction to that done in EIGEN equation 3.11.

END LOOP ON BEAMS

END LOOP ON BEAM FILES

LOOP ON FREQUENCY

The limits of the frequency loop have been specified in [Scope] and have a maximum range of 55 to 880 Hz. The step size is set at one twelfth octave or one semitone.

[Main] Build the system matrix. The upper part of the system matrix is a square n by n matrix representing the isolated braced plate system. EIGEN solved this system for natural frequencies and mode shapes. The number of assumed modes is denoted by n. The frequency has been chosen allowing the simple computation for these system matrix elements.

3.12)

$$S_{i,j} = k_{i,j} - \omega^2 m_{i,j}$$

i = 1, n
j = 1, n
n = number of assumed modes

[Main] The port model system elements are computed from equations 2.49 and 2.50.

3.13)

$$S_{n+2,n+2} = i\omega r_{port} - \omega^2 m_{port}$$

[Main] The action of the net pressure across the plate is derived from the box cavity back pressure and the simple source radiation pressure. The pressure is accounted for in equations 2.53, 2.55, 2.56 and the volume displacement 3.7.

3.14)

$$S_{n+1,i} = (P_{box} + P_{rad}) \cdot Vol_i$$

[Main] A similar term is generated for the soundhole piston.

3.15)

$$S_{n+1,n+2} = (P_{box} + P_{rad}) \cdot A_{port}$$

[Main] The pressure equation 2.52 requires;

3.16)

$$S_{n+1,n+1} = 1$$

[Main] The pressure loading is then applied to the structural system through the coupling elements. For the braced plate;

3.17)

$$S_{i,n+1} = -Vol_i$$

And for the soundhole piston;

3.18)

$$S_{n+2,n+1} = -A_{port}$$

[Main] all other terms in the system matrix are zero. The right hand side of equation 2.65 has been constructed. The matrix is complex.

[Main] The forcing vector is constructed from the drive point information acquired in [String]. The constant force magnitude is multiplied by the assumed mode displacement at the drive point following equation 2.61.

[Main] The next call is to Linpack subroutine cqrst which solves the system of equations using a least squares algorithm. The matrix is square and could be inverted directly.

[Acus] Upon return from the system solution subroutine a set of assumed mode magnitudes are in hand. These magnitudes are used to scale the assumed mode shapes to arrive at displacement on the plate. A piston array is constructed, the size of the pistons being equal to the soundhole. The array is centered on the soundhole. The plate displacements are averaged over the piston areas and converted into piston velocities for acoustic radiation calculations. The self and mutual radiation impedances are calculated using equations 2.57 and 2.58. Radiated power is calculated using the radiation impedances as in equation 2.59.

END LOOP ON FREQUENCY

[Ans] the acoustic power levels computed by SPECTRA are plotted and stored in a file {filename.ans} for future use.

3.2 Program Verification Tests

The three programs MODEL, EIGEN and SPECTRA calculate a simple model of a cavity-backed braced-plate radiator which is being used to describe a guitar soundboard. The theory is approximate, the boundary conditions are

simplified, the knowledge of material properties limited. The desired result of the modeling exercise is to compute major trends.

In this section the solution of well documented problems have been used to verify the computer code generated for this study. The code has been checked out using simple geometries. Any guitar soundboard model can only be verified with experimental data beyond this point.

3.2.1 MODEL and EIGEN Tests

Predictions will be made for clamped and simply supported circular plates for the purposes of computer code verification. The circular plate has been studied in great detail with both exact and approximate methods of analysis. Experimental data is available for the braced clamped plate providing an opportunity to validate the beam model. A guitar shaped plate, a Sloane classical guitar pattern, will also be used in the verification studies. The guitar shape is used to see if the convergence criteria for the circular plate holds for the guitar shape. No exact solution for the guitar shaped plate is known to the author.

The first study is aimed at determining the number of Chebyshev polynomial terms needed to represent the outline of the plate. The stiffness and mass terms used in computing the system dynamics are the result of integrations over the area of the plate. The ability of the truncated Chebyshev polynomial version of the

boundary curve to estimate the plate area is a criterion for determining the number of terms needed in the boundary curve expansion. The area of a circle is known, pi times the radius squared. The integral of the boundary function over the length of the plate is an approximation to the area of the plate. A ratio of these two numbers should approach one as the number of approximation terms increases. To normalize the area of the guitar plate a hand estimate of the area was made from the drawings provided in Sloane's book on guitar construction[32].

---

32) Irving Sloane. Classic Guitar Construction. New York: E. P. Dutton & Co., Inc.,: 1966.

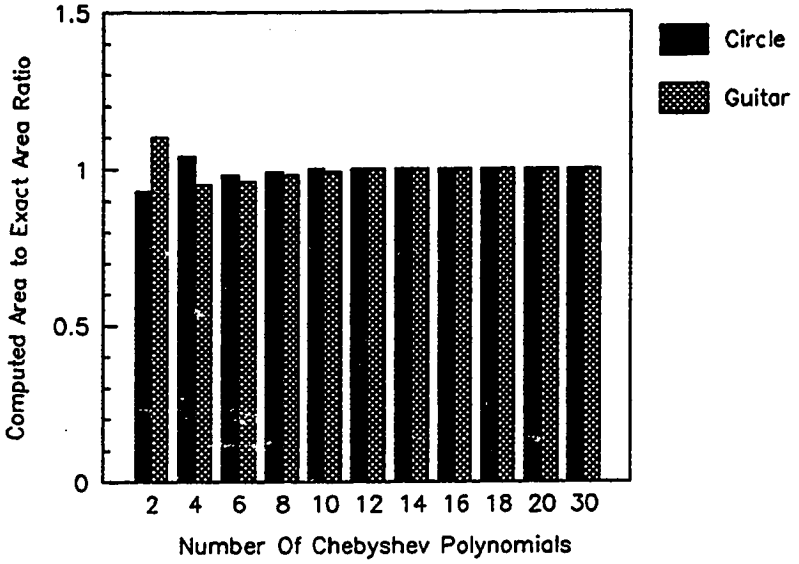

Figure 3.5 Chebyshev Polynomial Term Requirements

The assumed mode series selected in Chapter 2 is an infinite series, for computational reasons the series must be truncated. To estimate how many assumed modes will be required to represent the dynamics of the guitar soundboard system two circular plate models, one clamped and one simply supported, were run with increasing numbers of modes. The assumed mode function family for a circular plate have the following patterns, as generated by equation 2.20. The actual modes of vibration are built up from a weighted sum of these assumed modes.

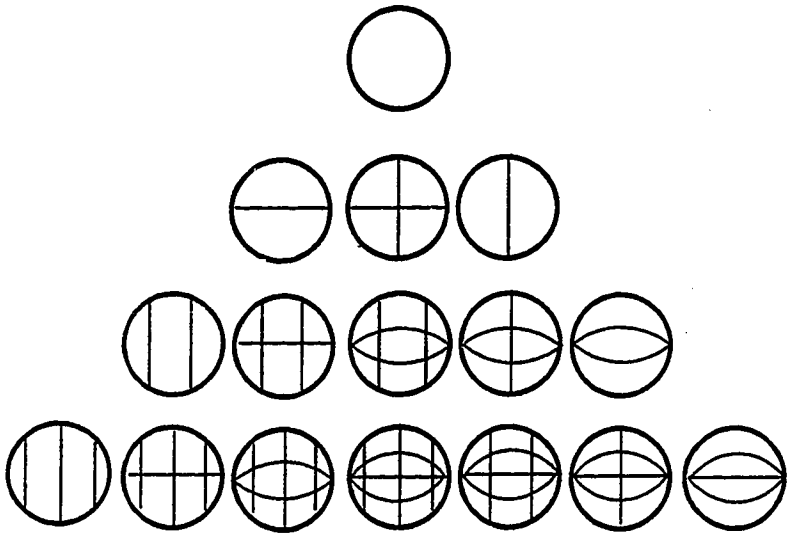

Figure 3.6 Assumed Mode Shapes for Circular Plates

The frequency of the fundamental mode of vibration of a circular plate was used as an indicator how well the model was predicting. Natural frequencies for isentropic simply supported or clamped circular plates are well documented[33]. The ratio of the established frequencies to those estimated in this study provide an indication of the validity of the current technique.

---

33) Robert D. Blevins, Formulas for Natural Frequency and Mode Shape. New York: Van Norstrand Reinhold Company, 1979.

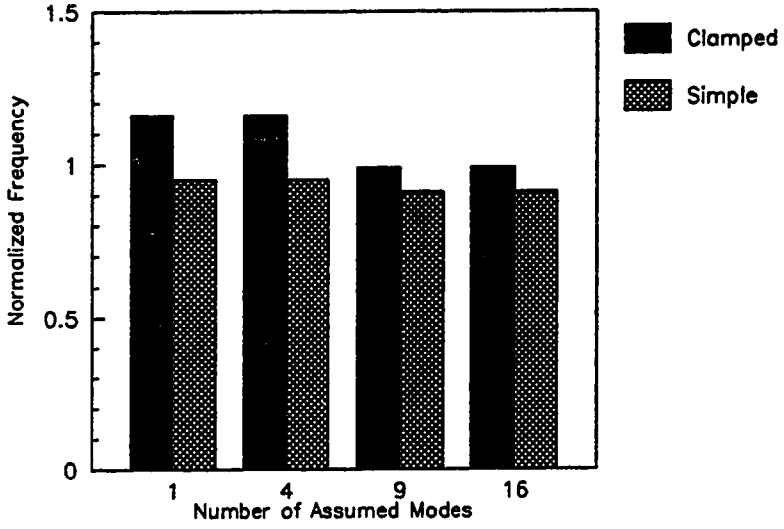

Figure 3.7 Effects of the Number of Assumed Mode Terms

Both predictions are systematically low, the simply supported plate by less than ten percent and the clamped plate by less than one percent with a nine or sixteen term assumed mode series. This level of accuracy is acceptable for the current studies. Larger uncertainties will be encountered in the estimation of material properties used in these models.

The number of integration points needed to accurately determine the value of the integrals using an equally spaced computational grid has been determined. The number of integration points is a function of the highest order mode shape selected in the assumed mode series. Five integration points per half wave or

"bump" in the assumed mode displacement function was found to be a good rule of thumb in determining the number of integration points required. In the sixteen assumed mode case this criterion translates into a twenty by twenty point integration grid.

The modeling of the soundhole in the guitar plate has been approached in a simple manner. The mass and stiffness integrals used to model the system are computed over an area which is bounded by the edge of the plate and soundhole. This is a crude approximation at best. The free edge boundary condition of the soundhole edge are ignored. This modeling approach has been used to model annular plates with both clamped and simply supported boundary conditions.

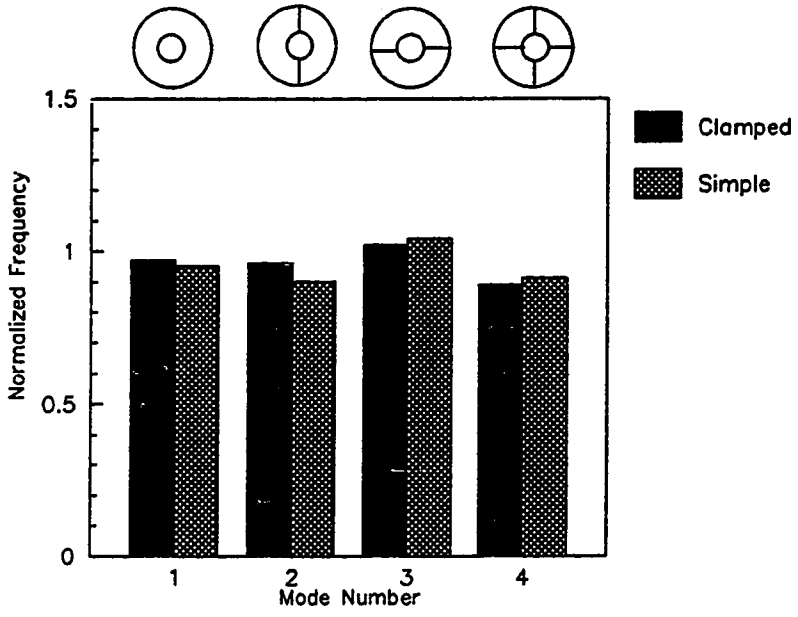

Figure 3.8 Annular Plate Predictions

Note that the predicted mode shapes for the second and third modes are identical except for a rotation of the nodal line, this dual prediction is a result of the selection of the assumed mode shape series.

The simple plate model has been checked against a number of solutions; unfortunately the literature is not as generous with data for the braced plate. In Leissa's book[34] on plates one can find a reference to an experiment by Hoppmann involving a clamped braced

34) Authur W. Leissa. Vibration of Plates. Washington D.C.: NASA SP-120, 1969

plate. The study measured the natural frequencies and mode shapes for a ribbed circular aluminum plate. Thirteen parallel ribs are milled into the plate the dimensions of which were found in a paper by Desiderati and Laura[35]. In that paper the authors applied the Galerkin technique and estimated the first natural frequency.

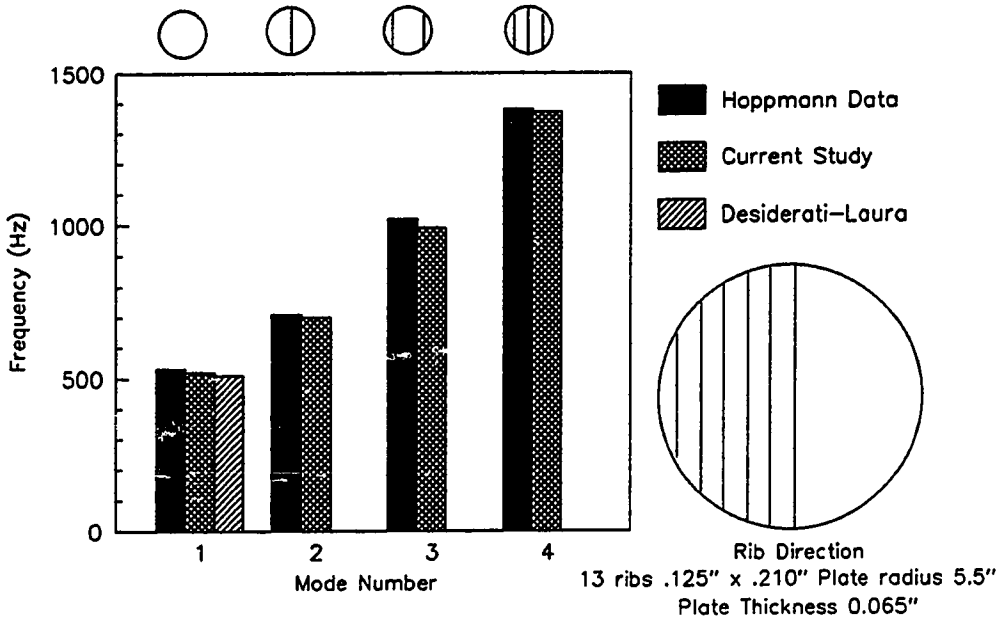

Figure 3.9 Clamped Braced Plate
Data and Model Comparison

35) Frank W. Desiderati, Patricio A. Laura, "Vibrations of Rib-Stiffened Elliptical and Circular Plates" J. Acoust. Soc. Am. 48(1) part 1 1970.

All aspects of the braced plate with sound hole computer program have been checked out using circular plates. The prediction of natural frequencies has been used to determine the figure of merit for each new complication. The model in this form is acceptable for the determination of the major design trends in soundboard studies.

3.2.2 SPECTRA Tests

The radiation model is based on the building of an acoustically equivalent array of simple piston sources. A seven piston model is used to predict the radiation impedance of a rigid piston over a large non-dimensional frequency range. The ratios of the predicted real and imaginary parts of the radiation impedance to the classical analytical results are presented in a logarithmic format.

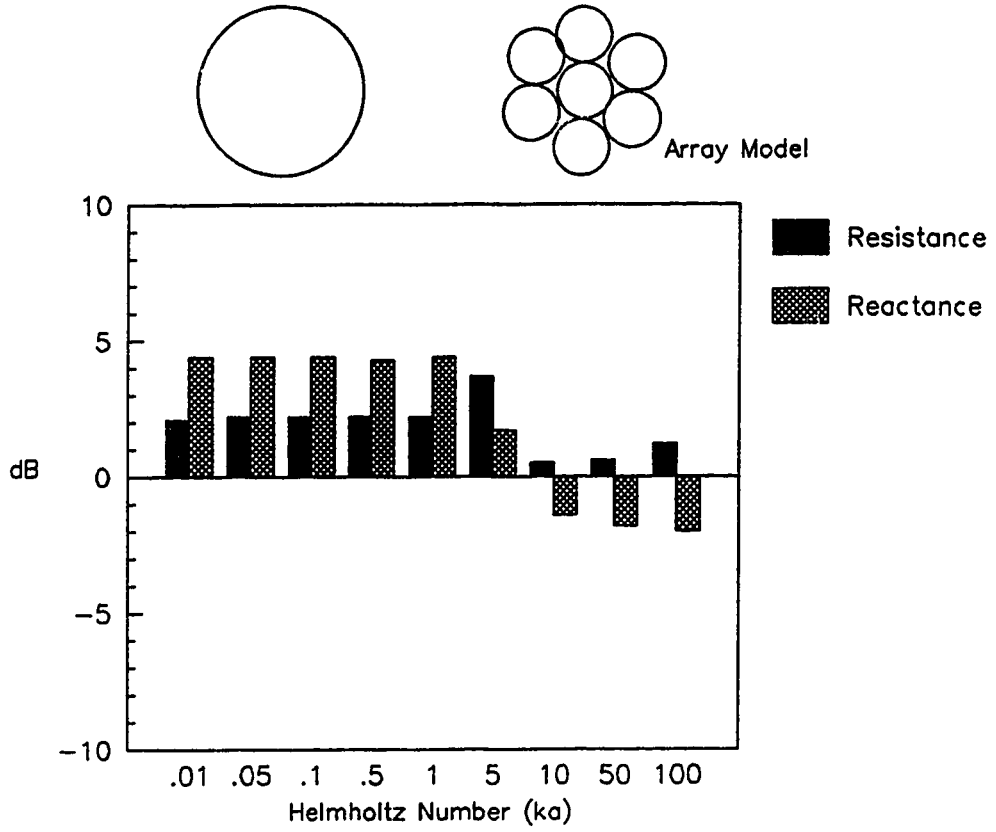

Figure 3.10 Rigid Piston Simulation via Array Model

The array model over predicts the radiation resistance throughout the modeled frequency range. This error in radiation resistance will translate into a 2 dB bias in the predicted acoustic power spectra. A prediction bias on this order is acceptable in the establishment of design trade studies. The radiation reactance acts

as an additional mass to the dynamics of the system. The radiation mass is relatively small compared to the plate mass and this modeling bias should be of secondary importance to the plate dynamics. The soundhole or port mass is dominated by its own radiation mass and will be the most sensitive parameter to errors in the predicted radiation mass. If there is relatively small motion around the soundhole this radiation mass loading error should not significantly influence the predictions.

In this section the solution of well documented problems have been used to verify the computer code generated for this study. The desired result of the following exercises is to compute major trends in the dynamics of guitar soundboard systems. The code has been checked out using simple geometries and any guitar soundboard model can only be verified with experimental data beyond this point.

4 Computer Model Exercises

The computer models developed in Chapters 2 and 3 for the prediction of guitar soundboard mechanical-acoustical behavior are exercised in this chapter. All the data presented in this chapter are computer generated. Six basic plate shapes have been used in the study of the unbraced plate. Three of these plates have been used to examine bracing patterns. Two of the braced plate configurations that have been selected are documented in the open literature and serve as check cases. The data from the previous studies are not discussed in this chapter.

4.1 Simple Plates

The outline shape of the guitar plate is the product of many physiological, artistic and mechanical compromises. The guitar is played in both standing and sitting positions. It is the sitting position constraints that define the maximum limits of the guitar body profile. The lower bout of the instrument must be designed such that the average arm can reach over it and pluck the strings of the instrument. The sitting position also requires the instrument to straddle the thigh of the player in some playing positions. The classical playing position requires the positioning of lower bout of the guitar between the thighs of the player which constrain the shape of the lower bout and overall body length. The upper bout must not adversely effect the ability of the player to address the fretboard. The instrument/player interface defines an envelope in which a guitar shape can be realized. The

maximum envelope is roughly a rectangular box with dimensions of 0.5 by 0.4 meters (20 by 16 inches). The maximum lower bout diameter is on the order of 0.425 meters (16 3/4 inches).

The guitar is also an art object of fine craftsmanship. An awkward appearance may preclude a musician from picking up the instrument and giving it its due. The selection of the body shape may be strongly influenced by a visual as well as acoustical considerations.

A guitar soundboard is designed to radiate sound while maintaining structural integrity. The body outline will influence the vibrational mode shapes of the basic plate. The plate shape will also influence the top thickness, the top material and bracing pattern layout. The evolution of the guitar suggests that the body shape was initially defined by physiological and artistic constraints not mechanical-acoustical constraints.

4.1.1 Plate Shape Designs

Six guitar shapes have been used to examine the effects of body shape, boundary conditions and material properties on plate mode shapes. Three of them, the Hauser, Sloane, and Dreadnought patterns, will be used for bracing and radiation studies. The basic shapes are those of Childers[36] with the location and diameter of the sound holes estimated from photographs and general building practices.

---

36) Richard L. Childers, "An Analytical Expression for the Shape of a Guitar". Catgut Acoustical Society News Letter # 41 1984.

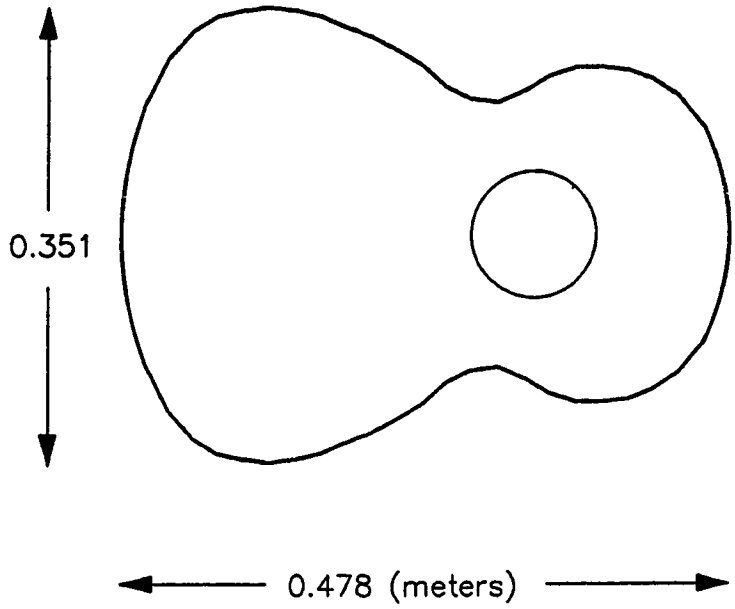

Figure 4.1 Torres Pattern

The Torres pattern is the first of the modern classical guitars in body shape. In its time it was a large body pattern but appears as one of the smaller modern patterns.

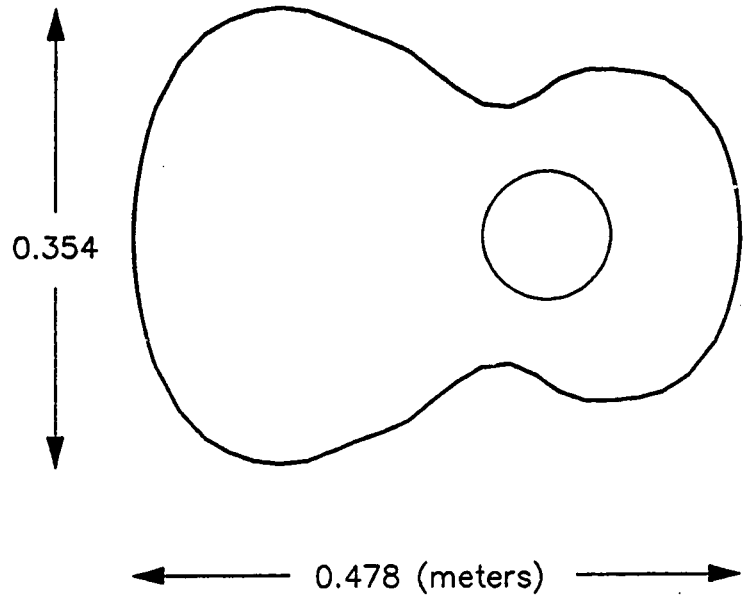

Figure 4.2 Hauser Pattern

The basic Torres pattern is still being produced as evidenced in the Hauser pattern. The Hauser pattern is also similar to the patterns used in the construction of inexpensive parlor guitars produced at the turn of the last century. The Hauser pattern will be used to study the simple transverse bracing patterns of the turn of the century parlor guitars.

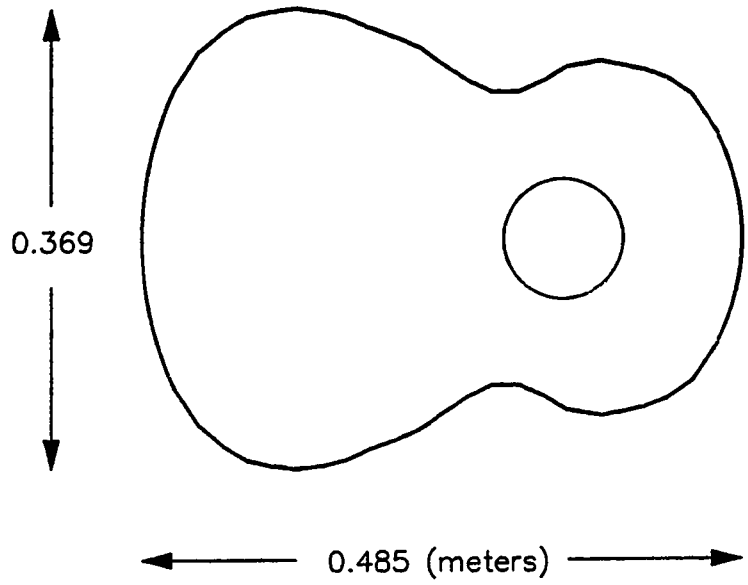

Figure 4.3 Sloane Pattern

A modern variant of the classical guitar is the Sloane pattern. This guitar is well documented due the writing ability of its designer Irving Sloane, however the artistic merits of this design have not been established. The design incorporates a modified Torres fan bracing system. The Sloane guitar will be used to study the fan bracing system.

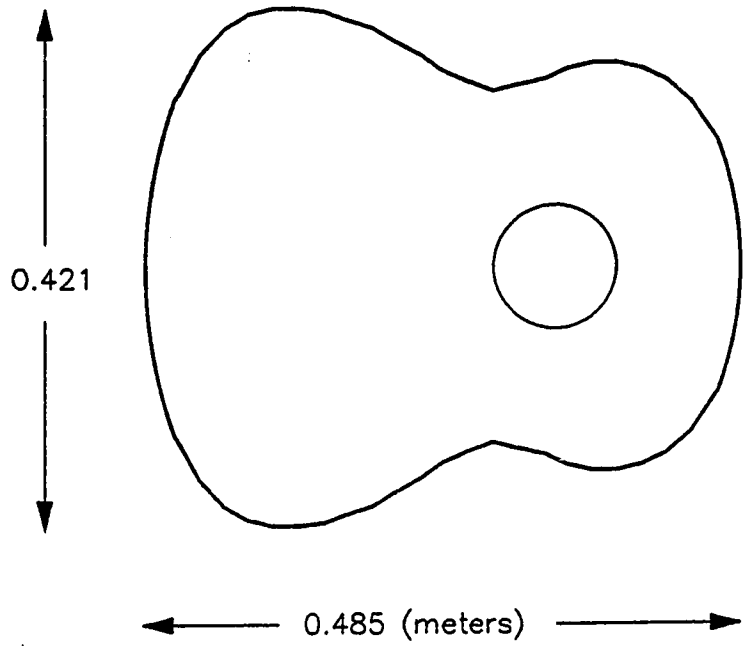

Figure 4.4 Conde Pattern

One of the larger patterns included in this study is the Conde pattern. The instrument is designed as a classical guitar. The body shape is similar to a number of steel string body designs.

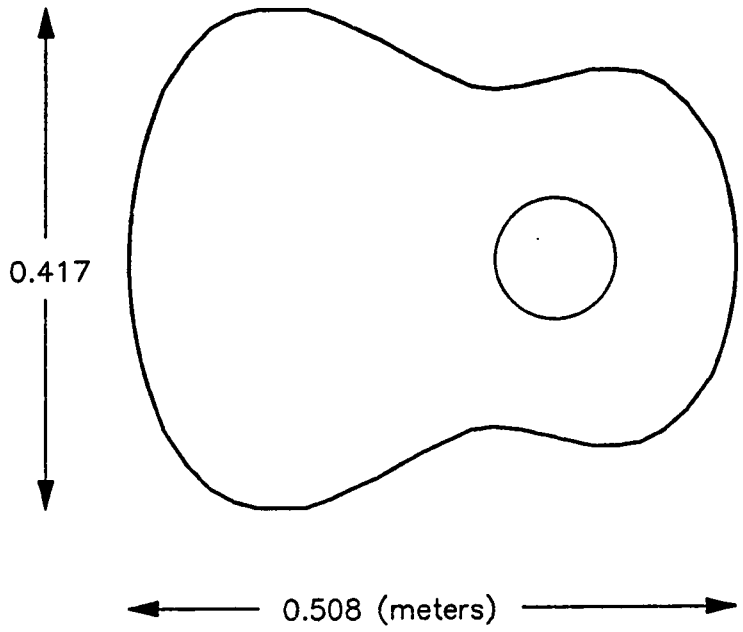

Figure 4.5 Dreadnought Pattern

The best known steel string pattern is the Dreadnought shape. This design and its characteristic X-bracing pattern date back to the period of the first world war, the name Dreadnought being taken from the largest battleships of the time. The X-bracing system will be studied from this pattern.

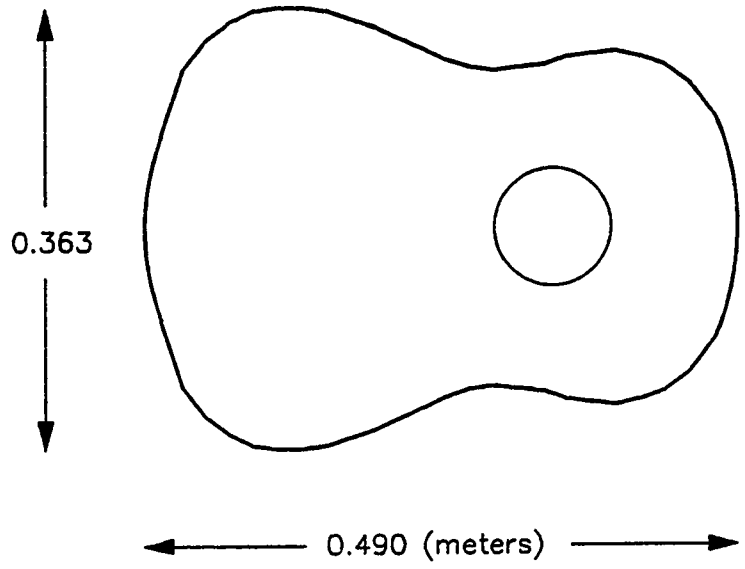

Figure 4.6 Wallo Pattern

The Wallo pattern, another representative steel string design, is a bit smaller than the Dreadnought and reflects the modern trend to slightly smaller guitar patterns. Playing comfort issues can be given a higher priority because acoustic output requirements can be meet with electronic amplification.

There are probably as many guitar patterns as there are guitar builders. Each of the historical guitar builders have modified their plate patterns across their building careers and there is no reason to expect the behavior of modern builders to be any different. The

plate patterns which are examined in this work are typical in shape and dimension from small to large patterns and should give an indication of the basic behavior to be expected for plates which are similar to those analyzed here.

4.1.2 Plate Boundary Conditions

The first study on plate shapes will examine the effects on boundary conditions on the first four mode shapes of the plates. The plates will be modeled with isentropic materials and with three boundary conditions. The first boundary condition will be a clamped condition at the outside edge of the plate. The second boundary condition will be a simply supported condition at the outside edge of the plate. The third boundary condition will be a simply supported condition at the outside edge of the plate with a soundhole cutout.

For an isentropic plate with uniform thickness the natural frequencies may be expressed by;

4.1)

$$f = \lambda_n^2 \left(\frac{h}{2\pi(2L)^2} \sqrt{\frac{D}{\rho}} \right)$$

λ_n^2 = Form factor

$2L$ = Plate Length

h = Plate Thickness

D = Bending Stiffness

ρ = Mass Density

For a given axial plate length, plate material and thickness the quantity in parenthesis is a constant. In the following studies on boundary conditions this quantity has been set to one. The numbers associated with each of the following figures can be interpreted either as frequency or the form factor. The nodal line placements are estimated from the calculation of displacement and phase at 144 points on the plate. In regions where the amplitudes were very small, phase shift "ripples" were observed in the predicted data, these ripples appear to be the result of a truncated assumed mode series and the computional limitations of finite arithmetic.

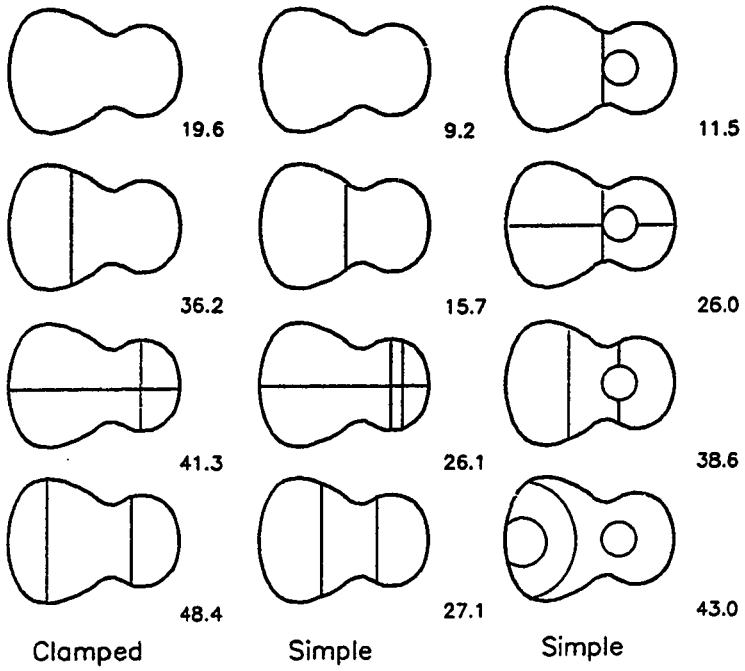

Figure 4.7 Torres Mode Shapes

The Torres pattern is presented as the starting point. The clamped modes have resonances above the simply supported plates as expected. The mode shapes for the clamped and simply supported solid plates are similar in form and progression. The third set of boundary conditions including the soundhole can be interpreted as shifting the modal progression up one mode, the second simply supported mode of the solid plate mapping into the fundamental mode of the plate with the soundhole. The third simply supported mode has a dual

nodal line in the upper bout. This dual nodal line is due to a low amplitude ripple in the predicted mode shape.

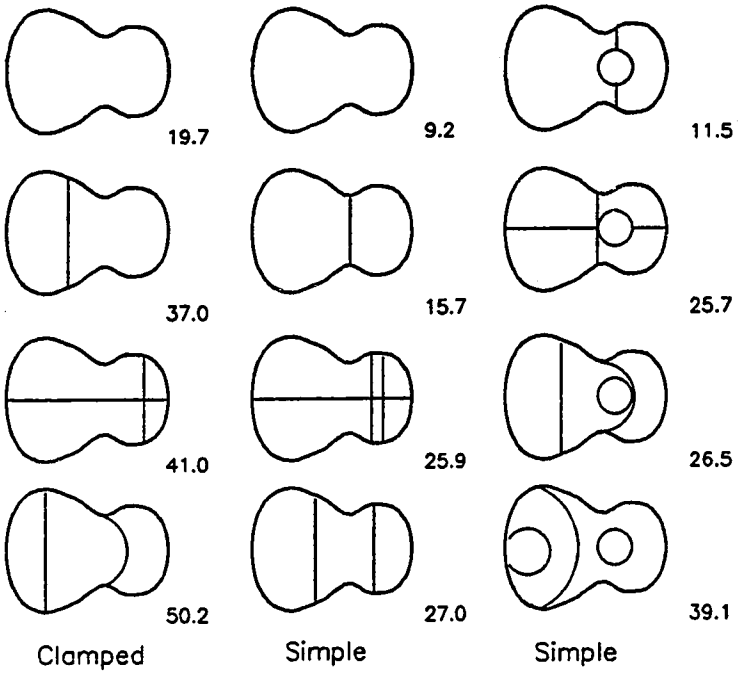

Figure 4.8 Hauser Mode Shapes

The Hauser pattern is very similar to the Torres pattern and the mode shapes are essentially identical in shape and order for the solid plates. When the soundhole is introduced the third mode, which has a nodal line in the waist area, introduces a modal difference between the two patterns. The Hauser and Torres pattern differences lie primarily in the waist

definition. The third simply supported mode has a dual nodal line in the upper bout as seen in the Torres pattern. This dual nodal line is due to a low amplitude ripple in the predicted mode shape.

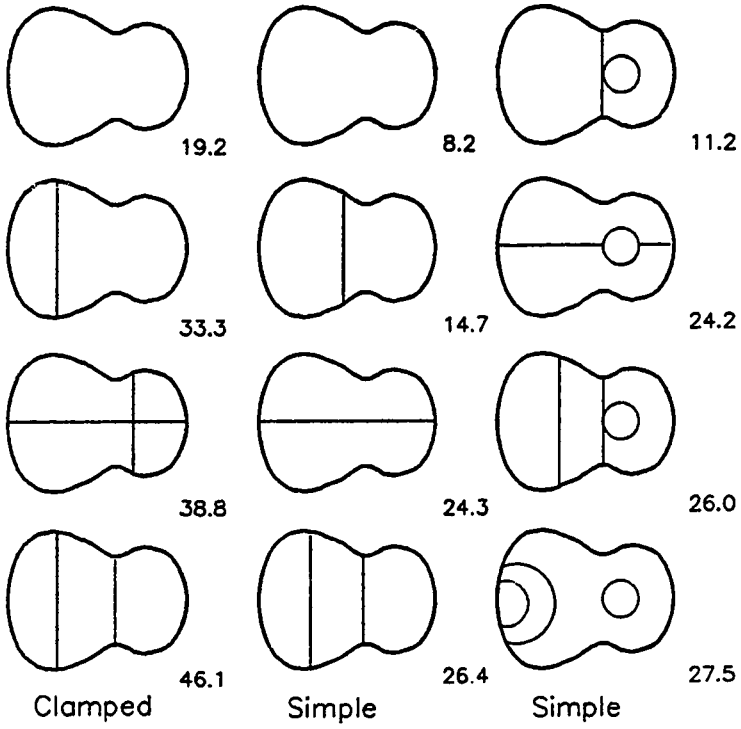

Figure 4.9 Sloane Mode Shapes

The Sloane pattern generates modes in much the same way as its narrower forerunners for the solid plate cases. The soundhole based modes differ primarily in the second mode. The Sloane pattern has a single axial nodal

line whereas the Torres and Hauser patterns have two nodal lines dividing the plate mode into four quadrants from their geometric centers.

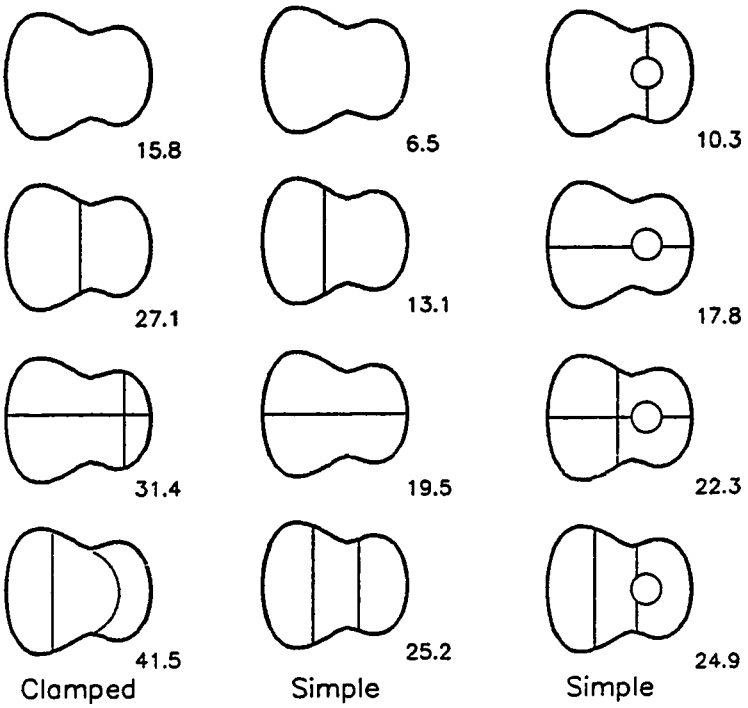

Figure 4.10 Conde Mode Shapes

The Conde pattern shows the same basic modal structure as the Torres pattern for the solid plate cases. The plate with soundhole modes generate an orderly set of mode shapes. The nodal lines run either axially or perpendicular to the plate axis. The curved lower bout nodal lines seen in the previous guitar patterns are not present.

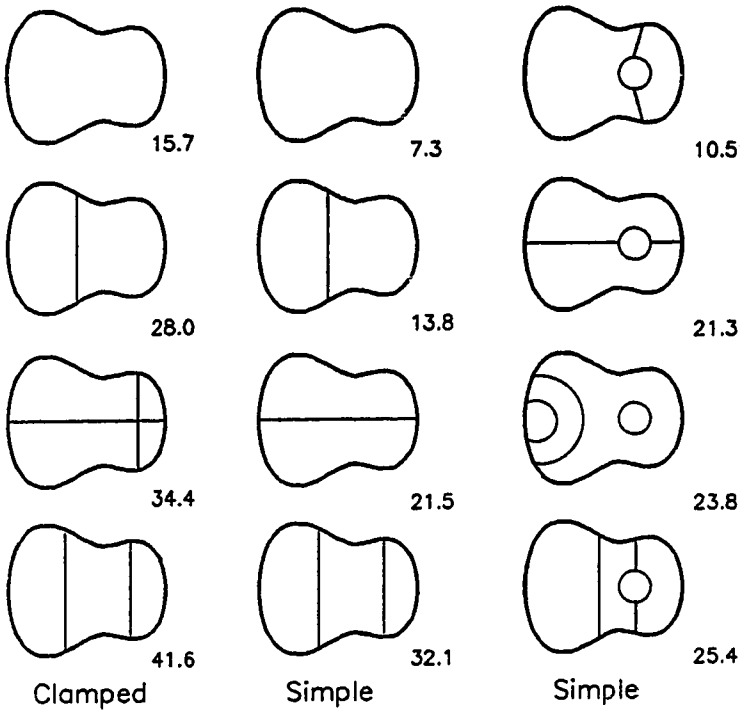

Figure 4.11 Dreadnought Mode Shapes

The solid plate modes for the gentle curves produced by the Dreadnought body shape generate the same basic mode shapes as those found in the more severe curves of the Torres pattern. The soundhole modes are similar to those first encountered in the Sloane design with the third and fourth mode shapes reversed. The frequencies associated with these "interchanged" modes in both the Dreadnought and Sloane patterns are within six percent of one another.

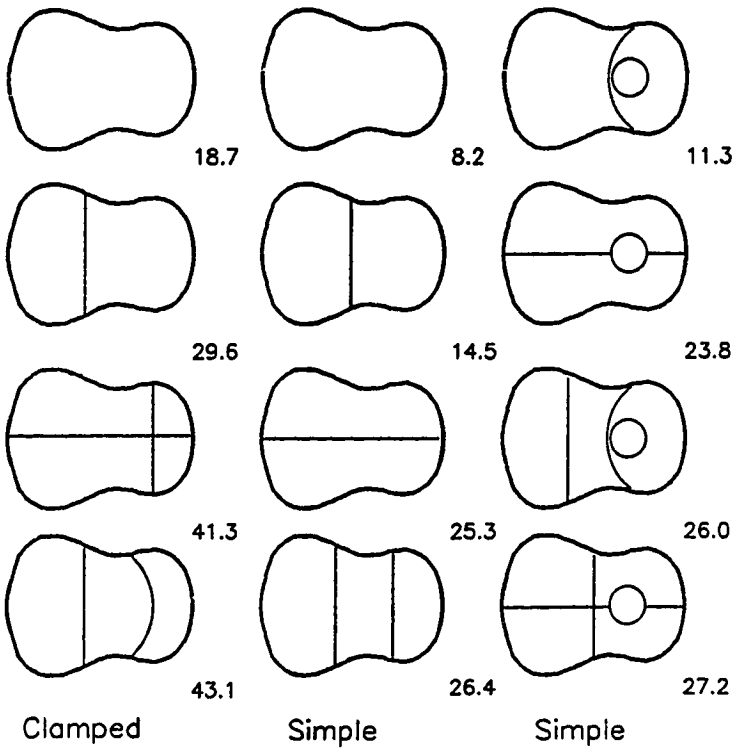

Figure 4.12 Wallo Mode Shapes

The Wallo pattern mode shapes follow the now familiar solid plate mode shape progressions first observed in the Torres pattern. Subtle new differences lie in the soundhole influenced plate. The soundhole modal shapes are seen to curve away form the lower bout. In the narrower Hauser pattern the nodal lines were seen to curve toward the lower bout.

The modes in the isentropic case are deceptively well behaved and drawing sweeping conclusions about the insensitivity of the modal patterns and frequency ratios on body shape should be avoided.

4.1.3 Plate Material Sensitivities

Guitar top plates are not generally made from isentropic materials and therefore guitar shape studies must be made using orthotropic materials. Two common materials used in guitar top construction are spruce and cedar. Spruce and cedar are unfortunately not well defined engineering materials. Wood properties vary from tree to tree and environmental factors as well as the past history of the given sample may influence its effective material properties. In the following calculations generic spruce and cedar materials have been defined for the purpose of comparison. The Spruce I material is 3 times stiffer along-the-grain than the Cedar I material. The across-the-grain modulus for the two materials are approximately equal. The material properties are those of Spruce I and Cedar I as detailed in the appendix.

Three predictions are made using the simply supported edge plate with soundhole boundary conditions. In these predictions the plate thickness is held constant (3 mm) and the plate material changed. A spruce plate, a cedar plate and an aluminum plate prediction is made for the first four modes of vibration. The aluminum plate modes shapes are the same as those generated in the preceding section.

The resonant frequencies for plates of different thickness may be obtained from scaling the resonant frequencies with the plate thickness ratio.

4.2)

$$f_{new} = f_{3mm} \cdot (h_{new}/3)$$

This equation is a direct result of equation 4.1 when the material properties and form factor are held constant. Re-scaling the resonant frequencies for orthotropic materials with different along-the-grain to cross-grain stiffness is not as simple. Mode shape order and resonant frequency relationships are strongly affected by the stiffness ratios as demonstrated below. In the following figures the numbers associated with each mode shape sketch are the calculated natural frequencies in Hertz.

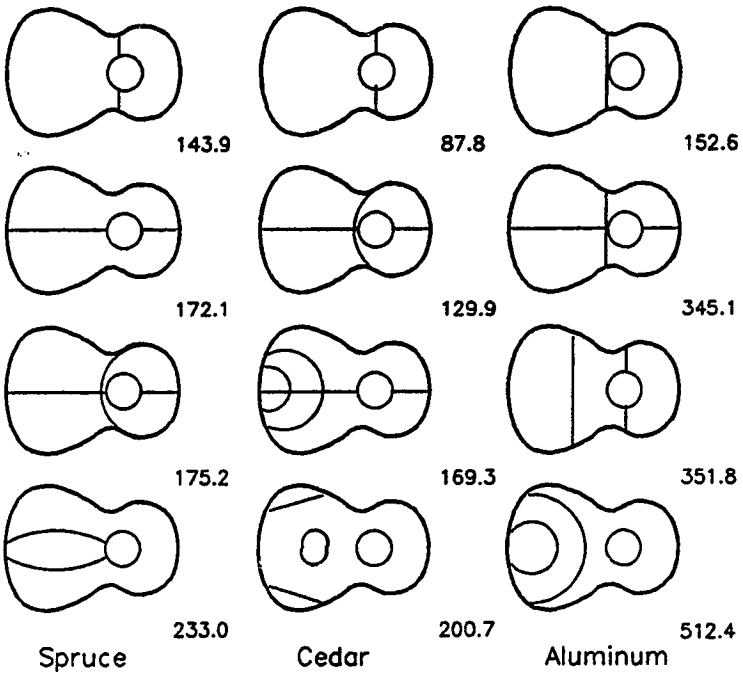

Figure 4.13 Torres Top Mode Shapes

The traditional Torres guitar is specified with a spruce top. Modern builders of the classical guitars often build cedar and spruce guitar tops on the same pattern. Spruce and cedar instruments have distinctly different tone colors. The similarities in the lower bout motion in the first two modes may indicate why the material interchange is possible, whereas the differences in the following two modes may give some insight into the tone color differences between the two materials.

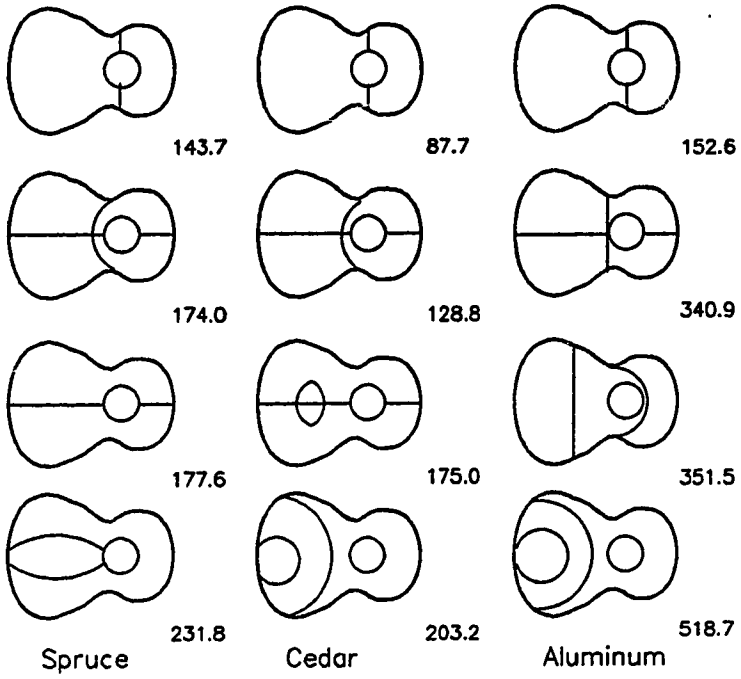

Figure 4.14 Hauser Top Mode Shapes

The Torres and Hauser patterns which appeared to be interchangeable in the isentropic case show their differences in the orthotropic case. The Hauser pattern would appear to be insensitive to the differences between spruce, cedar and aluminum in the first two modes. The third and fourth modes in the spruce and cedar plates appear to have the same basic form although the nodal lines favor an axial nodal alignment in the spruce plate.

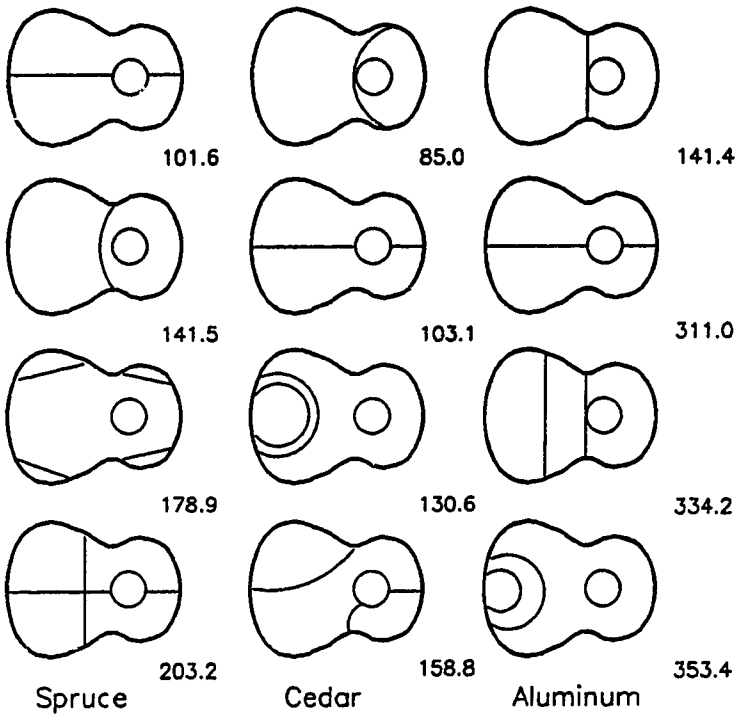

Figure 4.15 Sloane Top Mode Shapes

The Sloane pattern reverses the order of the first two modes shapes between the cedar and spruce cases. This mode order inversion suggests that a bracing pattern design for one material may be inappropriate for the other. The third spruce mode introduces nodal lines running off the boundary of the plate. The fourth cedar mode has an interesting shape appearing to be a modified form of the cross mode seen in the fourth spruce mode. The low amplitude of the mode in the

center of the plate suggest that the unsymmetric model shape may be a result of the modal truncation ripple observed in the Torres pattern.

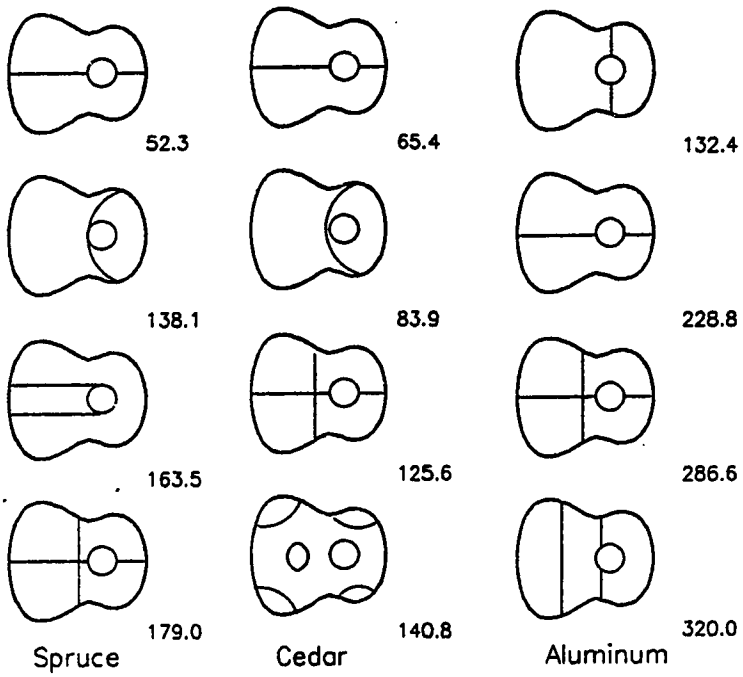

Figure 4.16 Conde Top Mode Shapes

The Conde pattern's mode sequence has the first two modes matching one another in the spruce and cedar tops. Note that these first two orthotropic modes are in reversed order of those predicted for an isentropic plate. The fourth cedar mode has a nodal boundary sur-

rounding the bridge area. In the spruce plate the third mode employs the soundhole as part of the nodal boundary.

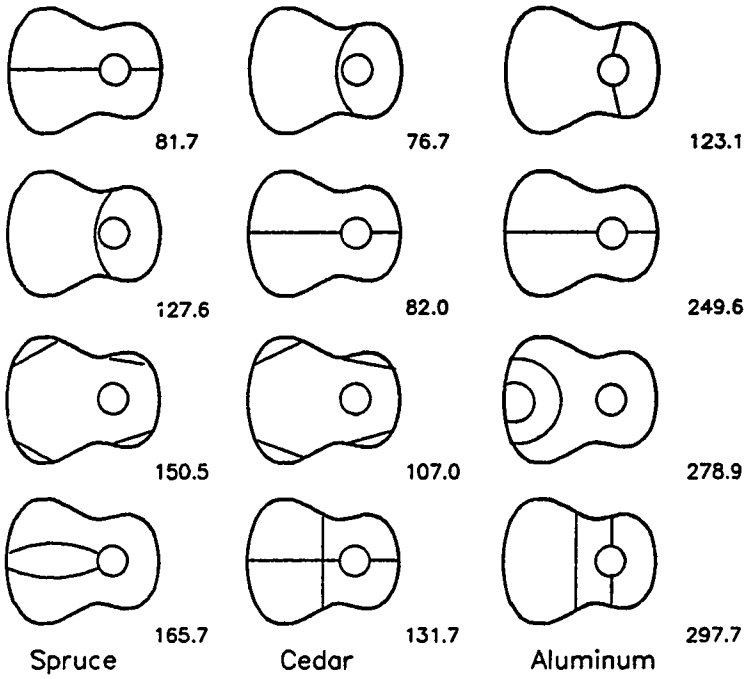

Figure 4.17 Dreadnought Mode Shapes

The Dreadnought pattern, like the Sloane pattern, interchanges the mode shape order between cedar and spruce for the first two modes. The third mode in both the cedar and spruce plates has the double bending nodal lines which run along the boundary which were seen in the Sloane plate.

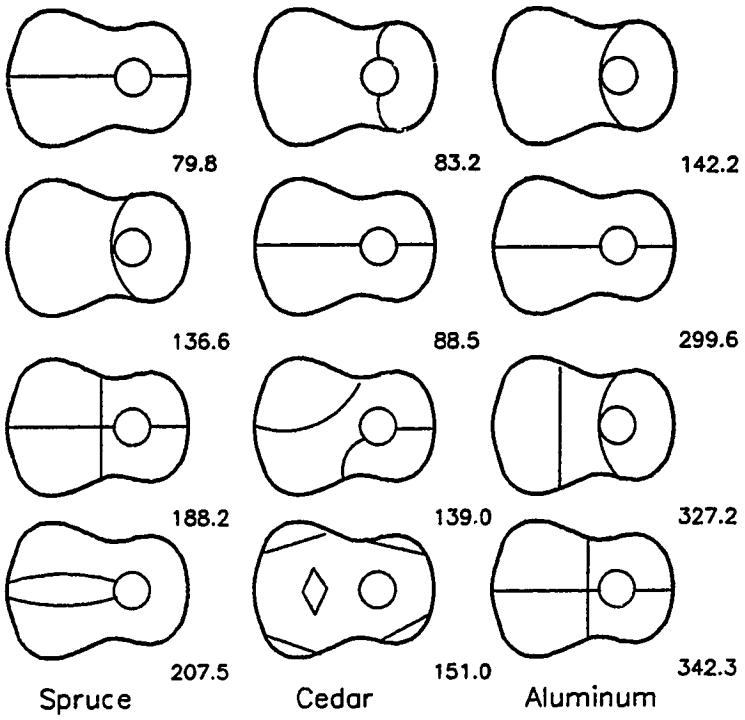

Figure 4.18 Wallo Top Mode Shapes

The Wallo pattern, like the Dreadnought and Sloane patterns, inverts the mode shape order between cedar and spruce plates in the first two modes. This pattern has a modified cross mode pattern in the third cedar mode which was observed in the Sloane pattern.

Each of the guitar patterns has its own set of mode shapes, resonant frequency relationships and sensitivity to material property changes. The plate is only the starting point in guitar construction; the bracing

pattern must also be modeled. The bracing pattern must work with the plate to establish a net volume displacement across the complete playing range. There have been a large number of symmetric plate modes predicted for these patterns and the bracing patterns must reshape these modes into more effective radiators.

4.2 Braced Plates

The guitar soundboard is a braced plate system. The braces serve two purposes the first to react the static string loads the second to improve the radiation characteristics of the instrument. The fundamental frequency of an isolated braced top plate is typically in the 160 to 200 Hertz range. By scanning preceding plate predictions it is evident that a considerable amount of stiffness must be added to the Dreadnought, Wallo, Conde and Sloane patterns to move their fundamental resonant frequencies into the 180 Hertz range. The smaller Torres and Hauser spruce plates could reach the 180 Hertz range by thickening the plates without bracing. The second and third modes of these unbraced guitars would be dipole and quadrapole radiators which are acoustically inefficient. Bracing systems are needed in all guitar shapes to increase their radiation efficiencies.

4.2.1 Simple Transverse Bracing

The simplest bracing patterns found in guitar constructions are transverse braces. Transverse braces run

perpendicular to the grain direction of the wood in the top of the guitar. This form of bracing dates back to medieval lute designs.

The Hauser guitar pattern has been chosen to study the transverse bracing system because it is similar in size and profile to many small bodied guitars sold at the beginning of this century. The modern Hauser guitar does not use this form of bracing pattern and therefore this discussion does not pertain to the Hauser guitar. The bridge and neck of the instrument are treated as part of the bracing system. The stock braces in the following designs are 6 mm wide by 18 mm in height with semielliptical cross sections. The fingerboard of the neck which is glued to the soundboard has a rectangular cross section 4 mm in height and 57 mm in width. The bridge geometry is more involved as shown below;

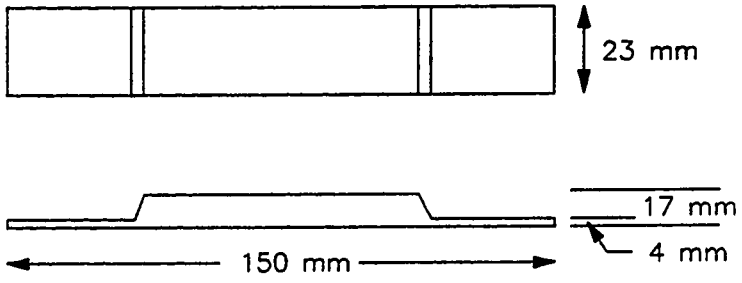

Figure 4.19 Hauser Bridge Geometry

The bridge and neck may be considered to be a bracing system built on the exposed side of the soundboard.

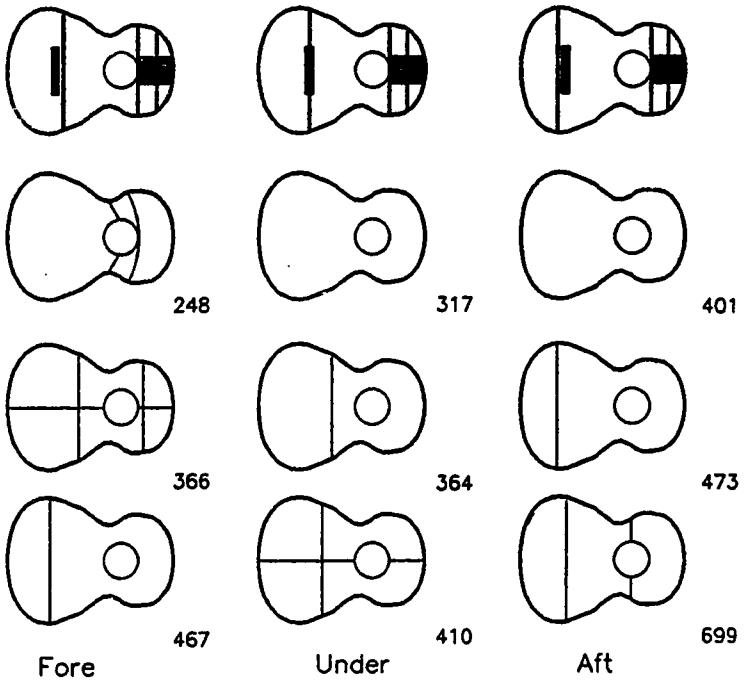

Figure 4.20 Simple Transverse Bracing

The current discussion is limited to the transverse bracing pattern in its three dominant forms. The dominant forms are named after the placement of the transverse brace in the lower bout. The lower bout transverse brace may be forward of the bridge, under the bridge or aft of the bridge. The fundamental frequencies of the plates range from 248 to 401 Hertz, the aft brace providing the highest frequency. These fundamental frequencies are higher than the target system resonance of the assembled guitar at 200 Hertz. By

tailoring the lower bout brace height one can retune the plates to the same fundamental frequency and reexamine their mode shapes and resonant frequency series. The goal for the braced plate fundamental frequency was selected to be 180 Hertz.

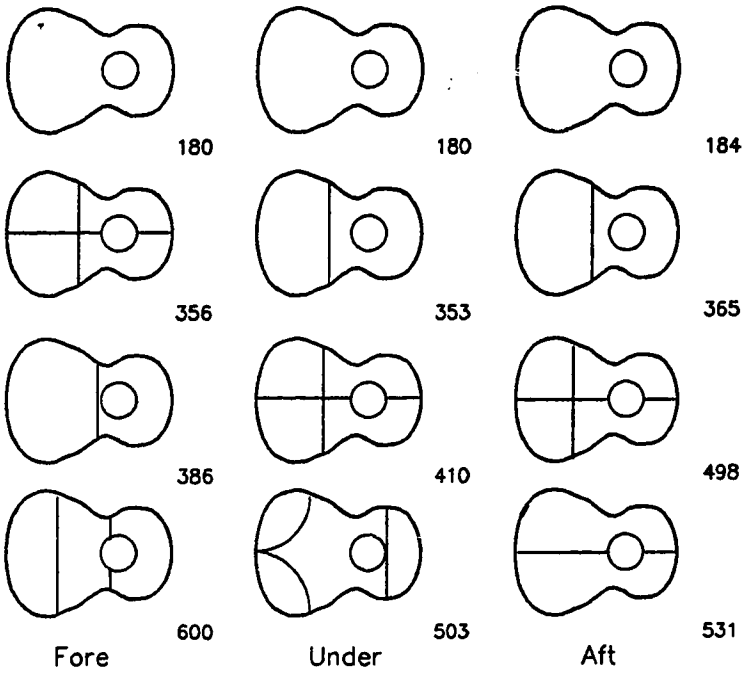

Figure 4.21 Tuned Transverse Bracing

In order to tune the top plate, the brace forward of the bridge was trimmed from 18 mm to 11 mm, the brace under the bridge was trimmed to 9.5 mm, and the brace aft of the bridge was trimmed to 8mm. The target plate fundamental resonance of approximately 180 Hertz was

obtained in each case. The modal series differ in both mode shape progression and resonant frequency for each bracing configuration.

The modal differences need to be mapped into the acoustic domain to estimate what these differences may mean in terms of tone and projection. The acoustic power response calculation is used to generate this type of information. The guitar plates are driven with a .1 newton force at the position of the A string on the bridge. The A string drive point is somewhat arbitrary, and for the time being will be used because it is the middle position between the extreme E strings and the interior D and G strings yielding a mean drive point for rocking modes of the plate about its center line. The arbitrariness is due to the fact that the preceding logic indicates the B string is an equally desirable drive point location.

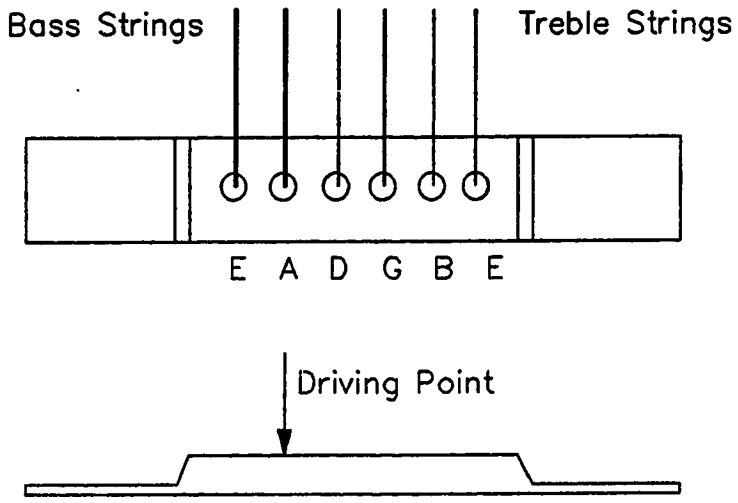

Figure 4.22 Drive Point Location

A study of the acoustic power response translates the observed modal differences into the acoustic domain. The three tuned transverse guitar plates are coupled with a backing cavity volume of 10 liters and driven at the A string location. The 10 liter backing volume is typical of the small body guitars being studied.

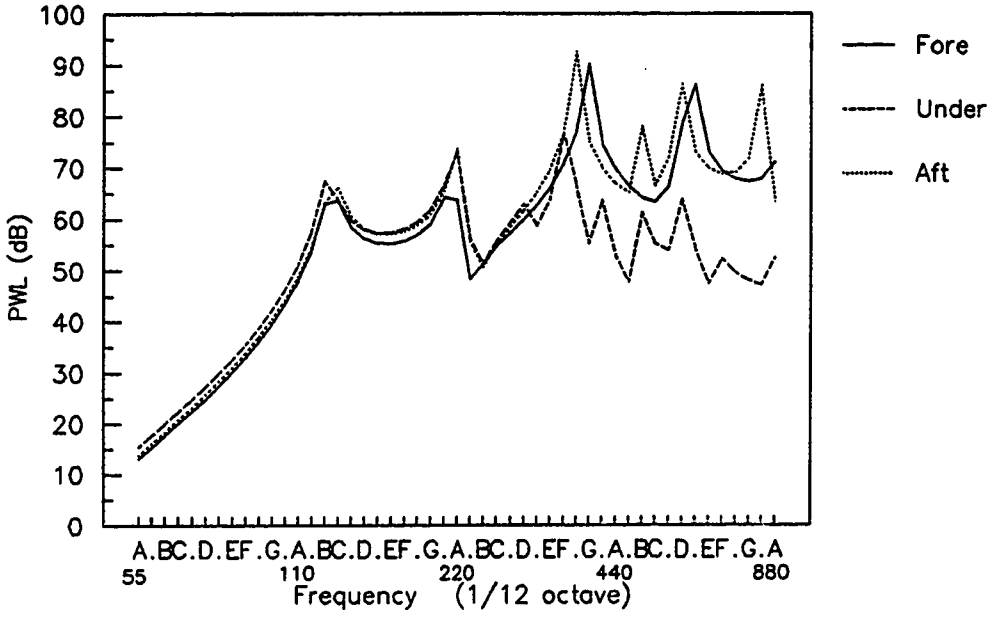

Figure 4.23 Tuned Transverse Bracing Acoustic Power Spectra

The acoustic power responses for the three tuned bracing systems differ primarily in the upper frequency response. The first resonance is due to the interaction of the backing cavity, the slug of air in the soundhole and top plate. This mode is commonly referred to as the air mode in violin research. In all three cases this mode fell near 123 Hertz. The top plates were tuned to the same frequency (180 Hz) and when coupled with a cavity of 10 liters were retuned to approximately 220 Hertz. The second resonance peaks do

differ in both level and frequency. The large differences between the bracing patterns appear above these first two resonances. The forward and aft bracing patterns follow a similar pattern with a substantial output in the high frequency range whereas the under the bridge brace drops off rapidly. The spectra of the forward and aft bracing systems have resonances at 392 and 370 Hertz respectfully. At higher frequencies the forward and aft bracing systems demonstrate resonances near 587 and 622 Hertz. Minor resonances lying on either side of these features also differentiate the two bracing patterns.

The prediction capability can estimate spectra features which would make instruments distinguishable from one another, however it may not be possible to select the preferred guitar from these spectra. The suggested quality criteria of Chapter 1 stated that resonances near 100, 200 and 400 Hertz were desirable. In these three spectra the behavior at the third resonance is different between the under the bridge design and the forward and aft designs leading to the possibility of a figure of merit for the designs.

4.2.2 Modern Dreadnought Guitars

The modern dreadnought guitar, strung with steel strings, has spawned a large number of bracing patterns. In this section three of these bracing systems will be examined. The models will all use the same body shape. Holding the body shape constant requires interpretation of the modeled bracing systems to fit

the chosen body shape. The three bracing patterns are based on the Gibson low-X system, the Manzer A-brace system, and the Martin slant-brace system.

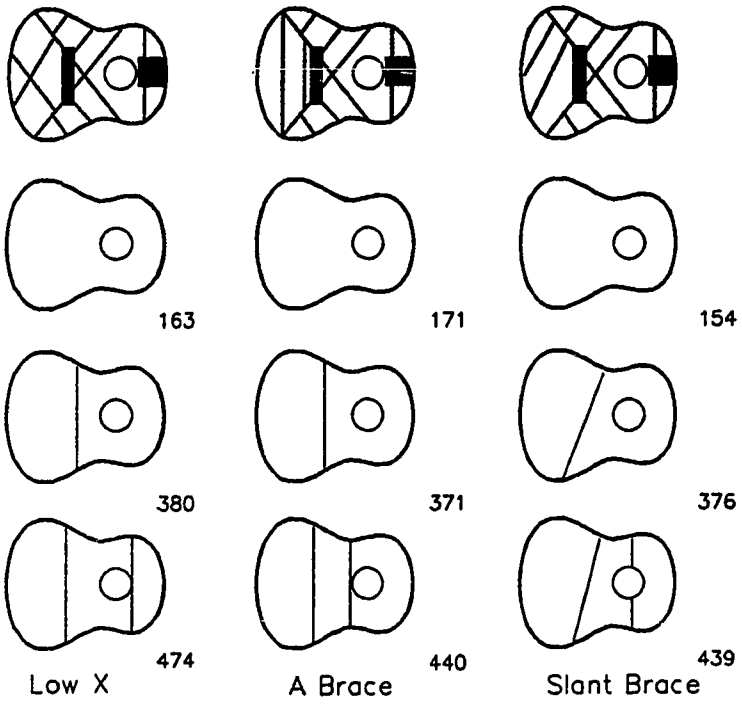

Figure 4.24 Dreadnought Bracing Patterns and Mode Shapes

In these models the main X-brace, the neck transverse brace, and small finger braces running from the X-brace to the sides of the top are constant. Shown in solid black are the bridge and the neck fingerboard overlay also held constant in this study. The lower bout secondary braces differ in each case. The stock width and

height of the lower secondary braces have been kept in proportion with the source bracing pattern drawings. In each case the unbraced plate resonance has been raised approximately an octave above the fundamental plate resonance of 81.7 Hertz.

The radiated power response for each top driven at the A string with a .1 newton force is generated to assess the differences between the designs. In each case a typical Dreadnought box volume of 16 liters was used. The single value of the box volume tends to aline the performance of the instruments in the lower frequency range.

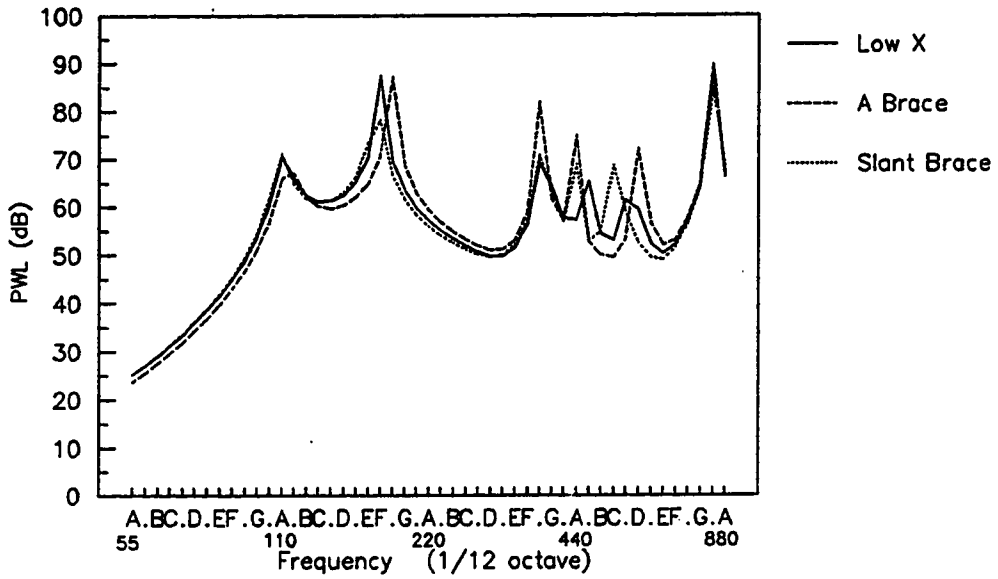

Figure 4.25 Dreadnought Bracing Patterns Acoustic Power Spectra

The first three peaks in the radiated power spectra in the X-braced instruments fall on top of one another with slight variances in maximum levels. The area where the spectra differ is above 400 Hertz and below 800 Hertz. All three bracing systems demonstrated strong activity just below A-880. The single strong peak observed in the 400 Hertz region in the transverse bracing designs is replaced by a family of evenly spaced peaks in these X-braced designs.

The asymmetric design of the slant bracing system raises a question on how sensitive is the acoustic power response to changes in the drive point location. To test the sensitivity to the location a number of predictions were made on a Dreadnought soundboard model. The drive point was moved to each of the six string locations on the bridge and sound power spectra computed.

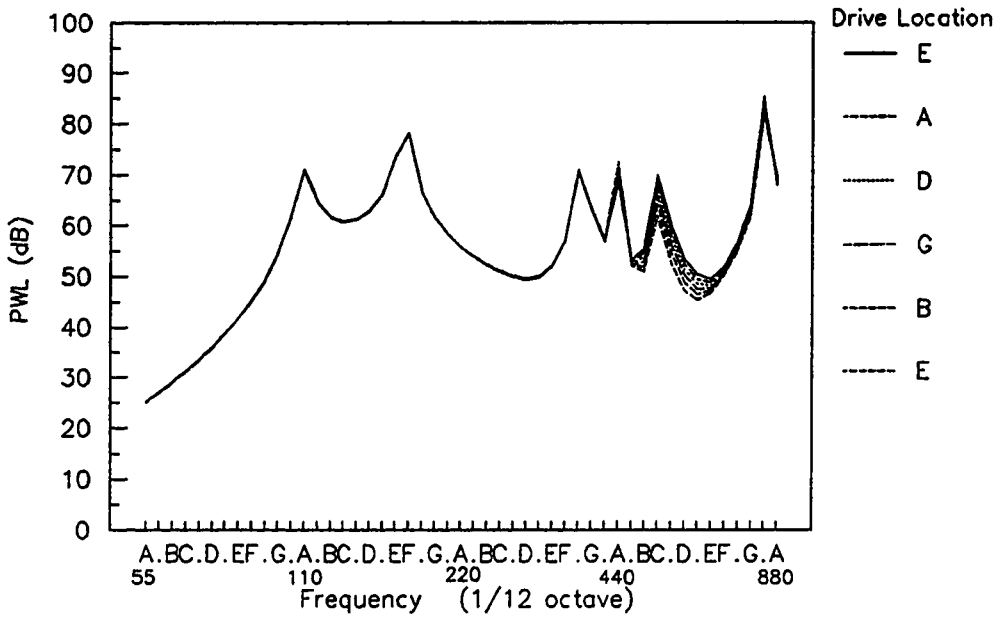

Figure 4.26 Dreadnought Slant Brace
Drive Point Sensitivity

The variation of the location of the drive point generates difference on the order of 6 dB near the fifth resonance peak. At low frequencies, in the Dreadnought design, the bridge is very stiff and drives the top in a uniform manner. At higher frequencies where rocking modes of the top come into play the drive point is important to the excitation of these rocking modes. At very high frequencies, generally beyond this modeling range, bridge bending modes will come into play and these are expected to be sensitive to changes in drive point location.

In the lumped element models discussed earlier the first two resonances were tightly coupled by the backing volume. To explore that coupling in the current model the A braced top was modeled with three backing cavities. The model volumes correspond approximately to a guitar with thin 5 cm (2 inch), normal 10 cm (4 inch), and thick 15 cm (6 inch) sides.

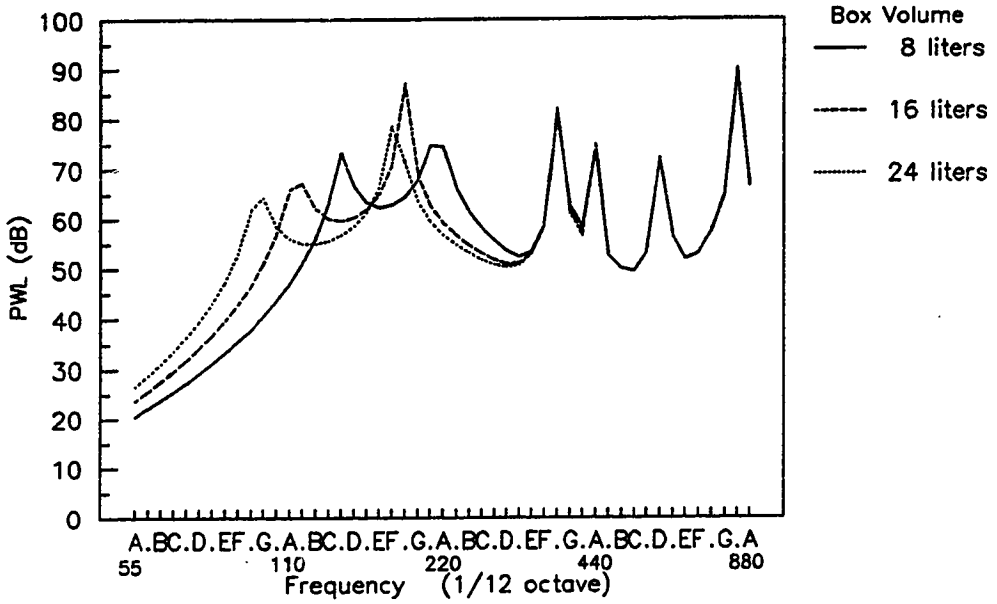

Figure 4.27 Dreadnought Backing Volume Sensitivity

There is a strong influence on the first two modes of the system with little alteration of the high frequency behavior. The air mode has dropped with increasing box volume from 139, to 114, to 98 Hertz. The main plate mode followed in kind from 215, to 185, to 175 Hertz. The eigenvalue solution for the plate in vacuo was 171 Hertz indicating increase of the box volume will not lower the plate resonance much more. The 16 liter box design is normal for a dreadnought guitar leading to 114, 185 Hertz resonances near the typical figures of 100, 200 Hertz.

4.2.3 Sloane Classical Guitar

The classical fan brace patterns will be represented by the Sloane design. This particular design is well documented in the widely circulated book by Irving Sloane on classical guitar construction[37]. The bracing pattern is a modified Torres seven ray fan.

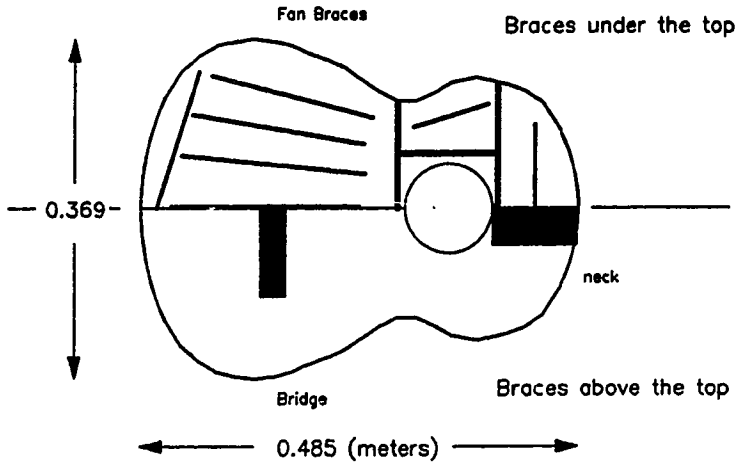

Figure 4.28 Sloane Classical Fan Bracing

The Sloane classical guitar has a backing cavity of 13 liters and produces a few well spaced peaks in the acoustic power response.

---

37) Irving Sloane, Classical Guitar Construction. New York: E. P. Dutton & Co. 1966.

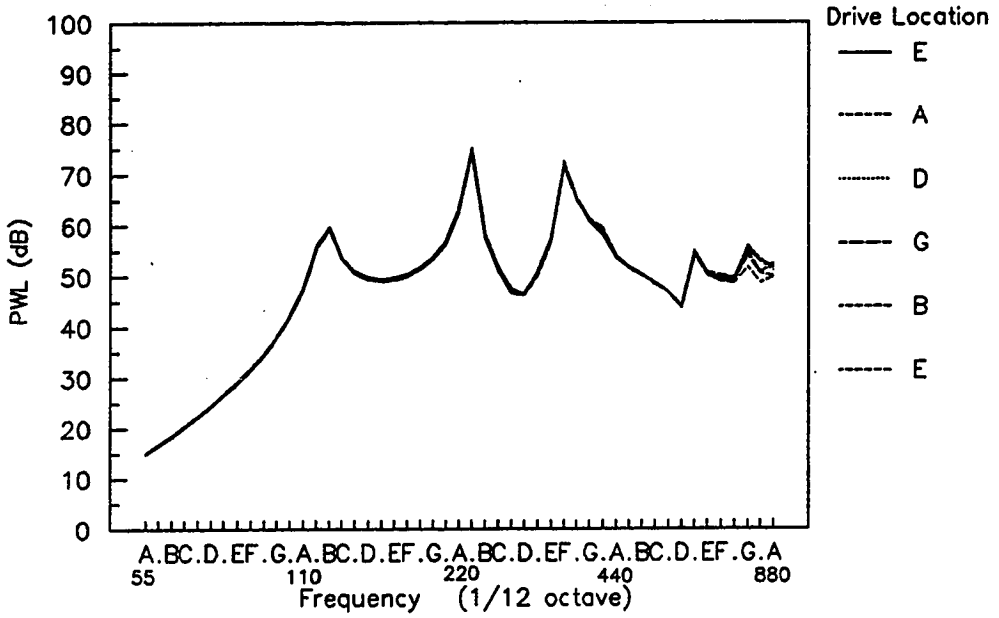

Figure 4.29 Sloane Classical Brace Drive Point Sensitivity

The guitar is insensitive to the location of the driving position through most of the modeled frequency range. At the highest frequencies modeled difference of a few dB can be seen. The placement of the spectral peaks indicate a good classical guitar according to work done by Meyer on classical guitar tone quality[38].

---

38) Jurgen Meyer, "Quality Aspects of Guitar Tone", in Function, Construction and Quality of the Guitar, edited by Erik V. Jansson, Stockholm, The Royal Swedish Academy of Music 1983.

In particular Meyer found that a strong spectral peak in the 400 Hz region was the dominating feature correlating quality in his study.

Classical guitars are often built using cedar instead of spruce as a top material with the same bracing pattern. The next exercise models the same guitar bracing system and backing cavity for five woods. Material properties for the woods are presented in the appendix.

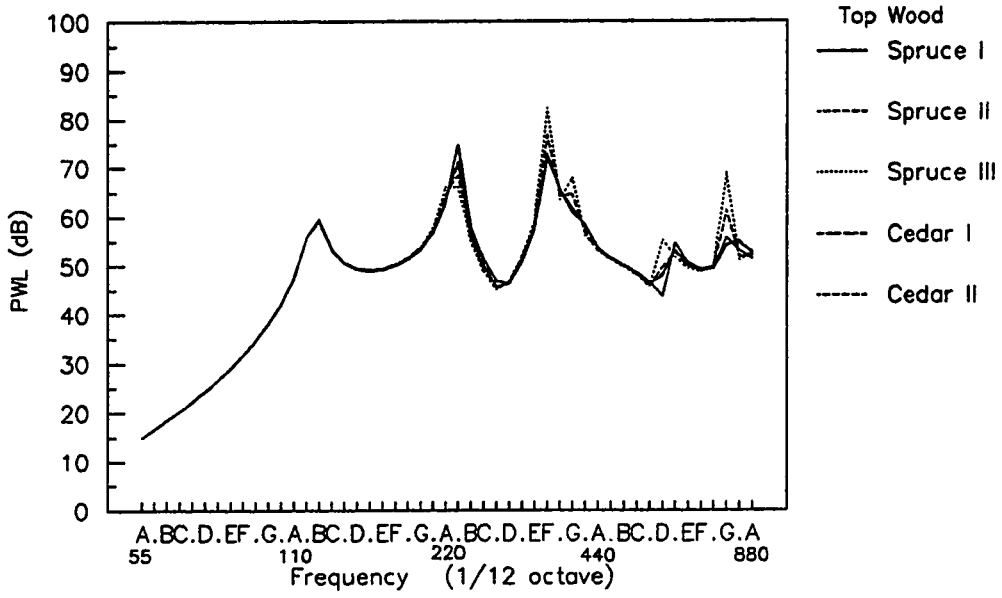

Figure 4.30 Effect of Top Wood on a Classical Guitar

The most striking feature of this study on the effects of the top wood is the general insensitivity of the acoustic response to the top wood. The peak levels of

the dominant peaks vary but the frequencies do not wander. The bracing pattern is clearly dominating the motion of the plate.

The age old concern over the application of finishes becomes a moot point after examining the above results. In the study of finishes, modeled with unconstrained layer damper theory and data on violin varnishes, the changes in the radiated spectra are imperceptible in this format. Small changes on the order of 0.1 dB are calculated. The added mass of the plate, roughly 10% in a well finished spruce plate, is not sufficient to alter the frequencies of the braced top plate. The damping factors are increased but not sufficiently to greatly alter the resonance Q's viewed with 1/12 octave filters.

4.3 Estimation of Modeling Uncertainty

The largest uncertainties in the modeling process is in the determination of material properties. The three samples of spruce taken from the literature and used in this project have densities that vary by 6.5 percent. The axial moduli vary by almost a factor of two. Given that the top plate and its braces are made of "spruce" with no further information any frequency estimate has an uncertainty of 33 percent, if the current data base covers the range of typical values. The lack of knowledge of the material constants associated with the design fundamentally limits the ability to predict within an arbitrarily set tolerance.

Secondary questions on material constants will remain unworked but should be brought up lest we forget them. What is the variation of material properties in a given log, or across the growth rings and are these variations important? Should humidity and age factors be introduced? The bond lines of the glues used to assemble the instrument have been ignored; do they need to be accounted for in terms of stiffness and damping? The only answer to these questions at this time is in the testing of wood samples from the instrument which is to be modeled.

Another source of uncertainty is in the selection of boundary conditions in the modeling process, both the mechanical boundary conditions of the edge of the plate and the acoustical space into which the sound radiates. The mechanical boundary conditions at the edge of the plate have been modeled as either clamped or simply supported. Guided by the earlier work of others the simply supported boundary condition has been used to model the guitar plates. The simply supported plate gives a lower bound on the frequency range, the clamped plate an upper limit. The sides of the guitar presents a boundary condition to the plate which is neither of these extremes.

The acoustic boundary is a mathematical abstraction of the top plate radiating into a semi-infinite space. The forward radiation from this model is an indication of what a guitar plate may radiate but it neglects radiation from the back of the instrument and the possible interactions between those two sources. The

internal acoustics have been reduced to a simple stiffness. In the frequency range of interest there can be internal acoustic modes in the cavity of the guitar but these have been neglected. It has been assumed that these modes neither radiate efficiently through the sound hole nor have strong interactions with the plate which would substantially alter the plate behavior from what has been predicted.

The ideal confirmation of this model is not in the study of actual guitars but in a laboratory where a very carefully constructed guitar top would be placed in a very large hemi-anchoic chamber and driven with a "massless" shaker mounted on the bridge of the guitar top. Acoustic sound power measurements would be made in the field above the guitar top plane.

This description of an ideal confirmation test configuration would close the loop on a study of a model. This model is not designed to be an end point but a process and the process is intended to provide insight into the design of guitar sound boards. This model with all its uncertainty and limitations is ready to aid in that process and prepared to address the behavior of guitars as they are built and played.

5 Model Confirmation Experiments

A series of model confirmation experiments have been conducted to evaluate the analytic model's ability to predict the performance of guitar top configurations. Realizable experimental hardware cannot completely reproduce the constraints embodied in the ideal analytical model. Differences between the model and experimental results maybe related to either inappropriate modeling assumptions, material property constants, or to the limitations of the experimental hardware and measurement techniques.

Certain elements of the analytic model are based on assumptions which may be updated using experimental data. The soundhole model element is updated using experimental results. The goal of these confirmation studies is to evaluate and, if possible, improve the ability of the analytical model to estimate the experimental trends.

5.1 Port and Cavity Model

The port and cavity models used in the prediction method are based on the low frequency asymptotic behavior of air in a confined volume. The cavity is modeled as a volume of air bounded by a rigid structure with a constant acoustic pressure. The possibility of acoustic modes in the cavity is ignored in the model. The acoustic modes in the guitar box have been experimentally determined and suggest that the simple cavity model is appropriate below 300 Hertz. The port has been modeled as a mass slug of air, the equivalent

mass of which has been initially selected based on textbook Helmholtz resonator analysis[39]. A revised equivalent mass is established for guitar type Helmholtz resonators in an effort to refine the analytical model.

5.1.1 Helmholtz Resonator Studies

The cavity backing the soundboard has been modeled as a simple stiffness element. The examination of the low frequency cavity and port system behavior is based on a simple Helmholtz resonator model.

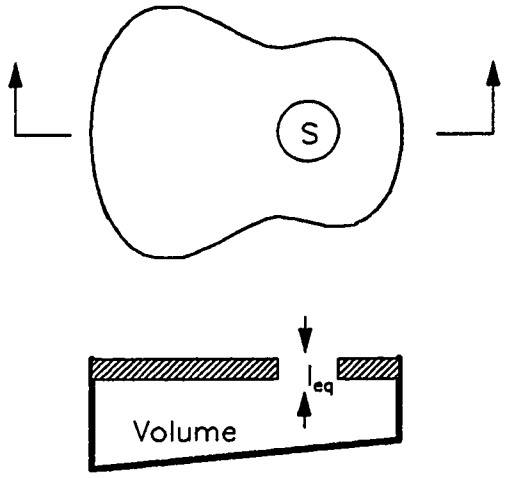

Figure 5.1 Helmholtz Resonator

39) Leo L. Beranek. Acoustics. New York: McGraw-Hill: 1954.

The resonant frequency of the Helmholtz resonator is a function of the cavity volume and the port geometry. If the walls of the cavity are rigid, the stiffness of the system is inversely related to the cavity volume. The mass of the system is determined by the plate thickness, the soundhole radius and the port termination conditions. The natural frequency of the Helmholtz Resonator is;

5.1)

$$f_H = \frac{1}{2\pi}\sqrt{\frac{(\rho c^2/V)S^2}{\rho l_{eq} S}} = \frac{c}{2\pi}\sqrt{\frac{S}{V l_{eq}}}$$

V = Cavity Volume

S = Soundhole Area $= \pi a^2$

a = Soundhole Radius

l_{eq} = Equivalent Neck Length

The Helmholtz resonator equation is valid for rigid walled cavities. In guitar structures additional compliance is added to the system due to the motion of the plates of the instrument. This compliance can be accounted for by assigning an equivalent volume to the system.

The effect of the added compliance on the experimental results can be monitored by measuring the second system resonance. The guitar has a "main wood" resonance above the "air" resonance. The "air" resonance is the focal point of this section. The wood resonance was measured in each configuration and moved from 245 to

240 Hertz over the range of the experiment. The coupling between these modes has been neglected in the determination of the end correction factor.

The mass of the system is a function of the soundhole radius and the equivalent length of the neck of the resonator. The equivalent length of the neck includes a correction factor which is a function of the neck termination. A correction factor for the guitar can be established by varying the geometric length of the neck and measuring the change in Helmholtz frequency. For ports mounted in an infinite baffle the classical correction factor for the neck length is a constant multiplied by the soundhole radius;

5.2)

$$l_{eq} = l + \left(\frac{8a}{3\pi}\right)_{external} + \left(\frac{8a}{3\pi}\right)_{internal}$$

$$l_{eq} = l + \frac{16}{3\pi}a = l + 1.7a$$

The general form of this equation is;

$$l_{eq} = l + \beta a$$

l = Neck Length

a = Soundhole Radius

β = End Correction Factor

Cardboard tubes were placed in the soundhole of a Dreadnought guitar increasing the neck length of the Helmholtz resonator. The tubes were mounted in two configurations, in the first the tubes were internal to the body of the guitar and in the second the tubes were above the plane of the soundboard. The body depth of the guitar under the soundhole was 110 mm.

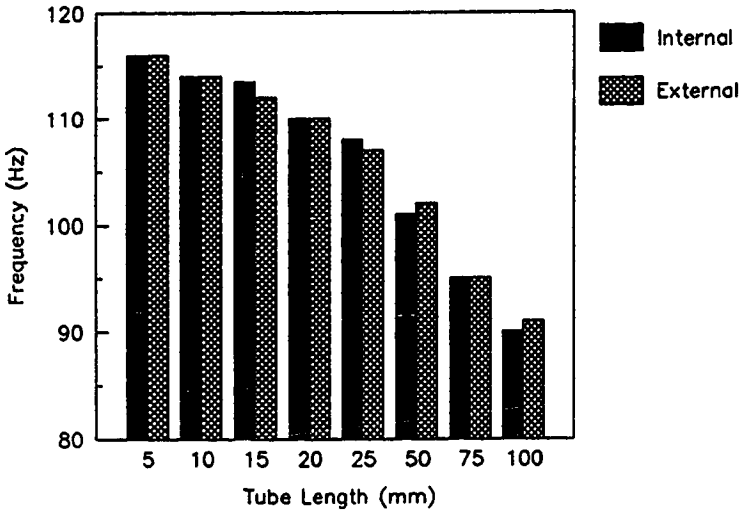

Figure 5.2 Dreadnought Helmholtz Tube Length Study

It is interesting to note that the measured frequencies in these experiments show little difference between the internal and external tube configurations. The termination impedance on either end of the tube is expected to be different. The external termination is into a large room and the internal termination is into a small

box with a surface in close proximity to the end of the tube. The combined effect however appears to remain constant.

If two Helmholtz resonators are identical except for the tube length, then the two resonance frequency equations can be solved for the end correction factor. The end correction factor is expressible as a simple function of the frequencies and tube lengths of the two configurations.

5.3)

$$\beta = \frac{l_1}{a} \frac{(f_1/f_2)^2-(l_2/l_1)}{1-(f_1/f_2)^2}$$

$f_n = n^{th}$ Helmholtz Frequency

$l_n = n^{th}$ Tube Length

From the data collected from a Dreadnought guitar using eight tube lengths in both the internal and external configurations an average end correction factor has been computed.

5.4)

$$l_{eq} = l+\beta a = l+2.7a$$

The measured end correction of 2.7 is larger than the computed classical Helmholtz end correction factor of 1.7. Two additional measurements were made using a

full soundboard size foam-core-board baffle at the end of a 10 mm and 25 mm tubes. The average equivalent length correction factor for these cases was 1.46.

The use of an internal tube is a practical method for adjusting the Helmholtz resonance of a guitars. The use of thick plates or the use of external baffled tubes is not a practical way to adjust this resonance. The larger correction factor of 2.7 will be used because it matches the basic data (without tubes) and can be used to predict the performance of tubes placed in the guitar to retune the Helmholtz resonance.

Equipped with an equivalent tube length and soundhole diameter the equivalent backing cavity volume can be computed. The equivalent backing volume of the guitar used in this study is computed to be 12.4 liters. The volume of the guitar based on its external dimensions is 16.5 liters, after a correction is made for the thickness of the plates and the presence of the braces, heal and neck blocks a net interior volume of 13.0 liters estimated for the test instrument. The equivalent wall compliance which appears as an additional volume is negligible as initially assumed. The final variable which can be adjusted in the Helmholtz resonator is the diameter of the soundhole.

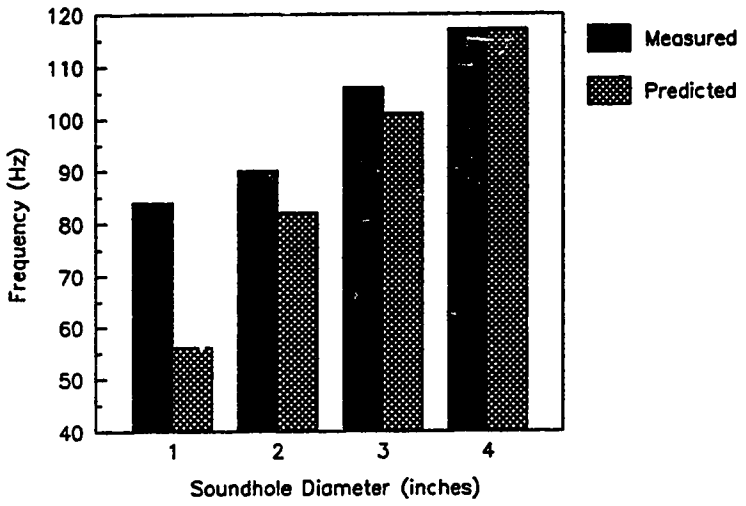

Figure 5.3 Dreadnought Helmholtz Port Area Study

Knowing the soundhole diameter, the effective backing cavity volume, the tube length and the tube length correction factor the natural frequency of the resonator can be computed. A number of soundhole areas were tested and predicted using the Helmholtz resonator model with the updated end correction factor. As the soundhole diameter was reduced the prediction error was increased. A likely source for this error is the algebraic form assumed for the end correction factor. The functional relationship between soundhole radius and tube length is probably an over simplification. In the narrow range of typical soundhole diameters encountered in guitar designs the model is considered adequate (3 3/4 to 4 1/8 inches).

Soundhole diameters have very little variation from small body to dreadnought guitars. The design of bass reflex speaker ports may shed some light on the stability of this dimension. The port radius which will reduce the port losses to a practical minimum in a bass reflex system is a function of the net volume displacement of the system. Gander[40] provides a dimensional equation for this minimum radius of the port in a recent article.

5.5)

$$a_{min} = \frac{10.15\sqrt{V_d}}{(f_H)^{1/4}}$$

a = Sound Hole or Port Radius (*meters*)

V_d = Volume Displacement $(meters)^3$

f_H = Helmholtz Frequency of Air Resonance (Hz)

Based on the typical sound power levels predicted at the fundamental "air" resonance of guitars a 0.1 meter (4 inch) diameter sound hole is estimated to be the practical optimum. This corresponds to the empirically derived dimension found in guitar designs.

---

40) Mark R. Gander, "Dynamic Linearity and Power Compression in Moving-Coil Loudspeakers", J. Audio Eng. Soc. 34(9) 1986.

5.1.2 Cavity Resonance Studies

The cavity backing the soundboard has been modeled as a gas spring. In order that the gas spring have an equal pressure across the volume, the dimensions of the volume must be much smaller than an acoustic wave length. The backing cavity of the guitar is large enough to have standing wave resonances in the frequency range of interest, 55-880 Hz. If a rectangular space, with dimensions similar to those of a guitar box, is used as a simple model the expected frequencies and mode shapes can be estimated[41].

5.6)

$$f_{x,y,z} = \frac{c}{2}\sqrt{\left(\frac{n_x}{l_x}\right)^2 + \left(\frac{n_y}{l_y}\right)^2 + \left(\frac{n_z}{l_z}\right)^2}$$

n_x, n_y, n_z = Integers

l_x, l_y, l_z = Box Dimensions

Let a dreadnought guitar body be modeled as a .5 x .3 x .1 meter box. The mode shapes associated with the resonances below 880 Hertz are two dimensional in form, the first mode in the thickness direction lying about an octave above the highest frequency of interest. Modes for a sealed, rigid rectangular box will differ from modes found in a guitar with an open soundhole but suggest a modal structure that may exist inside the guitar box.

---

41) Philip M. Morse. Vibration and Sound. New York: McGraw-Hill: 1948.

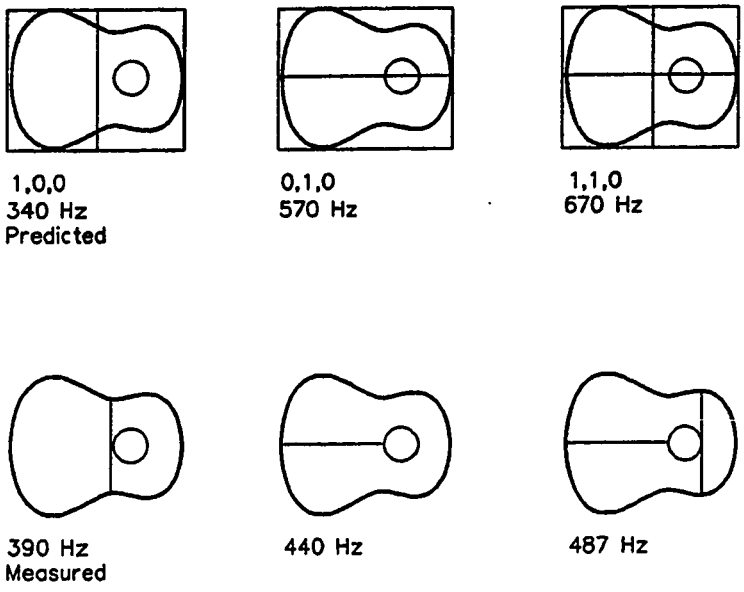

Figure 5.4 Dreadnought Cavity Acoustic Mode Shapes

The measured mode shapes were estimated from a six-microphone array. The heal block of the neck fills the volume forward of the soundhole so that the axial nodal lines appear to terminate at the soundhole. The mode order is similar to the simple model with the soundhole impedance conditions modifying the mode shapes and the resonance frequencies. There is no increase in the activity of the soundhole at these frequencies or any other indication that these resonances strongly influence the radiation from the guitar. The 1,0,0 mode has approximately the same frequency as a radiating plate mode and did not dominate the sound radiation near that frequency. In some guitar design evidence of the 1,0,0

mode driven soundhole sound radiation is to be expected. The simple port and cavity model with the updated soundhole length correction factor is suitable for the analysis of guitars in the frequency range of interest.

5.2 Plate Shapes

The plate shape experiments explore the effects of plate shape and soundhole cutouts on the plate resonances. Models of Sloane and Dreadnought guitar body shapes were used in this work. A set of test fixtures were constructed to simulate the simply supported boundary conditions used in the analytical model. The test plates were constructed of an isotropic material in order to isolate the shape effects.

5.2.1 Measurement Methods

Three solid plates were tested: a Sloane pattern, a Dreadnought pattern and a rectangular plate. In order to create a compliant joint which would approximate a simply supported boundary condition in the test fixture, the foam board plates were glued to the particle board frame with rubber cement. The rectangular plate was constructed to explore the boundary conditions of the assembly. The boundary conditions as built were not close approximations to the simply supported condition but neither were they representative of clamped boundary conditions.

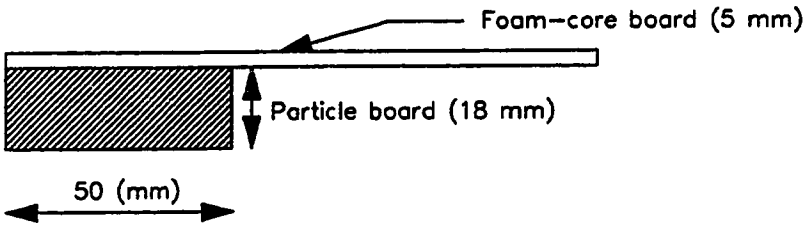

	Modal Frequencies			
Rectangular panel (515 x 380 mm)	85	189	254	287 (Hz)
Sloane Classical	114	198	271	383 (Hz)
Dreadnought	106	232	326	426 (Hz)

Figure 5.5 Simply Supported Plate Test Fixture

The resonance frequencies are measured using a set of six small piezoelectric pickups at several points on the plates. The responses of the pickups were monitored on an oscilloscope. Lissajous patterns were used to determine the relative phase between the pickups. These phase differences were used to estimate a mode shapes. This technique was found to be tedious and it was difficult to reproduce the result with a high degree of certainty. An alternate to the piezoelectric sensor measurement technique is the use of Chladni patterns.

Chladni patterns are generated by exciting a plate covered with a light weight powder. If the forcing function, in this case the acoustic output of a 15 inch loudspeaker in a sealed box, is exciting a plate resonance it is easy to produce acceleration of the plate of 1 g or larger. If the accelerations are greater than 1 g then the powder will bounce and migrate off the plate. Where there are nodal regions the accelerations will be low, the powder will not move and will begin to accumulate. The powder accumulations define the nodal regions. These nodal regions are reduced to nodal lines by inspection.

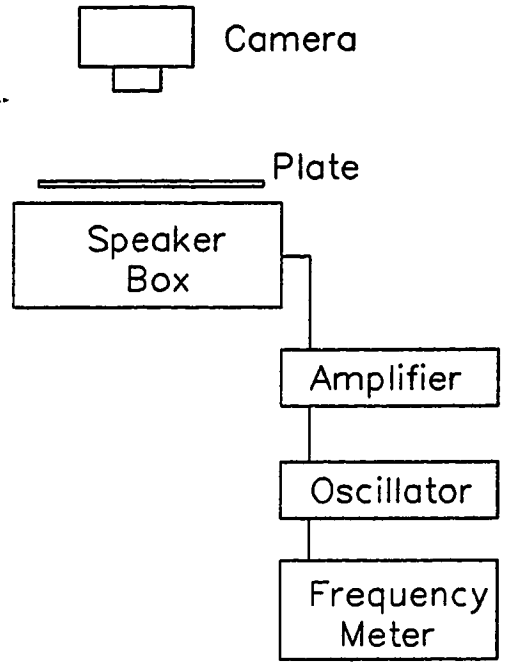

Figure 5.6 Mode Shape Observation Equipment System

The "powder" which has been found to be the easiest to work with is poppy seeds. The poppy seeds are light weight and black in color which stands out well against the white foam core plates. A useful procedure in the observation of the nodal patterns has been the use of a wide paint brush to push the seeds in different areas to refine the definition of a nodal area.

The Chladni pattern resonant frequency repeatability was within the one Hertz measurement resolution of the frequency meter. The modes which had a net volume displacement were easier to excite than the symmetric "zero" volume displacement modes though both were measured and documented.

5.2.2 Solid Plates

The initial experiments used foam core board to examine the basic relationships between the first four plate modes. Three plate shapes were used; a Sloane classical guitar pattern, a Dreadnought steel string guitar pattern and a rectangular plate with an aspect ratio similar to that of the Dreadnought guitar.

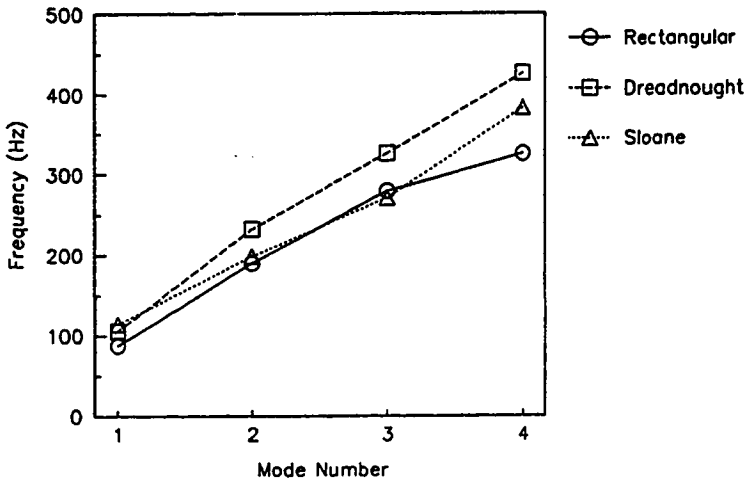

Figure 5.7 Solid Plate Resonance Frequencies

The relationships between the frequencies give some indication of the basic shape effect on the modal frequency series. A following study of a similar set of plates shows the mode shapes associated with the Dreadnought and rectangular plates (see figure 5.10).

5.2.3 Plates with Soundholes

The effects of the soundhole on the dynamics of plates were studied by cutting soundholes from the Sloane and Dreadnought foam-core board plates.

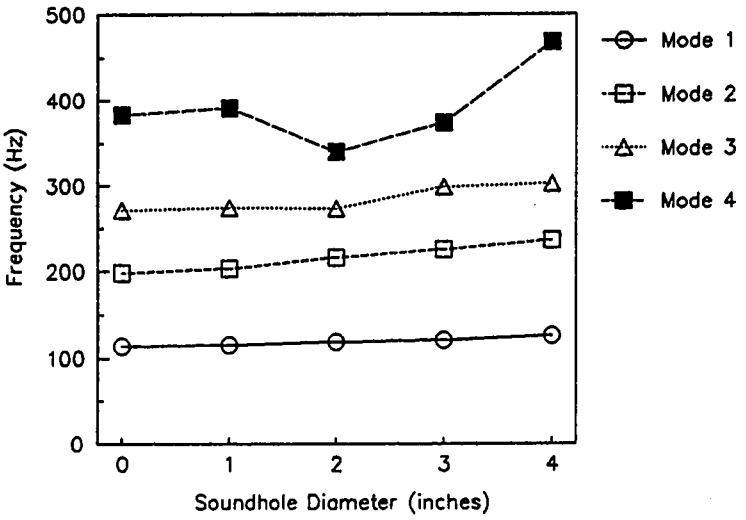

Figure 5.8 Sloane Soundhole Sensitivity

The Sloane guitar pattern showed an overall increase in the frequency of the first three modes with increasing soundhole diameter. The change in the fundamental frequency is small, almost unchanged.

The results obtained on the Dreadnought guitar pattern were similar the results of the Sloane study.

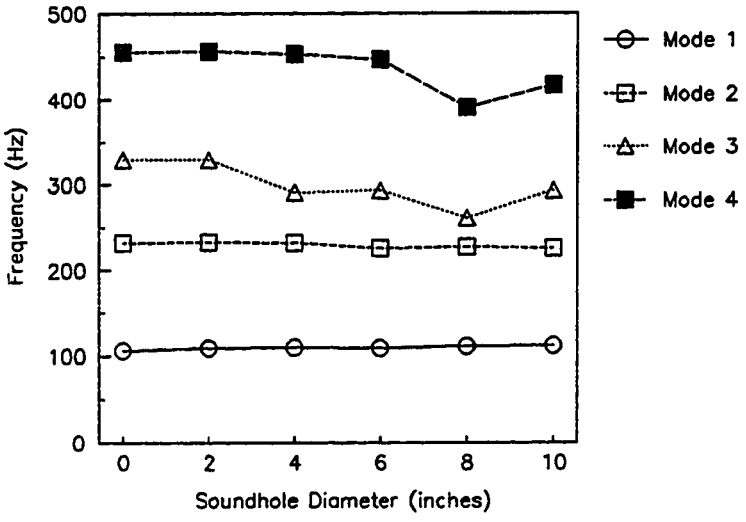

Figure 5.9 Dreadnought Soundhole Sensitivity

The Dreadnought fundamental was so insensitive to the presence of the soundhole that the soundhole size was increased to 10 inches. The upper bout of the plate was then removed with only minor changes in the resonances.

5.2.4 Plate Mode Shapes

The Chladni patterns can be used to trace the evolution of the mode shape through a number of geometric changes. The guitar soundboard can be viewed as a modified rectangular plate. The mode shape of a rectangular plate are well known and can be used as a reference point in the evaluation of the test fixtures.

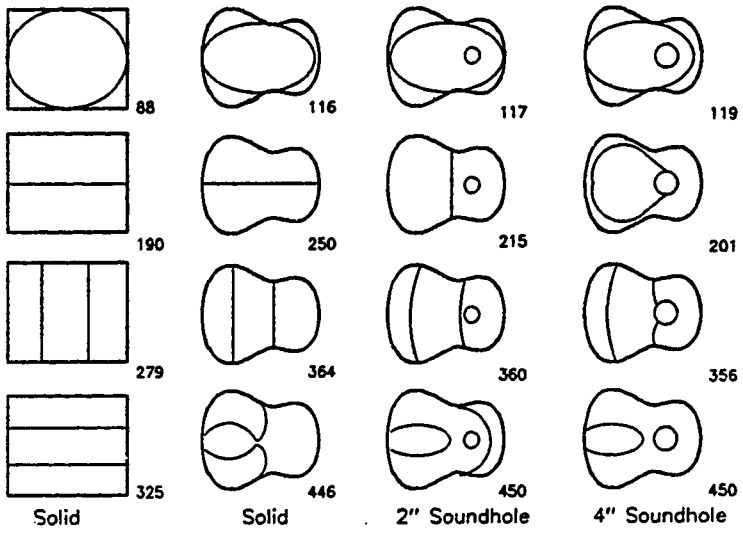

Figure 5.10 Foam Core Plate Mode Shape Evolution

The mode shapes of the rectangular plate are mapped into the guitar outline in a simple manner in most cases. The second mode is interesting in its sensitivity to the plate geometry while remaining modes are essentially unchanged in both mode shape and frequency.

5.3 Material Property Extraction

Material properties must be known if predictions are to be made. The material properties extraction methods are based on interpreting the resonance behavior of vibrating beams and plates with analytical models.

5.3.1 Vibrating Beam Method

The simplest system to be used for determining the material properties for musical instrument woods is a simple beam. Beam samples of wood have been tested using a number of flexural beam modes and support systems. Clamped-free and free-clamped-free test techniques have been developed in Europe by Holtz[42] and Rajcan[43]. Schelleng[44] and Haines[45] have developed free-free beam methods in the United States. The free-free method is used in this study.

The flexural beam test technique assumes a relationship between the resonance frequency of a sample and its material properties and geometry. The modulus of elasticity of the sample is calculated from these measured quantities. The determination of material properties

---

42) D. Holtz, "On Some Important Properties on Non-Modified Coniferous and Leaved Wood in View of Mechanical and Acoustical Data in Piano Soundboards", Archiwum Akustyki 9 (1) 1974.

43) E. Rajcan, "Some Differences in Physico-Acoustic Characteristics of 'Resonant' and Standard Spruce Wood", Acustica vol 48 1981.

44) John C. Schelleng, "Wood for Violins", Catgut Acoust. Soc. Newsletter #37 1982.

45) Daniel W. Haines, "On Musical Instrument Wood", Catgut Acoust. Soc. Newsletter #31 1979.

for orthotropic materials such as wood requires the testing of two beam samples, one cut along the grain and the other cut across grain. The geometry and weight of the beam samples are measured. The resonance frequency of the first mode of vibration and the damping factor are estimated from the resonance response of the sample. Using a model for the vibration of free-free rectangular cross sectional beams the modulus of elasticity of the material may be calculated.

5.7)

$$E = 0.946 f^2 m_b (ab/h^3)(a/b)^2$$

E = Modulus of Elasticity

f = Resonance Frequency

m_b = Mass of Beam

a = Beam Length

b = Beam Width

h = Beam Thickness

The loss factor is taken from the -3dB down points on the resonance curve.

5.8)

$$\eta = \frac{(f_2 - f_1)}{f}$$

$f_2; f_1$ = -3 dB frequency

The complex stiffness can be expressed using the real modulus and the loss factor;

5.9)

$$\overline{E} = E(1 + i\eta)$$

Loss factors reported in the literature for woods are independent of frequency below 2000-5000 Hertz[46]. The current modeling effort is limited to 880 Hertz and a constant damping factor has been assumed.

The experimental method used to measure the forced vibration of the wood samples is designed to minimize the influence of the test procedure on the collected data. A free-free beam support and instrumentation system has been developed to accomplish this goal. The clamped cantilever beam approach used by others requires great care in building a clamp which will not add damping or compliance to the sample. The free-free boundary is easily implemented by supporting the test specimen with small rods or threads at the nodal lines of the first mode of vibration.

---

46) D. Holtz, "Investigations on a Possible Substitution of Resonant Wood in Plates of Musical Instruments", Archiwum Akustyki 4 (4) 1979.

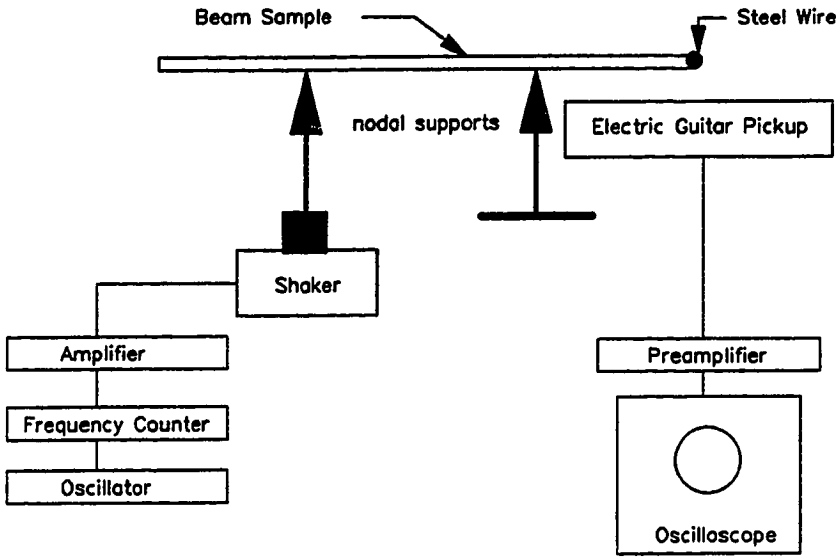

Figure 5.11 Beam Dynamics Measurement Fixture

In practice the free-free mode shape is obtained by supporting the beam at its nodal points 22.3 percent of the beam length from either end of the beam. The beam is excited by a small shaker under one of the supports. The pickup device produces a voltage proportional to the velocity of the moving magnetic target attached to the beam sample. A 0.009 inch diameter steel wire was used to minimize the mass and stiffness influence of the wire on the measurement.

5.3.2 Vibrating Plate Method

A superior method for determining the material properties of orthotropic materials such as wood is the plate method. The plate method is the two dimensional

version of the beam technique. In this method the two major bending moduli and the shear modulus are measured using free-free plate modes which are dominated by only one of these moduli. The cross moduli must be inferred from the measurement of an additional mode and the values of the other three moduli.

Blevins[47] has expressed the frequency equation for rectangular plates in a general form in which the boundary conditions and mode order are taken into account using constants. Using this equation and selecting certain modes allows for the estimation of the dynamic moduli in a manner similar to that employed in the beam technique.

5.11)

$$f_{i,j} = \frac{\pi}{2}\sqrt{\frac{h^2}{12\rho}}\left[G_i^4\frac{D_x}{a^4} + G_j^4\frac{D_y}{b^4} + 2H_iH_j\frac{D_{xy}}{a^2b^2} + (J_iJ_j - H_iH_j)\frac{D_k}{a^2b^2}\right]^{1/2}$$

ρ = Plate Mass Density

a = Plate Length

b = Plate Width

h = Plate Thickness

---

47) Robert D. Blevins, Formulas for Natural Frequency and Mode Shape. (New York: Van Nostrand Reinhold Company) 1979. Section 11.3.

For the case of a plate with free-free-free-free edge conditions the constants for the first few modes are;

G_l= 0.0, 0.000, 1.506 l=1,2,3

H_l= 0.0, 0.000, 1.248 l=1,2,3

J_l= 0.0, 1.216, 5.017 l=1,2,3

The modulus of elasticity and Poisson's ratio are bound together in the bending moduli in this formulation.

5.12)

$$D_x = \frac{E_x}{1-\nu_x\nu_y}$$

$$D_y = \frac{E_y}{1-\nu_x\nu_y}$$

$$D_{xy} = D_x\nu_y + 2D_k = D_y\nu_x + 2D_k$$

D_k= Shear Modulus

The computer models developed in Chapters 2 and 3 have been constructed using these bending moduli. The data collected using the resonance plate technique is in the desired form to support the modeling effort.

The implementation of the technique is predicated on the selection of appropriate modes in which the moduli can be separated. The frequency formula has been rearranged and restated in terms of the directly measurable

quantities, lengths, mass and frequency. Selection of vibration modes allows for the estimation of desired moduli.

The shear modulus is computed from a twisting mode with two nodal lines running perpendicular to one another.

5.13)

$$D_k = 0.822 m_p \left(\frac{ab}{h^3}\right) f_{22}^2$$

The bending moduli are calculated from "beam" modes which have mode shapes similar to the first mode of the free-free beam.

5.14)

$$D_x = 0.945 m_p \left(\frac{ab}{h^3}\right)\left(\frac{a}{b}\right)^2 f_{13}^2$$

5.15)

$$D_y = 0.945 m_p \left(\frac{ab}{h^3}\right)\left(\frac{b}{a}\right)^2 f_{31}^2$$

The cross modulus is computed from the measurement of a mode which involves the previously measured moduli.

5.16)

$$D_{xy} = 1.561 m_p \left(\frac{ab}{h^3}\right) f_{33}^2 - 30.32 D_k - 1.651\left[D_x\left(\frac{b}{a}\right)^2 + D_y\left(\frac{a}{b}\right)^2\right]$$

A check on the estimation of the cross modulus is the knowledge that the cross modulus is approximately equal to the geometric average of the bending moduli.

5.17)

$$D_{xy} \cong \sqrt{D_x D_y} \cong 0.945 m_p \left(\frac{ab}{h^3}\right) f_{31} f_{13}$$

This estimation of the cross modulus using the bending modulus is required if beam samples alone are being used to estimate the dynamics of a plate. The measured modulus of elasticity using the beam technique and the bending modulus using the plate technique are essentially equal for woods. The moduli differ by the reciprocal of one minus the cross product of the Poisson's ratios. The cross product of Poisson's ratios for woods is on the order of 0.01.

The experimental equipment used to implement the plate moduli material property extraction is basically the same as that used in the beam experiment. The magnetic sensor system has been replaced with a small piezoelectric sensor which is attached to the plate. The sensor is moved and re-attached to determine mode shapes. The support placement on nodal locations has been avoided by suspending the plate from its edge with loops of string.

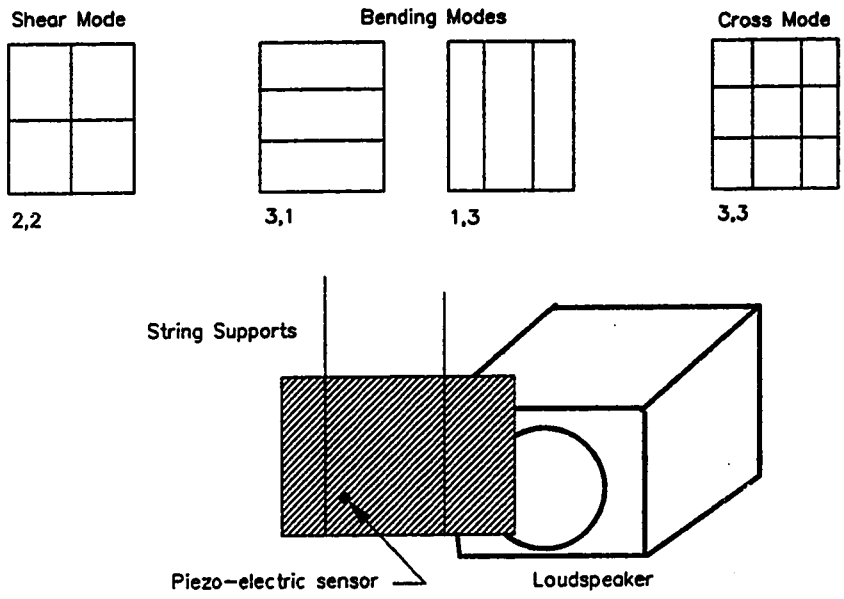

Figure 5.12 Plate Dynamics Measurement Fixture

The four measured modes can be identified by monitoring the phase shifts between the loudspeaker and the sensor signal. Lissajous figures on an oscilloscope gave a visual indication of the relative phase relationships between the loudspeaker and the sensors.

5.3.3 Material Properties Data

The material properties extraction methods were applied to selected samples with known material properties and to samples with unknown properties. An aluminum bar was used to calibrate the beam test method. The foam-core board was used to compare the procedures. The

rectangular plate fixture was used to determine the material constants of foam-core board in a "simply supported" condition.

Using the beam method of material property extraction, the aluminum bar sample had a density of 2680 kilograms per meter cubed and a Young's Modulus of 65 x 10^9 Newtons per square meter. These values are within a few percent of the handbook values. The foam core board had a density of 163 kilograms per cubic meter and Young's Modulus of 1.0 x 10^9 Newtons per square meter. There were small differences in the modulus value depending on the method of measurement.

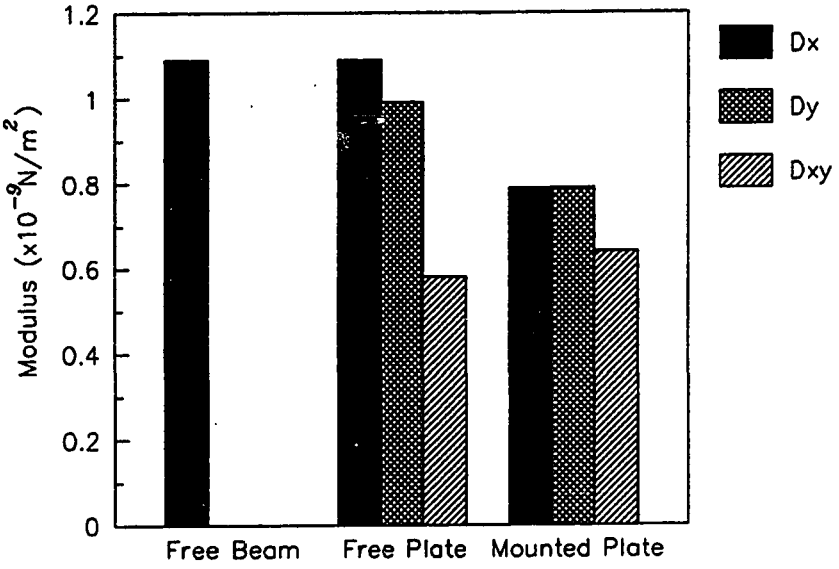

Figure 5.13 Foam-Core Modulus

The free beam and free plate methods yield essentially identical answers, however when the sample is mounted on the particle board fixture with rubber cement the effective modulus is 80% of its "true" value. This result casts doubts on the assumption the fixture is presenting the plate a simply supported boundary condition. As the fixture clamps the plate the effective modulus must drop in order to match the simply supported model. In using the experimental fixture in the determination of natural frequencies an additional experimental uncertainty has been introduced. The lowering of the effective modulus by 20% translates into a frequency error of approximately 10%.

5.4 Sound Power Measurement

Sound power measurement technology has been extended in recent years through the commercialization of acoustic intensity measurement systems. Before the invention of the intensity probes, techniques were developed to estimate the sound power of a source based on sound pressure measurements. The premise of these techniques is a relationship between the space averaged sound pressure levels (SPL) measured away from the source and sound power level (PWL) of the source under a number of special conditions. The special conditions include the use of reverberation, anechoic and hemi-anechoic test chambers. The precision techniques for the determination of sound power require a qualified anechoic chamber or reverberation chamber. Less precise measurements can be made in less ideal environments.

An adaptation of the standard method[48] for the determination of sound power levels in reverberant rooms has been used to estimate the sound power radiated from guitars. The standard deviation of the estimated sound power level to the actual sound power level is expected to be less than 5 dB at the lowest frequency of interest based on the procedures of the standard measurement methods, the measured data had a standard deviations on the order of 2 dB.

Guitars are commonly played in small rooms which are closer to semi-reverberant chambers than to anechoic spaces. The sound power levels are computed from sound pressure levels measured throughout the room. The variation of the sound field in space requires that the reverberant room be sampled at many points to reduce the standard deviation of the estimate. The sound power level in a reverberant room is related to the averaged sound pressure level by;

---

48) American National Standard. Methods for the Determination of Sound Power Levels of Small Sources in Reverberation Rooms. ANSI S1.21-1972. New York, 1972.

5.18)

$$PWL = \overline{SPL} - 10\log(RT_{60}/T_0) + 10\log(V/V_0)$$

$$+ 10\log(1 + S\lambda/8V) + 10\log(B/1000) - 14$$

V = Room Volume (m^3)

V_0 = Reference Volume (1 m^3)

S = Room Surface Area (m^2)

λ = Acoustic Wavelength (m)

T_0 = Reference Time (1 sec)

B = Barometric Pressure (millibars)

RT_{60} = Reverberation Time (sec)

The reverberation time of the room may be estimated by;

$$RT_{60} = 0.16\frac{V}{S\bar{\alpha}}$$

$\bar{\alpha}$ = Average Sabine absorption coefficient

The average sound pressure level is computed by summing the squares of the magnitudes of the acoustic pressures at each point in the sound field and converting that sum back into decibel notation;

5.19)

$$\overline{SPL} = 10\text{Log}\left(\frac{1}{N}\sum_{i=1}^{N} 10^{SPL_i/10}\right)$$

N = Number of Measurement Points

SPL_i = SPL at i^{th} measurement point (dB)

In these experiments the sound pressure levels were measured at 16 points using a hand held sound level meter. The room is a typical playing environment with rugs and furniture with dimensions of 17 x 12 x 7.5 feet. At the lower test frequencies the selected room is a poor approximation to an ideal reverberant chamber. At these lower frequencies of 80 to 220 Hertz the acoustic wavelengths are on the order of a few feet and the modal density of the room is very small. This low mode count leads to a nonuniform sound field. The Sabine absorption of such rooms is in the 0.2 to 0.3 range.

The guitar was driven by a small shaker. The guitar was supported by a shoulder strap on a manikin which was padded and dressed to approximate the player's body.

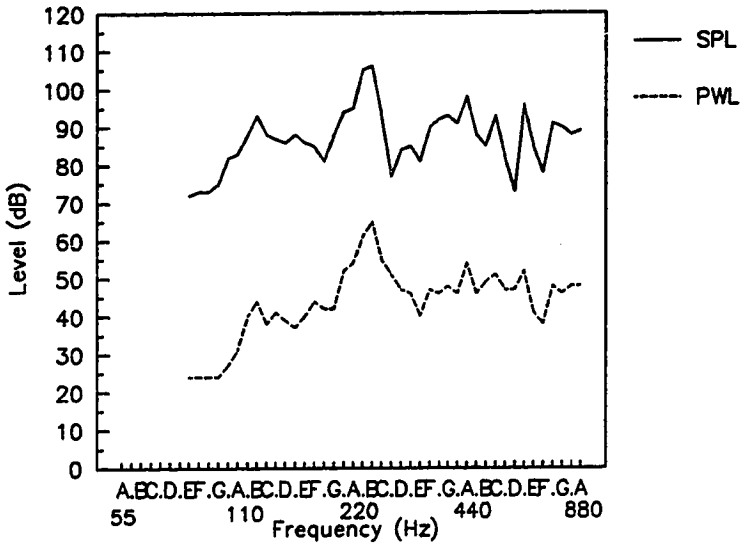

Figure 5.14 Dreadnought Sound Power Level

The measured sound power level (PWL) and the sound pressure level (SPL) measured 1/2 meter over the geometric center of guitar top have the same basic shape. A strong resonance near 240 Hertz dominates the radiated spectra. A low peak near 120 Hertz is the "air" resonance defining the low frequency roll off of the system.

The measured sound power level is a function of the average sound pressure; in order to interpret the sound power level measurement the standard deviation of the estimated SPL data is needed.

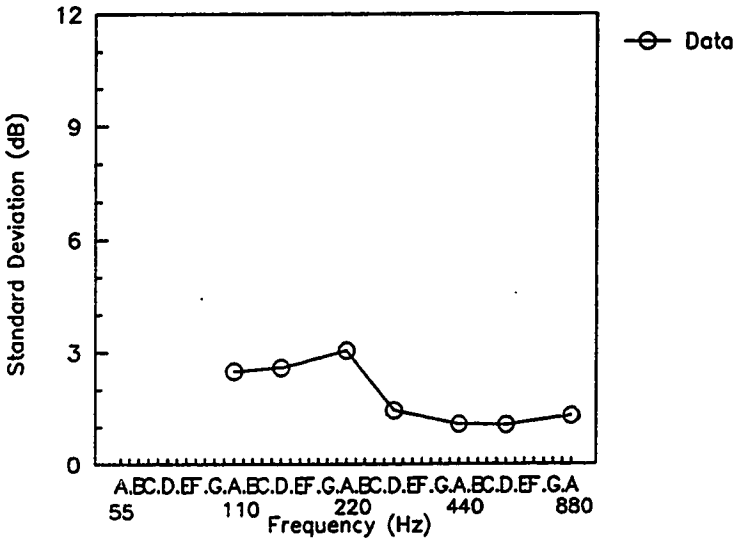

Figure 5.15 Dreadnought Sound Power Standard Deviation

The sound power estimates in the high frequencies above 300 Hertz have a standard deviation of approximately 1 dB. In the lower frequencies the standard deviation is 3 dB or less.

The sound power level of a Dreadnought guitar has been measured using a reverberant room technique (Figure 5.15). The dominant features of the radiated power spectra as expected from earlier analytic estimates are clearly visible (recall figures 4.25, 4.26 & 4.27). The definition of the upper resonances, those above 300 Hertz, are not as sharp as predicted. This may be due to the motion of the back plate which has not been

modeled or an under estimation of the frictional damping or an overestimation of the radiation resistance at these frequencies. No attempt was made to match the drive level in the experiment to the levels used in the predictions, therefore the absolute magnitudes of the two are not expected to match.

An alternative procedure to the use of a reverberant room is the use of an anechoic environment[49]. The information gathered using the anechoic approach is more appropriate for instruments which are being used in large concert halls or outdoor performances. The reverberant method is more appropriate for instruments in small rooms. The anechoic measurement technique lends itself to the measurement of source directivity. The standard anechoic method measures the sound pressure on an imaginary sphere surrounding the source. The standard requires that the radius of the measurement sphere should be at least one meter or twice the largest dimension of the source. Most guitar plates are less than one half a meter in length therefore a one meter radius is sufficient. The sound power of the source is directly related to the space averaged sound pressure level. If the sound pressure measurements are made on an imaginary sphere with the source at its center then;

---

49) American National Standard. Precision Methods for the Determination of Sound Power Levels of Noise Sources in Anechoic and Hemi-Anechoic Rooms. ANSI S1.35-1979. New York, 1979.

5.20)

$$PWL = \overline{SPL} + 10\log(S_m/S_0) + C$$

PWL = Sound Power Level (dB)

$\overline{SPL}$ = Space Averaged Sound Pressure Level (dB)

$S_m = 4\pi R^2$

R = Radius of Measurement Sphere ($meter$)

S_0 = Reference Area = $1 meter^2$

$C = 10\log(400/\rho c)$

Each microphone measurement position is taken to be representative of sound pressure over a given area.

5.21)

$$\overline{SPL} = 10\mathrm{Log}\left(\frac{1}{N}\sum_{i=1}^{N} 10^{SPL_i/10}\right)$$

N = Number of Measurement Points

SPL_i = SPL at i^{th} measurement point (dB)

In a less ideal sound field the measured sound pressure levels are a function of the outward going waves moving away from the source and any back traveling waves due to refections. Guitars are played primary in small concert halls, practice rooms and homes in the presence of one or more reflecting planes. The room effects can

be accounted for by using simple room model. The simple correction will not take into account the placement of the source in the room and possibility of standing waves. The average room correction factor is based on the Sabine absorption and is added as a correction to the sound power estimation equation.

5.22)

$$PWL = \overline{SPL} + 10\log(S_m/S_0) + C + K$$

$$K = 10\log\left(1 + \frac{4}{A/S_m}\right)$$

$$A = \bar{\alpha} \times S_r$$

$\bar{\alpha}$ = Average Sabine absorption coefficient

S_r = Total Surface Area of Test Room

These two alternative procedures for the calculation of the radiated sound power level have been introduced together for comparison. The information gathered in this chapter used the reverberant method. The anechoic method is used in the following chapter. The sound power spectra measured by either method are equal within experimental error.

6 Guitar Soundboard Experiments

A dreadnought guitar kit was purchased with the objective of measuring the mode shapes of the soundboard at various stages of construction. The experimental guitar is based on the Stewart-MacDonald dreadnought guitar kit. The bracing pieces supplied with the kit were completely shaped and therefore unsuitable for the documentation of the step-by-step evolution of the mode shapes as planned. Additional bracing stock was provided by master luthier Linda Manzer of Toronto, Canada for use in these experiments. The construction geometry is based on Martin D-18 guitar top loaned for use in this project by Bob Rothstein and drawings supplied with the guitar kit.

6.1 Estimation of Material Properties

The methods for determining the material constants of plates and beams have been discussed in sections 5.3.1 and 5.3.2, these methods were used to estimate the material properties of the materials used in the experiment. The estimation of the material properties of the plate were hampered by the condition of the plate supplied with the kit. The top plate as received, was not rectangular and there was not enough material to square it up. The soundhole area had been routed to accept the soundhole binding material and soundhole edge had been routed to approximately one half the thickness of the plate. The soundhole bindings were installed in the plate before any measurements were made. The free plate resonances of the approximately rectangular plate with the soundhole

bindings installed were used to estimate the material constants of the plate. Under these less than ideal conditions the material properties of the top plate were estimated and are documented with the experimentally determined mode shapes.

The bracing stock material properties have been determined by the free beam method, as described in the preceding chapter. The bracing stock was also not ideally configured for material property extraction experiments. Data contamination due to unmodeled twisting modes of the beam samples is suspected. The material properties of each bracing group are given as they are added to the plate. The bracing patterns have been given short names which will be used for identification throughout out this and the following chapter. The location of the start, stop and break points along the beams are described in a plate based coordinate system.

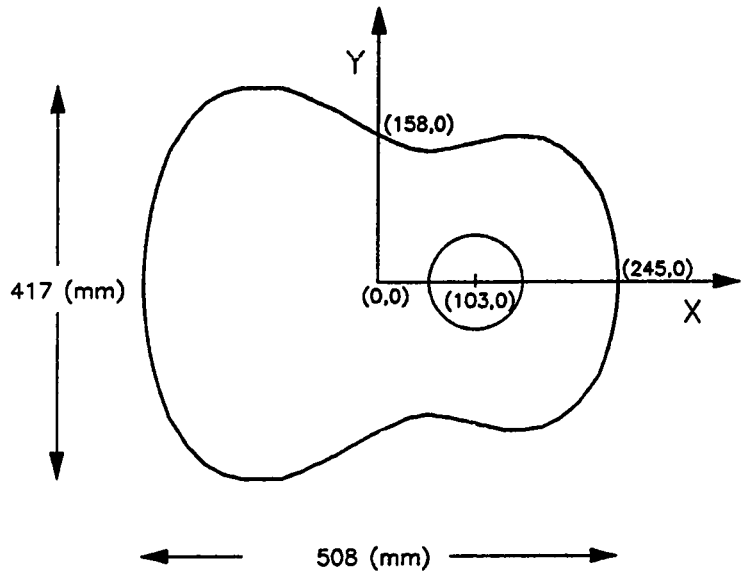

Figure 6.1 Plate Coordinate System Definition

The origin of the coordinate system is the center of the plate and the coordinate unit is one millimeter. All brace length measurements, such as taper lengths, are measured and documented as distances along the brace.

6.2 Soundboard Construction Mode Shapes

The wood working techniques used in the construction of the experimental soundboard were standard. Yellow wood glue was used for assembly and hand chisels, scrapers, small planes and sandpaper were used in the shaping of the braces. Conventional construction practice has been modified with the use of a wooden frame. The

wooden frame is intended to provide a boundary condition to the plate which can be approximated by the computational model. The frame is attached on the unbraced side of the plate so that gluing and carving on the braces can proceed in the traditional manner. A guitar shaped board sits inside the frame during brace work to provide a solid working surface. The wooden frame is the same frame used in the earlier plate work (figure 5.5 of section 5.2.1).

The mode shapes presented here are schematic representations of modes observed with the use of Chladni patterns. These Chladni patterns are generated by exciting a plate covered with a light weight powder.

6.2.1 Soundboard on Fixture

The purpose of these experiments is to document the evolution of the plate mode shapes as the bracing structure is added. The plate is mounted on a guitar shaped particle board frame. The frame is intended to produce a boundary condition similar to that of the bent wood sides of the guitar. A simply supported boundary condition has been used in the computational model. The guitar frame allows the use of standard guitar construction techniques whereas building the braces inside the guitar box would not. Building the soundboard brace-side-out on a set of sides was considered however the proper main brace interfaces to the sides could not be reproduced. Evolutionary data is taken on the frame fixture until the bracing pattern is completely carved. When the bracing pattern is finished the soundboard is the joined to a set of bent

guitar sides in the traditional manner. A stiff honeycomb back has been used to seal the box for box-cavity studies. In the following mode shape sketches the soundhole is drawn and should be understood to represent the routed grove at the soundhole edge.

The mode shapes sketches are collected from a survey of the plate using the Chladni pattern method. The modes are the distinct modes found below 800 Hz. The figures are arranged to track mode order and mode shape.

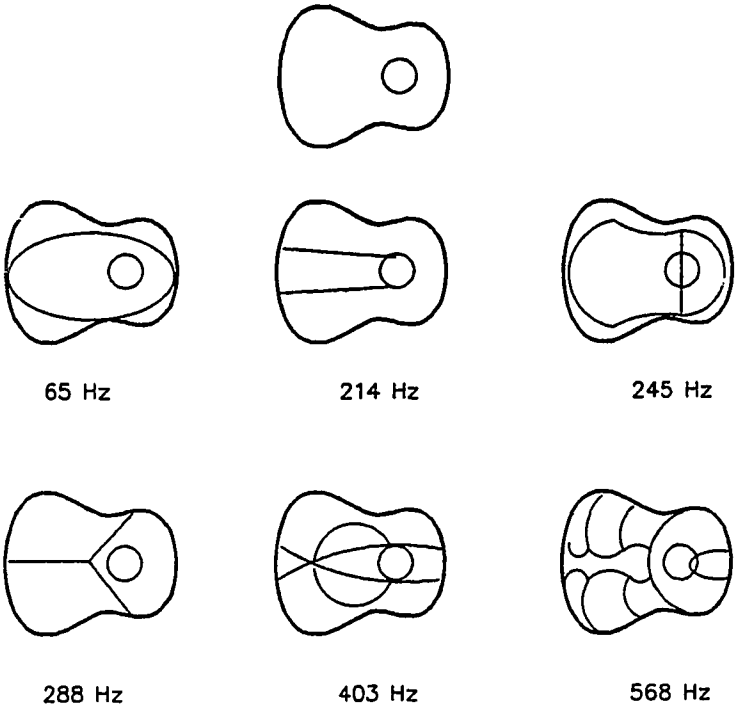

Figure 6.2 Modes of Spruce Plate on Test Fixture

The first configuration is that of the bare plate on the frame. The material properties of the plate as determined by the free plate experiment are; an along the grain modulus of 7.4 x 10^9 N/m^2, an across the grain modulus of 0.8 x 10^9 N/m^2, a shear modulus of 2.1 x 10^9 N/m^2 and a density of 537 kg/m^3. The plate was 3 mm thick.

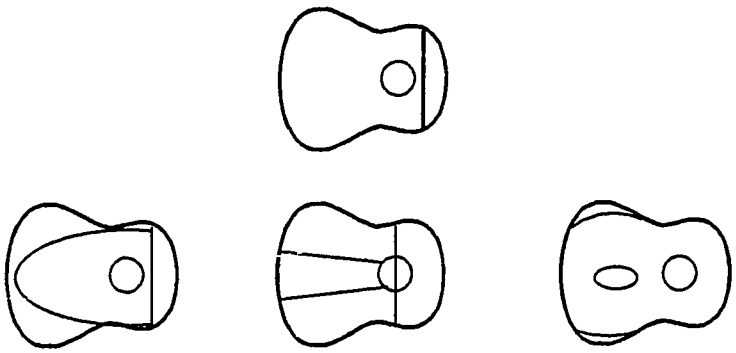

Figure 6.3 Modes of Plate with Upper Bout Brace Added

Brace-1 is the major upper bout brace running perpendicular to the grain direction of the plate. The material properties of this brace are a bending modulus along the grain of 6.1 x 10^9 N/m^2 and a density of 412 kg/m^3. Brace-1 is one of the largest braces used in the dreadnought guitar style with a height of 15.7 mm and a base width of 15.1 mm. The upper bout brace runs from plate coordinate (168, 145) to (168, -145). The center of the plate is the coordinate origin (0,0) and the coordinate unit is one millimeter.

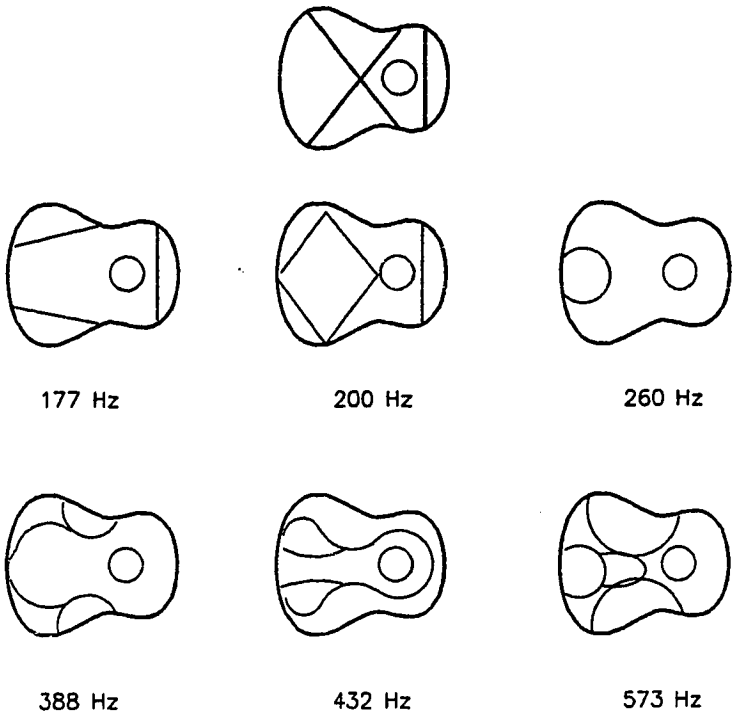

Figure 6.4 Modes of Plate with X-Brace Added

The X-brace is two braces treated as a single unit and form the major bracing of the lower bout. As the sketch suggests the mode shapes are measured in a construction sequence, this configuration is the assembly of the bare plate, Brace-1 and the X-brace. The X-brace stock cross section is 19.1 mm high and 8.3 mm wide. The material properties of the X-braces are a modulus along the grain of 4.3×10^9 N/m^2 and a density of 495 kg/m^3. The upper part of the X-brace runs from plate coordinates (132, 140) to (-158, -193). The lower part of the X-brace is the mirror image of the first running from plate coordinates (132, -140) to (-158, 193). The intersection between the braces does not form a right angle, this is consistent with the Martin guitar soundboard.

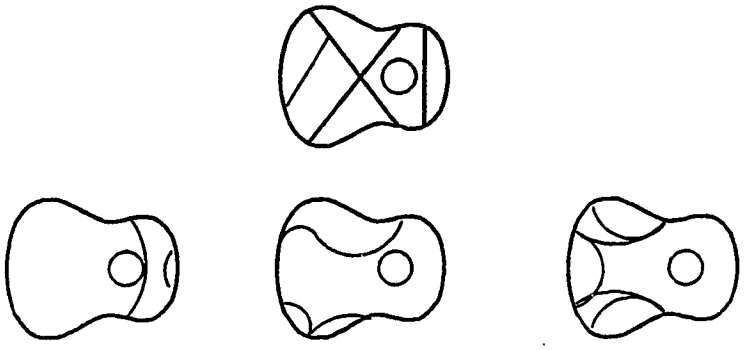

Figure 6.5 Modes of Plate with First Slant Brace Added

The slant braces receive much of the attention in the books on guitar construction in the control of guitar tone. The material properties of the slant braces are the same as the X-braces. The beam section was 15.5 mm high and 8.2 mm wide. The first slant brace (slant-1) runs from plate coordinates (-104, -125) to (-241, -114).

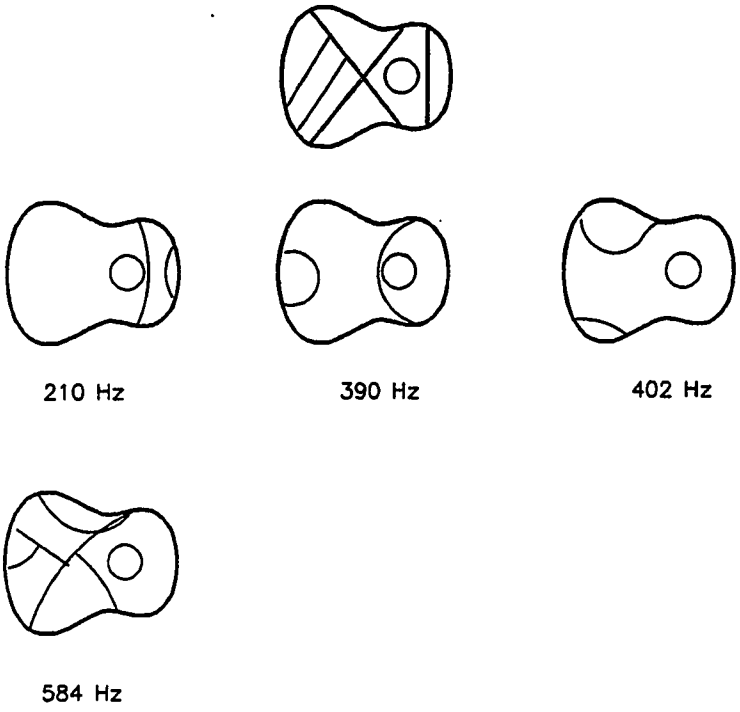

Figure 6.6 Modes of Plate with Second Slant Brace Added

The second slant brace runs from plate coordinates (-73, -86) to (-213, -198). The material and stock dimension of the second slant brace (slant-2) are the same as those of the first slant brace (slant-1).

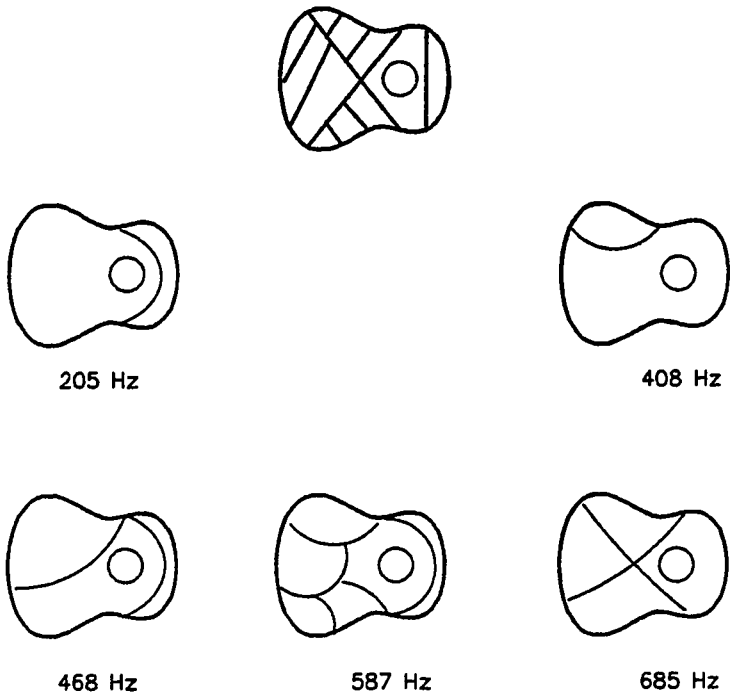

Figure 6.7 Mode Shapes of Plate with Fins Added

The next four braces are smaller than the major braces or the slant braces and are treated as a single unit. The fin braces were taken from the original kit materials and have the following material properties a bending modulus along the grain of 2.7×10^9 N/m^2 and a material density of 441 kg/m^3. The fin brace stock is 6.4 mm high and 6.9 mm wide. Fin 1 brace runs from (-74, 99) to (-10, 168) and fin 2 brace runs from (-38, 56) to (43, 145). The fin 3 and fin 4 braces mirror the first two braces running from (-38, 56) to (43, -145) and (-74, -99) to (10, -168) respectively. This configuration completes the blocking out of the bracing pattern.

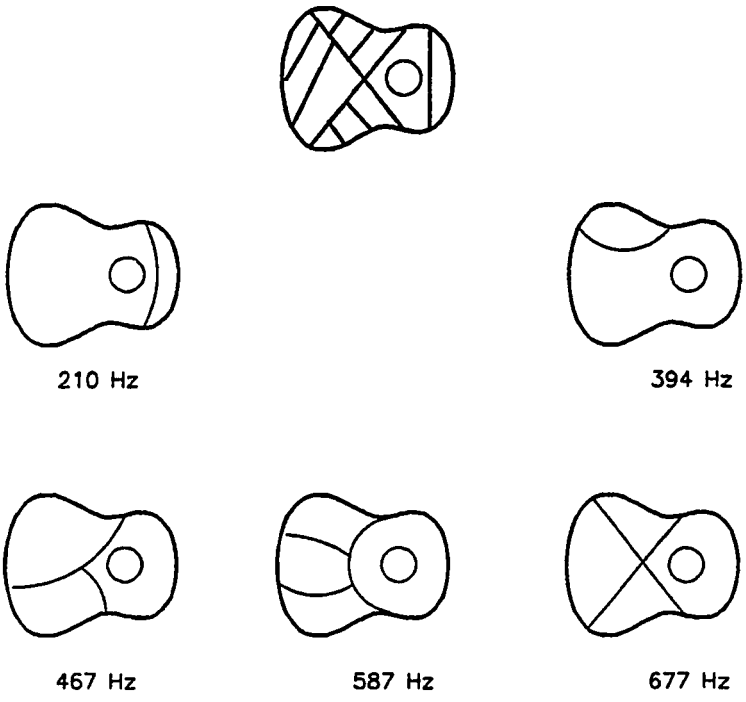

Figure 6.8 Mode Shapes of Plate with Major Braces Trimmed

The major braces, Brace-1 and the X-brace, are tapered to a height of 3.2 mm at the edge of the plate. The height of the tapers is eventually locked into the side of the guitar providing rotational constraint. All the tapers used in this experimental guitar are linear. Measuring along the braces, the X-braces rise to their full height 100 mm from the edge of the plate and Brace-1 rises to its full height in 50 mm from the edge of the plate.

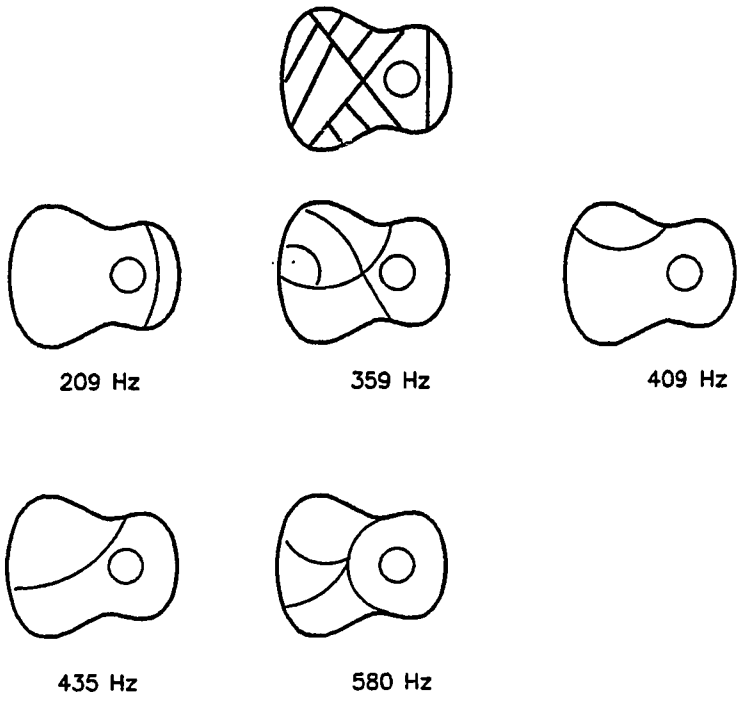

Figure 6.9 Mode Shapes of Plate with Slant Braces Trimmed

The slant braces are tapered to zero thickness at the plate's edge. There is no locking in of the slant braces with the guitar sides during final box construction. Slant-1 rises to its full height in 92 mm from the plate's edge and slant-2 rises to its full height in 90 mm.

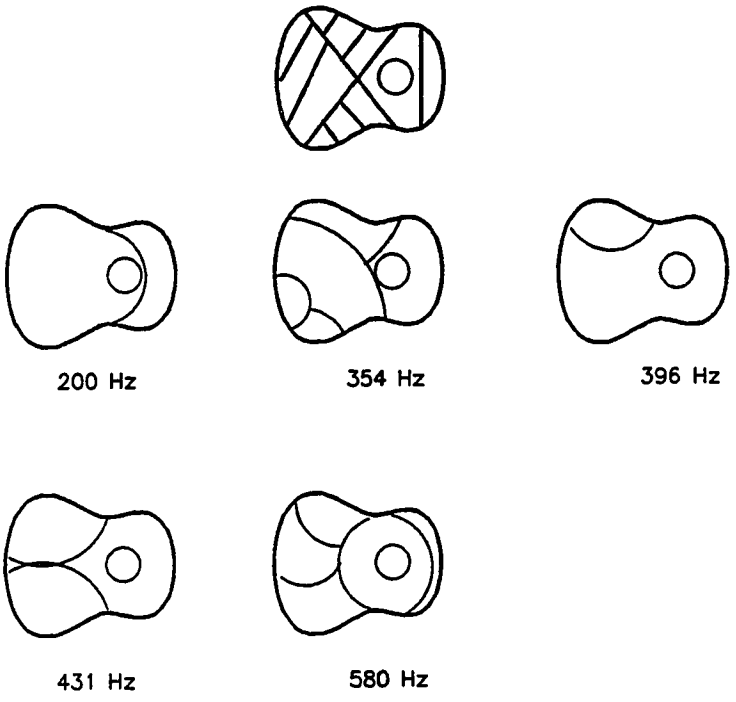

Figure 6.10 Mode Shapes of Plate with all External Braces Trimmed

The small fin braces are tapered to zero thickness at the plate's edge. The four tapers averaged 43 mm in length. The fins also taper to zero thickness at their interfaces with the X-brace the length of these tapers average 12 mm.

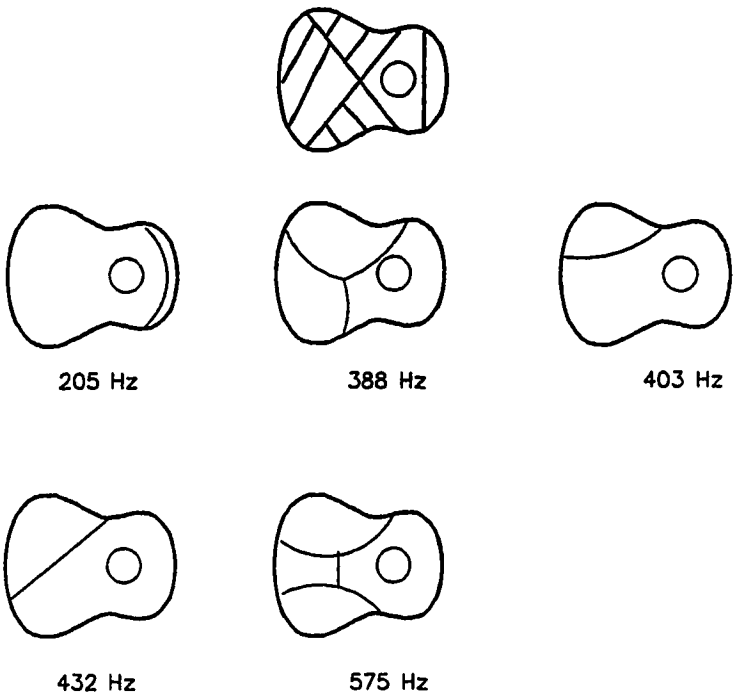

Figure 6.11 Mode Shapes of Plate with X and Slant Brace Interfaces Trimmed

The interface between the slant braces and the X-brace is tapered. The slant braces are tapered to a height of 4.5 mm at the interface. A taper length of 37 mm is carved on the slant-2 brace and 45 mm taper is carved on the slant-1 brace. The slant angle is determined by the Martin guitar top sample.

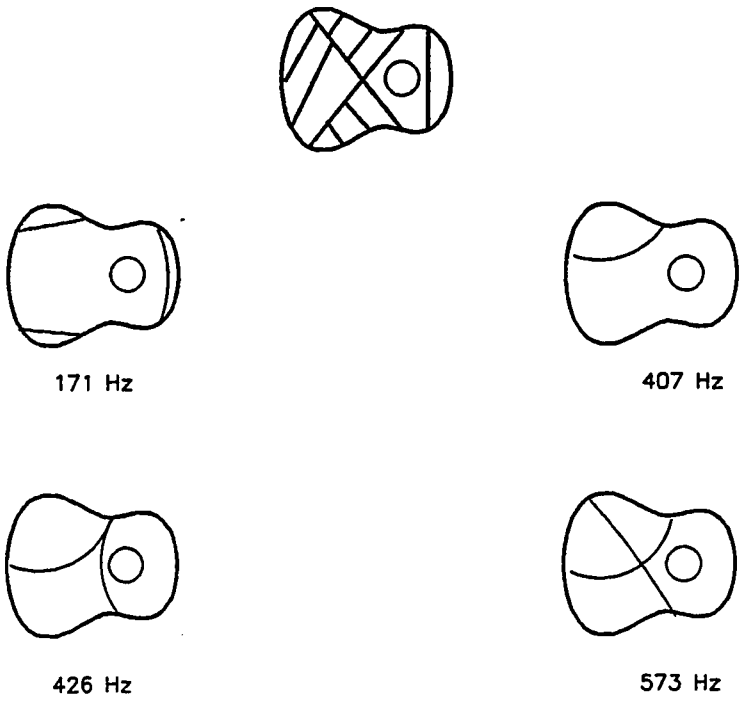

Figure 6.12 Mode Shapes of Carved Bracing Pattern

Up to this point the braces have been left in their raw stock rectangular cross sectional shape. In this step the more traditional semielliptical cross section has been carved on all the braces. The maximum height of the beam stock has not been altered.

6.2.2 Soundboard on Guitar Sides

The guitar soundboard bracing patterns have been assembled on a special fixture which was intended to represent a simply supported boundary condition. The

assumption that a simply supported plate is an appropriate model for the dynamics of the guitar soundboard is tested by moving the assembled guitar soundboard on to a set of rosewood sides. The traditional construction technique of using a kerfing strip to increase the gluing area at the edge of the guitar sides has been used.

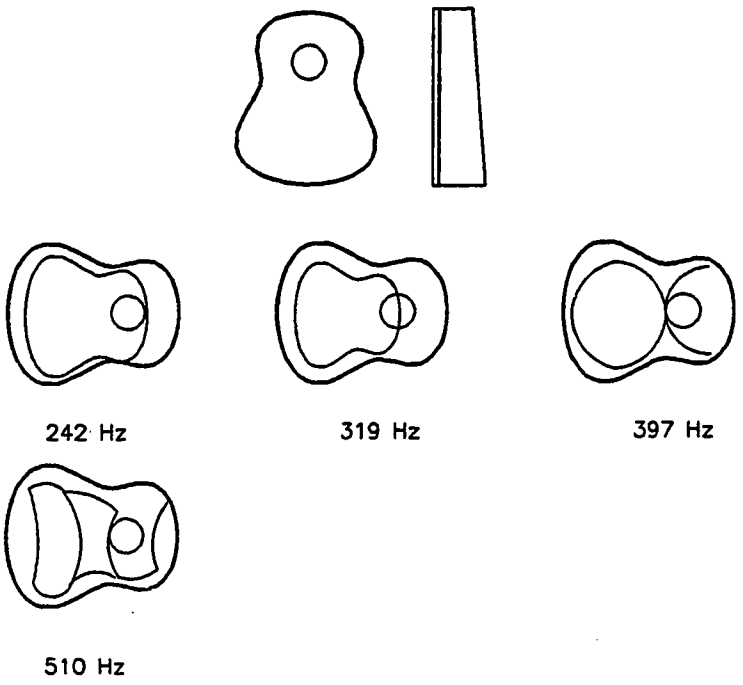

Figure 6.13 Mode Shapes of the Soundboard on Unconstrained Sides

The sides of the guitar are attached to the soundboard on one side but are unconstrained on the other. This configuration is not representative of a guitar construction but is presented as a transition case. The soundboard has been trimmed to match the guitar sides. This trimming removes the lip of wood which was required to attach the soundboard to fixture used in the earlier experiments.

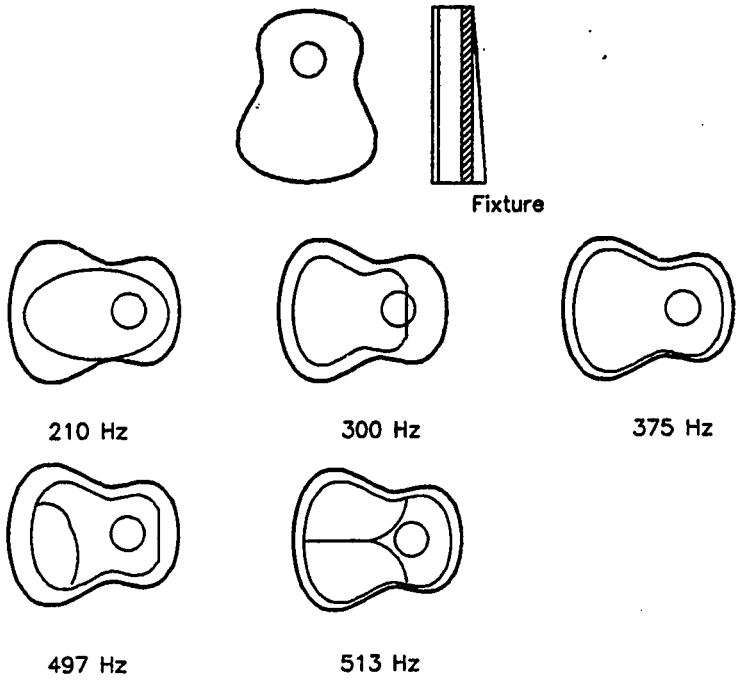

Figure 6.14 Mode Shapes of the Soundboard on Constrained Sides

The fixture, which used to establish the boundary condition for the plate alone studies, is now used to provide a constraint on the sides. The fixture was clamped at four points, the waist points and the heel and neck blocks to provide some rigidity to the sides. The clamped fixture configuration leaves the guitar box open and yet imitates the presence of a back plate to some degree.

The soundboard as supplied in the dreadnought kit was routed for the soundhole bindings and the soundhole. The bindings were installed before any measurements were make on the plate. The soundhole relief required a decision to either remove the soundhole material initially or build up the plate and remove the soundhole material late in the assembly of the instrument. Removal of the soundhole is traditionally delayed in order to reduce the possible cosmetic damage to the instrument top. The traditional approach was selected.

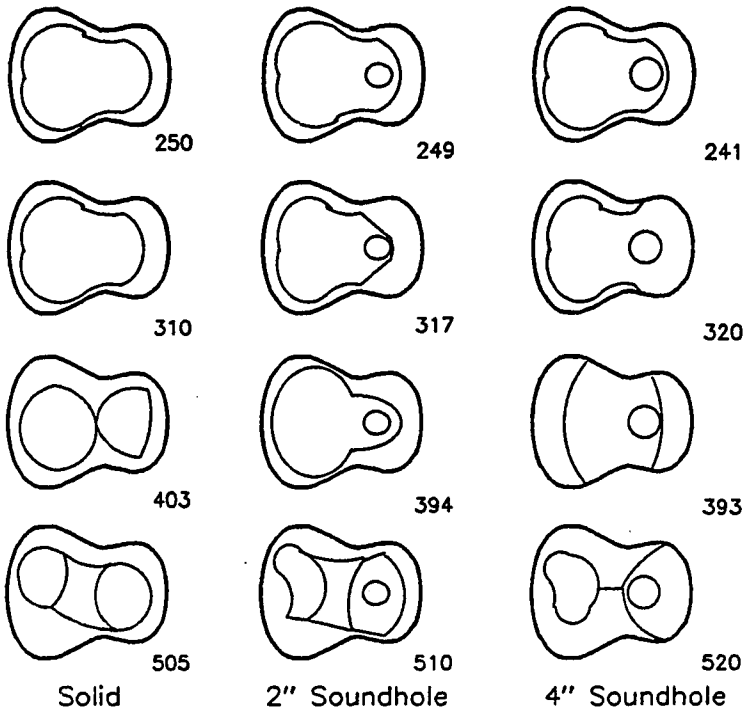

Figure 6.15 Soundboard Mode Shapes Dependance on Soundhole Size

The mode shape dependence on the soundhole size has been documented for a guitar with unsupported sides. The mode shapes of the soundboard change with the removal of the soundhole material indicating that the routed soundhole relief did not remove the soundhole material from affecting the soundboard's motion. The motion of the sides are seen to strongly effect the plate mode shapes in the case of the four inch diameter soundhole. Many of the nodal lines are running off the plate indicating important motion of the sides in the control of the modes.

The final brace to be added to the guitar box is the guitar bridge. The location of the bridge is critical to the ability of the guitar to play in tune and is traditionally the final step in the construction process.

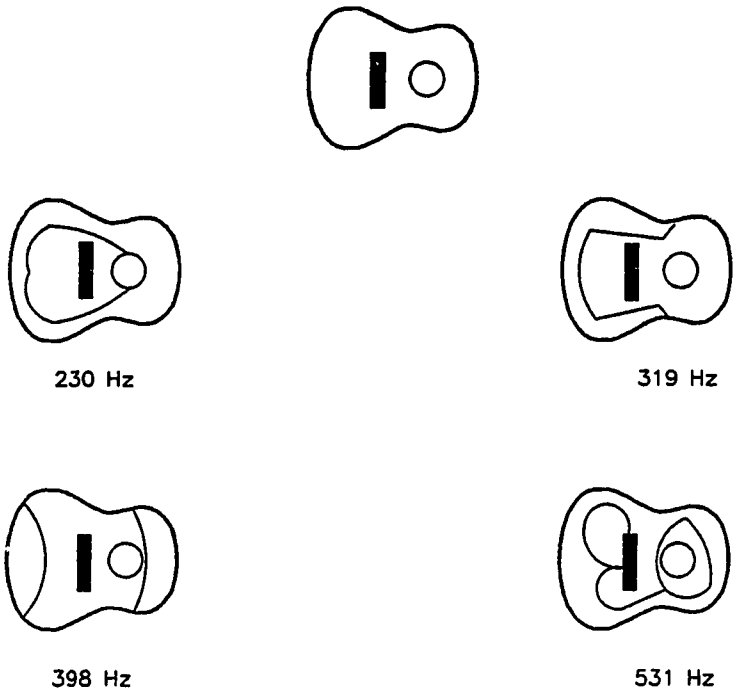

Figure 6.16 Soundboard with Bridge Mounted on Guitar Sides

The bridge used was an ebony Martin D-28 style dreadnought bridge which had been supplied completely carved with the basic guitar kit. The bridge placement was established by using the guitar body side at the neck block to determine the location of the fourteenth fret and then using a fret rule to locate the position of the bridge saddle from the fourteenth fret reference.

The soundboard has been completed, the braces, the bridge and the sides have been assembled the final assembly step is the completion of the box with a back. The standard dreadnought guitar back is an arched, braced plate structure. The arching of the back is accomplished by gluing a flat wood plate to curved beams. Modeling the arched, braced structure was beyond the scope of this work therefore a structurally simpler plate which would seal the backing cavity and fix the sides was desired. In order to include a back plate but isolate its resonances from those of the top, a honeycomb plate was build and used to complete these investigations.

6.2.3 Soundboard on Guitar Box

The guitar box is of an unconventional construction. The sides of the guitar are of the traditional bent rosewood. The back is a specially made honeycomb panel with 1/32 inch thick mahogany face sheets and a 1/2 inch thick nomex honeycomb core. The intent of the unique back is to produce a stiff back plate whose fundamental resonance is above that of the top plate.

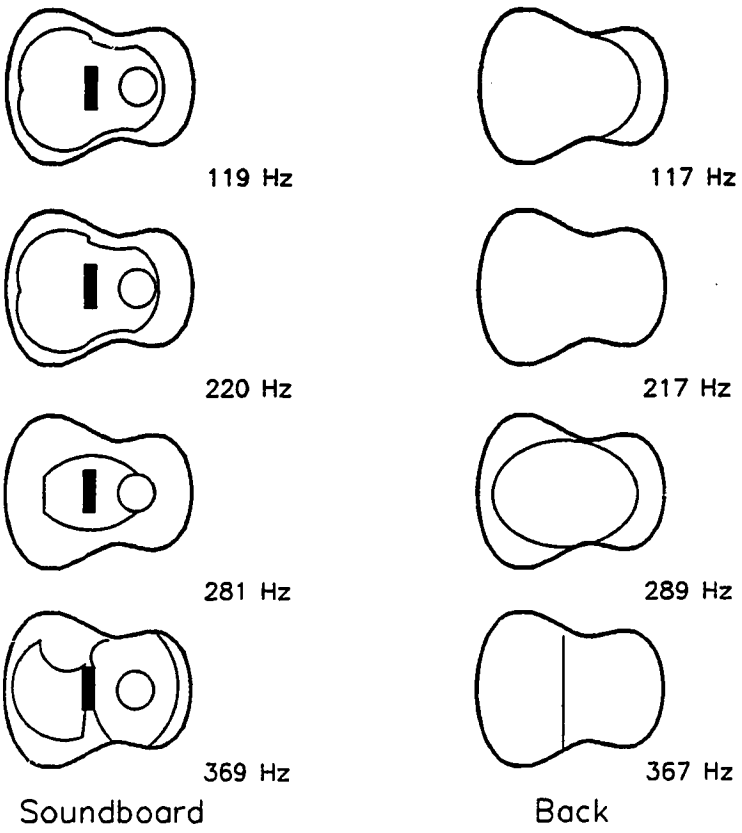

Figure 6.17 Modes of the Soundboard on the Guitar Box

A strong coupling of the soundboard and back modes is evident in the guitar box structure. The mode structure of the back is different than that encountered in the soundboard studies to date. The second back mode has no nodal lines. The fourth back mode has a nodal line running across the plate at the waist of the guitar and a nodal ring at the edge of the plate. The slight differences in the measured resonant frequencies of the top and back are within the repeatability of the frequency measurement system.

The ported box system should exhibit a Helmholtz resonator mode. At the Helmholtz frequency the soundhole radiation is particularly strong. A sound pressure level meter was placed near the soundhole during one of the frequency sweeps. The frequency of the lowest mode shape corresponds to the Helmholtz frequency of the system.

6.3 Sound Power Measurement

The sound power measurement was made in accordance to the ANSI standard on survey sound power measurements[50]. The sound power determination requires the measurement of the sound pressure on an imaginary sphere surrounding the source. The standard requires that the radius of the measurement sphere should be at least one meter or twice the largest dimension of the source. The guitar's dimensions are less than one half a meter in

---

50) American National Standard. Survey Methods for the Determination of Sound Power Levels of Noise Sources. ANSI S1.36-1979. New York, 1979.

length therefore a one meter radius is sufficient. The sound power spectra of the guitar was determined by measuring the spaced averaged sound pressure level.

The force input to the plate is not specified and absolute power spectra are not being sought, therefore the spaced averaged SPL is used as the power spectra without correction for measurement position.

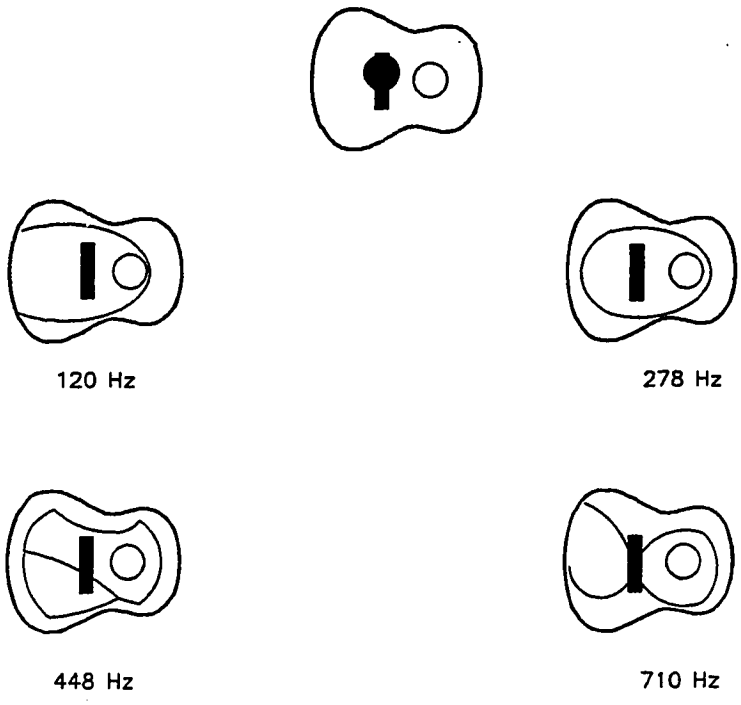

Figure 6.18 Soundboard Modes with Driver on Bridge

The driver available for these tests influenced the plate modes and resonances. The driven mode shapes are different than those of the guitar box. The mode shape differences can be observed by examining the modes in this figure with those in the previous figure (Figure 6.17).

Selection of the guitar mounting conditions for the estimation of the sound power levels is somewhat arbitrary. In order to produce an "typical" acoustic environment for the test a manikin was used to support the guitar. To the first order of approximation the acoustic and mechanical influences on the radiation characteristics of the guitar are reproduced with this approach.

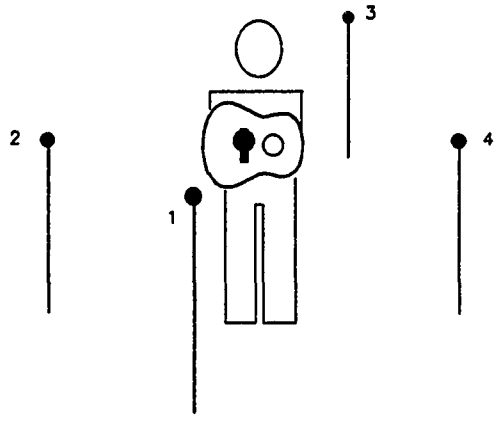

Figure 6.19 Sound Power Experimental Setup

A four point sound level survey was made to estimate the sound power level of the guitar. The measurement points were located at a height corresponding to the center of the guitar. Microphone point one was perpendicular to the center of the top plate of the guitar and the other microphones spaced at 90° intervals. A sound level meter using a slow-dBc setting was used to measure sound levels. These measurements were made outdoors on a cool windless day with a background level of approximately 60 dBc. Pauses in data collection were made to accommodate the occasional airplane and passing car. The measurement radius was 2.2 meters.

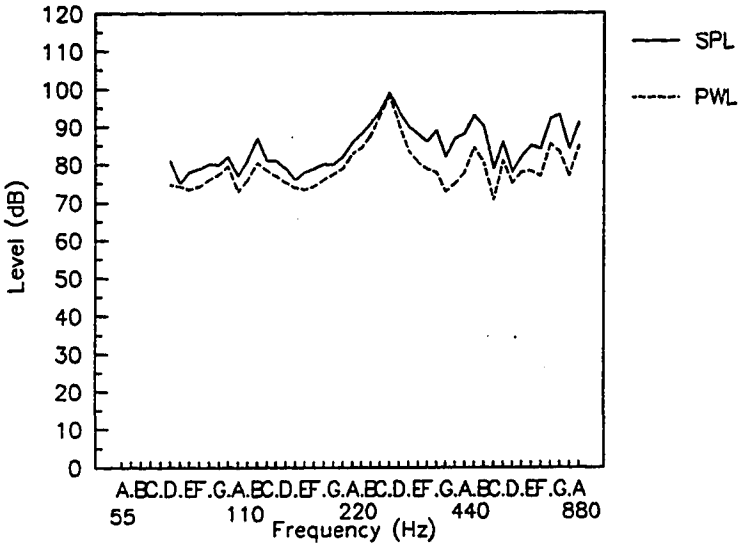

Figure 6.20 Measured Sound Power Spectra

The sound power level and sound pressure level, measured at microphone position 1 on figure 6.19, follow the same trends. Both levels peak at the major resonances of the box structure. The sound power level does not fall off below the "air resonance" as expected. This could be due to driver limitations and distortions or the fact the recording meter could not distinguish between fundamental and higher distortion harmonics produced by the driver. Subjectively, the driver working at the lower frequencies did not produce as pure a tone as it did in the upper ranges.

7 Prediction Model Evaluation

The analytic model and experimental mode shapes and resonance frequencies are compared in order to evaluate the ability of the model to predict soundboard behavior. The analytical model built to predict the dynamics of the guitar soundboard is limited to eight configurations. These eight model configurations can be represented in a graphical form as the corners of a cube in a model options space.

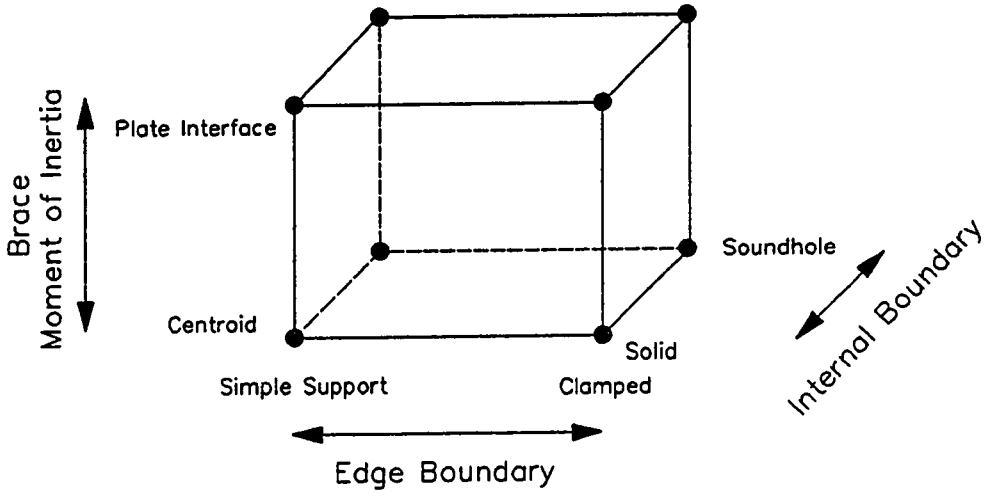

Figure 7.1 Analytical Model Options Space

The lower plane of the options space represents the various plate alone configurations which are modeled in the computer code. The outside edge of the plate can be modeled as a simply supported or clamped boundary

condition and the presence of an internal soundhole can be represented. The plate can be modified by adding braces which will modify the plate dynamics. The bending energies of the braces are dependant on the location of the neutral axis of the brace. Two of the options that are available are: (1) the neutral axis can be located at the centroid of the beam, and (2) the neutral axis can be located at the plate-beam interface.

The predictions presented in this chapter are based on the measured material properties of the various plate and brace elements unless specifically noted. The geometries are those described in the construction of the test instrument in chapter five. The fixtures used to support the plate assemblies are not modeled.

The first comparison is for the frequency of the fundamental mode of the braced plate system as the braces were added.

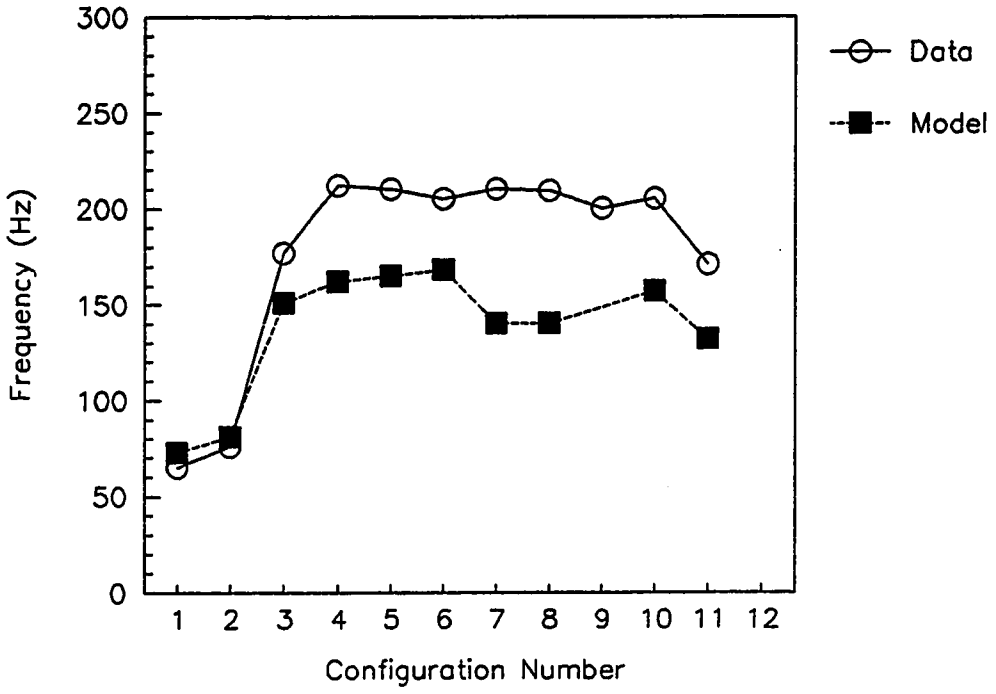

Figure 7.2 Fundamental Plate Frequency Prediction

In examining the fundamental mode of the plate as the bracing pattern is built up with the prediction model for a simply supported plate with the neutral axis of the braces lying at the plate-brace interface, the model predictions and the data track each other very well. The first configuration is for the bare spruce plate on the particle board fixture. The final config-

uration is for a fully braced guitar top with the braces carved into their final shapes. The intermediate configurations are detailed in Chapter 6.

The fundamental mode estimates are encouraging however a great deal of information on mode shape and higher order modes is neglected in this initial overview. The detailed mode shape predictions and measured mode shape data comparisons that follow should fill in some of this information.

7.1 Test Fixture Data Evaluation

In the following figures the measured data is presented on the left-hand side of the figure and the predictions on the right. The following data has been collected on the particle board fixture.

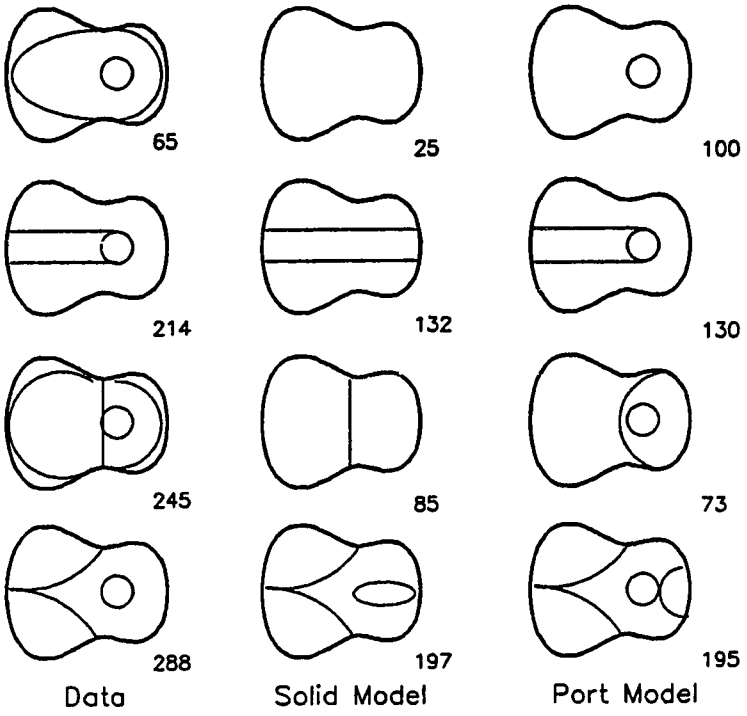

Figure 7.3 Simply Supported Bare Plate Predictions

The bare plate mode shape data are compared to the simply supported plate models for the spruce plate. The comparison based on mode shapes is good however the resonance frequencies differ. Note that the mode order of the predictions differs from that of the data. The resonance frequency predictions may be in error due to the inability to properly evaluate the plate's material properties due the limitations of the material sample as discussed in chapter six.

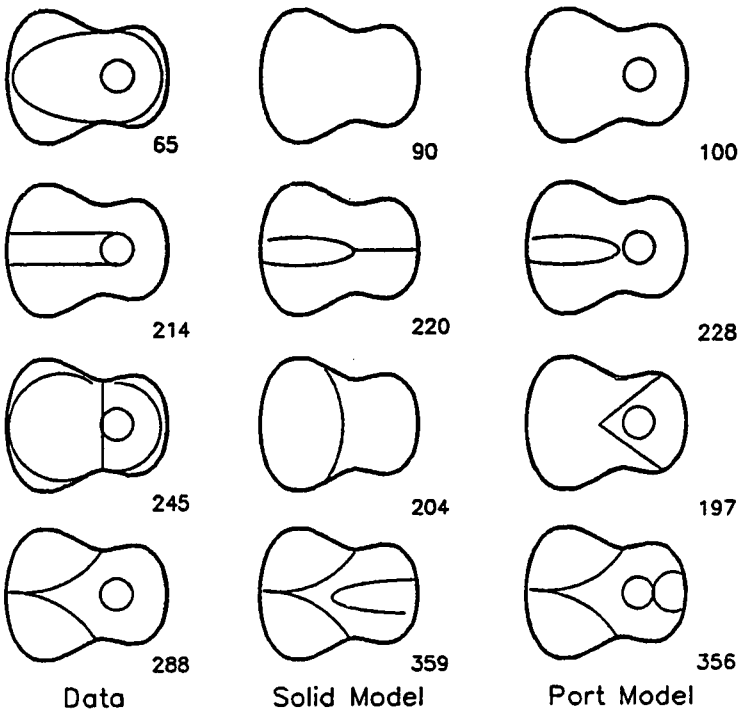

Figure 7.4 Clamped Bare Plate Predictions

An alternative analysis of the data is that the boundary conditions on the outside edge of the plate are not acting as if they were simply supported but are acting as if the were clamped. Using the model to predict the mode shapes of the clamped plate tend to over predict the resonant frequencies of the plate. The predicted mode shape order is once again different that of the data.

In reviewing the data neither the clamped nor simply supported models is superior in predicting the mode shapes of the bare plate. The plate data lies between the two extreme analytic models of a clamped or simply supported plate. This is to be expected.

The next predictions are on fully braced soundboards were the dynamics of the braces control the plate dynamics. Two locations for the neutral axis of the braces have been modeled and a selection between them for the best fit model is desired. The computational model which predicts the measured results most consistently is the simply supported plate with braces modeled as moving about the plate-brace interface. Only the simply supported plate model results will be presented.

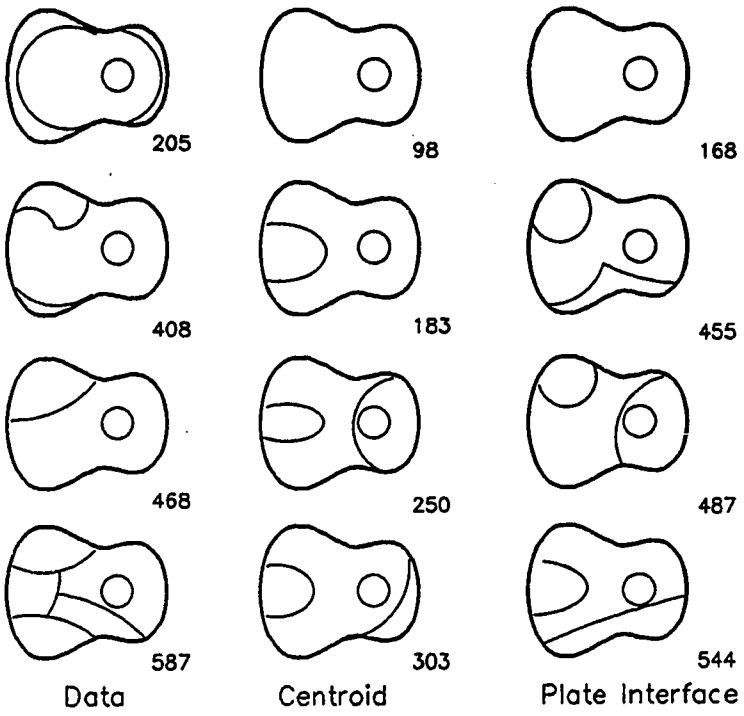

Figure 7.5 Simply Supported Braced Plate Predictions

In this configurations the braces have rectangular cross sections and have been tapered along their lengths. The plate is modeled as simply supported and the braces modeled with the two moments of inertia.

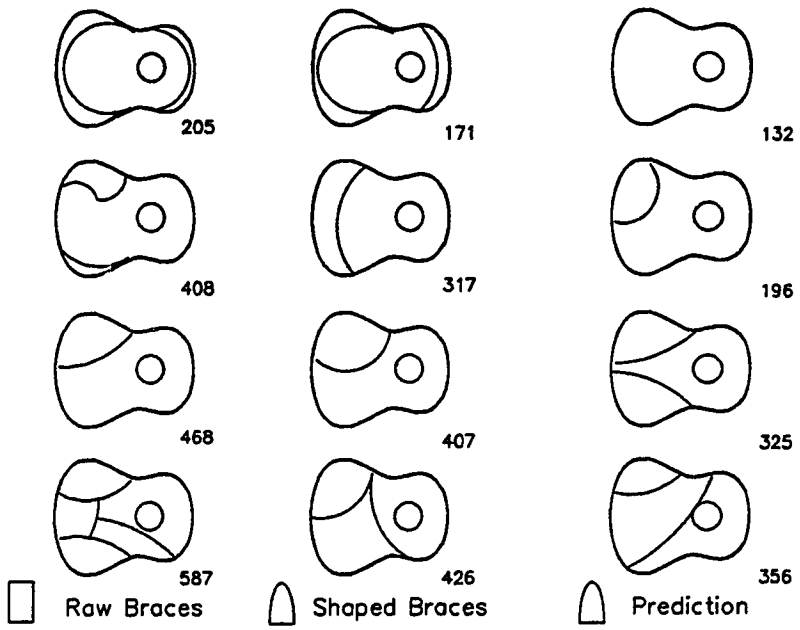

Figure 7.6 Simply Supported Carved Brace Plate Mode Shape Predictions

The influence of the cross sectional shape of the braces on mode shape is studied by caving the braces into the traditional semi-ellipitical shape and reevaluating the model predictions. The first two columns are the data before and after the braces are carved, the third is a prediction using the simply supported plate-brace neutral axis model. The predictions follow the same trends as the data.

The prediction of mode shapes and resonance frequencies are dependent on the material properties of the sound-

board and its braces. Errors in the determination of these material properties will result in errors in the prediction of the system response. The comparisons which have been presented in this chapter are based on the measured material properties of the elements. In the appendix a number of spruce materials have been defined from material properties collected from the literature. These spruces, designated Spruce I, Spruce II and Spruce III will be used to examine the influence of changing the material properties of the top plate and bracing stock.

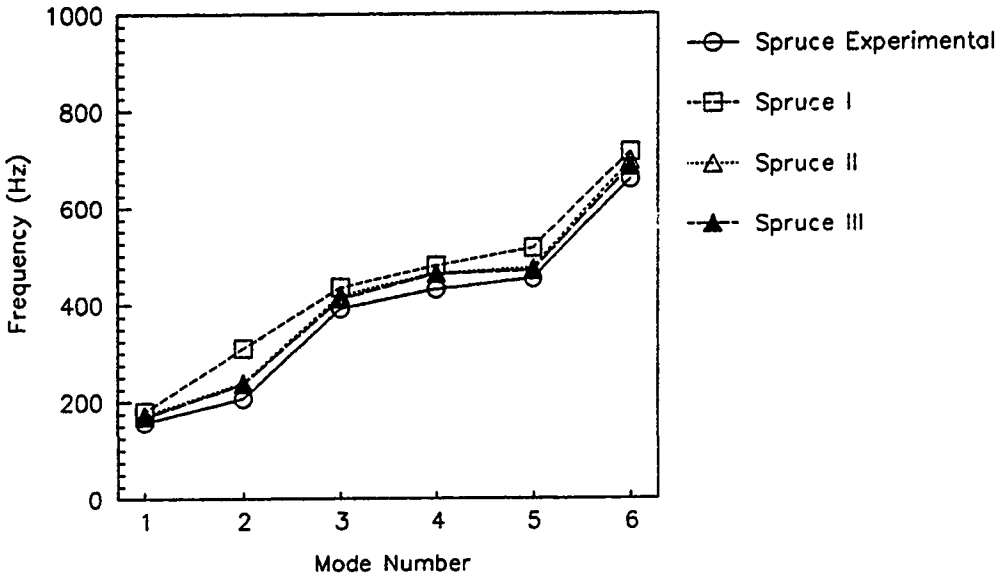

Figure 7.7 Influence on Top Material Properties on Plate Mode Predictions

The soundboard material substitution shifts the resonance frequencies up with increasing modulus. The ratio of the along the grain modulus between the baseline experimental spruce and Spruce I is approximately 1:3 (7.4:19.6). The frequency shifts indicate that the plate material is not dominating the dynamics of the plate in this configuration. If the plate had been dominating the plate dynamics the ratio of the fundamental frequency would shift as the square root of the modulus ratio. Changes in the bracing materials should demonstrate a larger control on the plate dynamics.

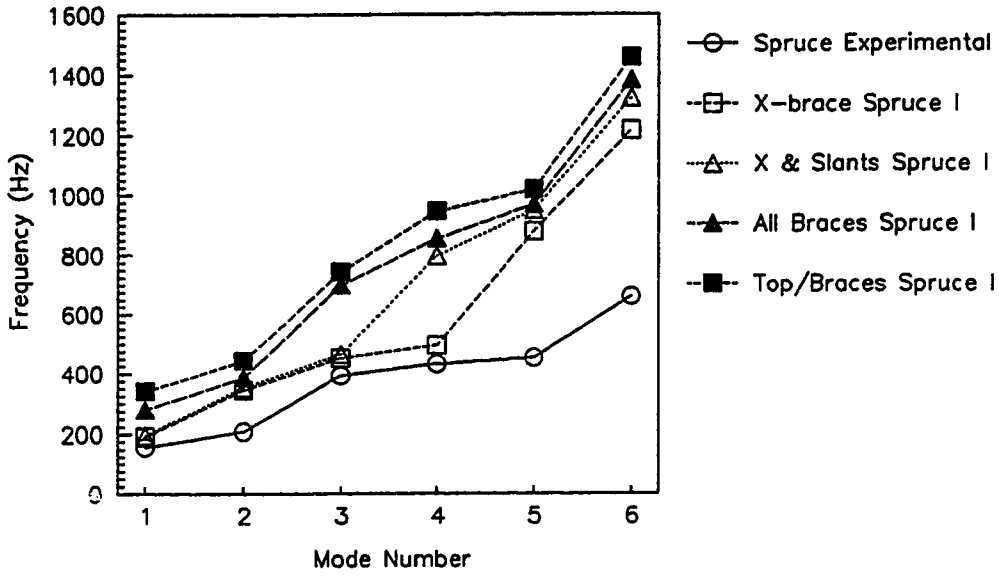

Figure 7.8 Influence on Brace Material Properties on Plate Mode Predictions

Dramatic changes in the natural frequencies are encountered when the bracing materials in the guitar plate are replaced with the Spruce I material. A noticeable shift in the resonance frequencies was observed when the main X-Brace material was replaced. The resonance frequency by mode order curve begins to sharpen when both the X-brace and the Slant brace materials are changed. The smaller secondary braces continue this raising of the frequency of the higher order modes as they are replaced with the stiffer material. A final prediction of a guitar constructed from the Spruce I material dramatically shows the variance which should be expected when predicting the dynamics of guitar soundboards with generic material properties.

The discussion on the influence of material properties on the prediction of guitar soundboard dynamics has been brief and has been included only to point out the requirement for good material property extraction methods in the pursuit of musical instrument modeling techniques.

7.2 Soundboard on Guitar Sides Data

The model and data comparison using the simply supported plate prediction model and the special particle board fixture are encouraging, however the validly of using the fixture as a representation of the guitar back and sides has not been established. The next set of comparisons are based on the soundboard mounted on a set of rosewood guitar sides and a specially constructed honeycomb back with the soundhole opened up and a traditional ebony bridge attached.

A number of experiments were conducted without the back to explore the type of boundary conditions the sides alone present to the soundboard.

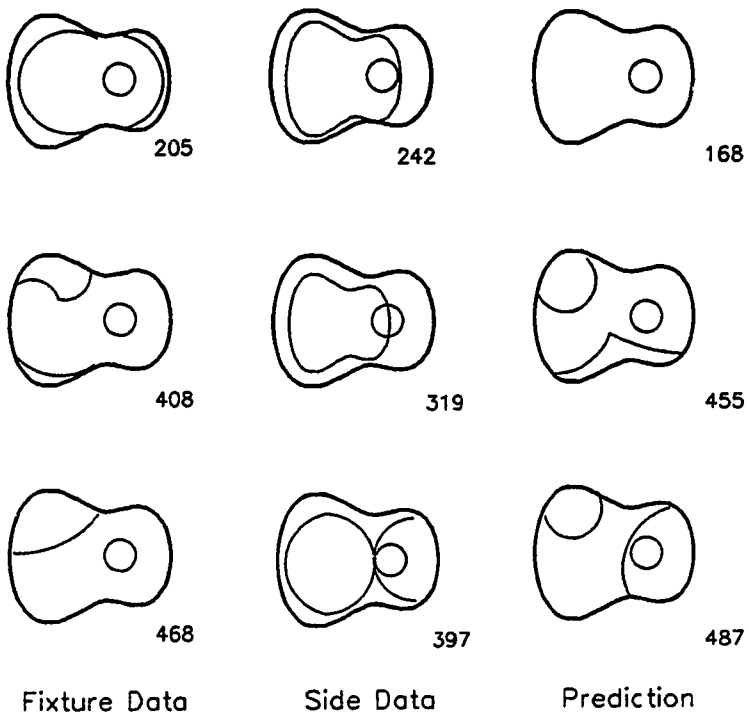

Figure 7.9 Experimental Boundary Condition and Simply Supported Model Comparison

The side alone data does not follow the trends established in the model or the fixture data. Note the presence of the two ring modes in the side mounted

data. The simply supported plate model fails to predict the plate dynamics in the case of the unconstrained sides.

The edge of the soundhole of the plate used in these experiments has been routed to one half the plate's thickness which adds some confusion to the study of soundhole diameter effect using this plate. Soundhole studies using the uniform plates showed very little influence on the resonance frequencies for a wide range of soundhole diameters. The braced spruce soundboard demonstrates the same result.

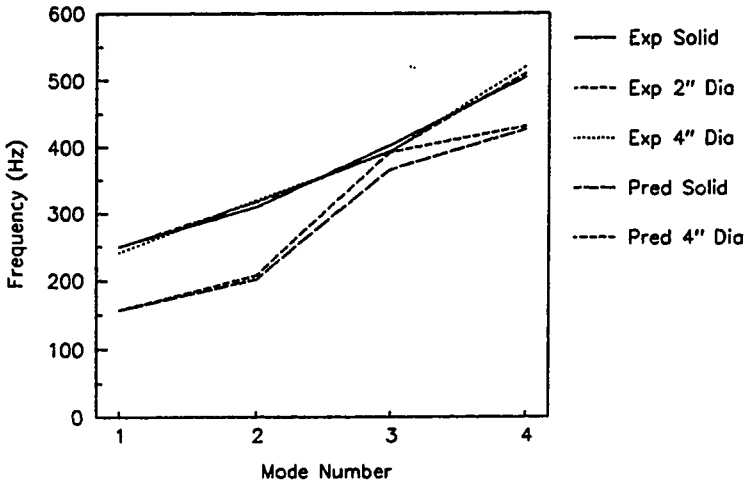

Figure 7.10 Soundhole Influence on Soundboard Dynamics

The mode shape evolution associated with the progressive removal of the soundhole material was presented in figure 6.15. The predictions and the experimental data agree on the limited influence of the soundhole size in the braced configuration.

The final stage of assembly was the addition of the bridge to the soundboard and then attaching the back plate, thus sealing the box. In completing the backing cavity the air mode is observed for the first time in these experiments. This air mode is associated with a Helmholtz type resonator mode.

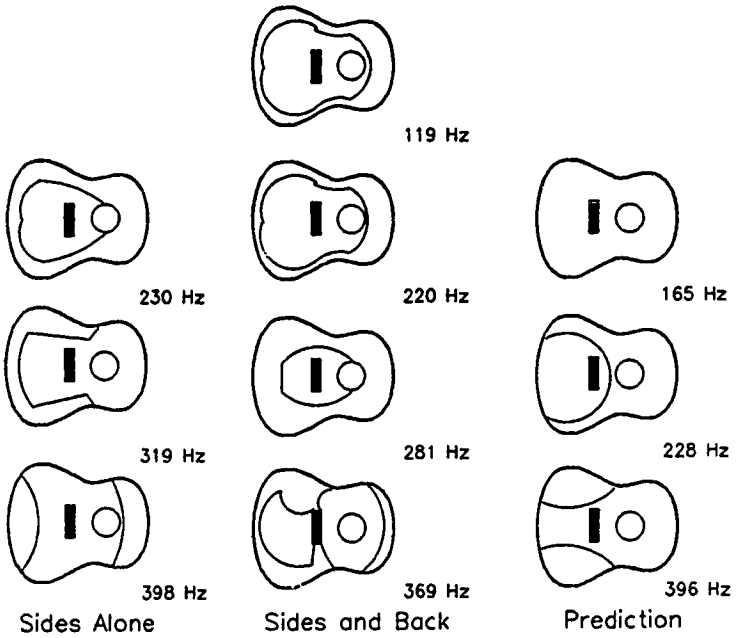

Figure 7.11 Final Assembly Data and Predictions

The frequencies of the top plate modes are lowered with the addition of the bridge. The fundamental is moved from 242 Hertz without the bridge to 230 Hertz with the bridge. The mode shapes are also changed and this can be studied by comparing figures 7.8 and 7.10. Mode shape predictions are not exact but do follow the basic changes observed in the experimental results.

7.3 Acoustic Radiation from Guitar Box

The acoustic power comparison are clouded by the consistent under prediction of experimentally determined modal frequencies by the prediction model. The model of the soundboard predicts the basic spectrum-shape shifted down approximately four semitones.

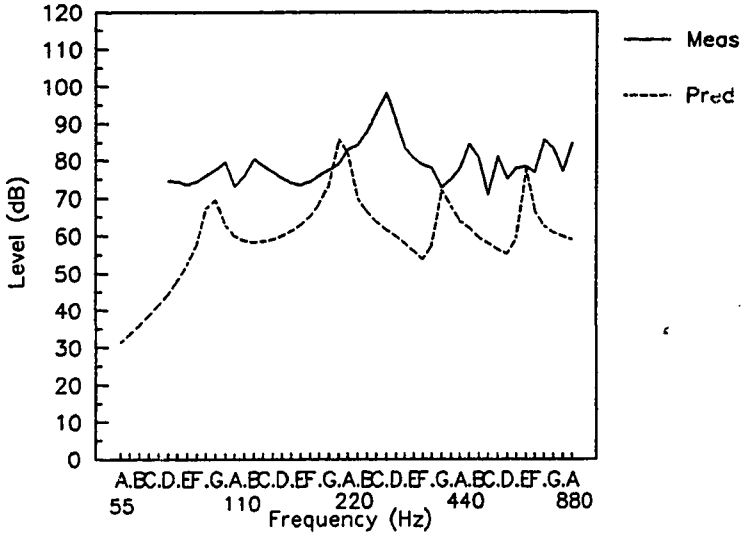

Figure 7.12 Sound Power Prediction

The "air" and "wood" resonances as well as the two upper resonances have the same positions relative to one another in both the data and in the prediction. Recalling that the soundboard models consistently under predicted the resonant frequencies it follows that the radiation prediction would have same trend. An intermediate peak between the two upper resonances in the measured spectrum may be due to unmodeled back or side modes.

There is a low-frequency double peak feature which is not explainable with a simple frequency shift. This feature may be a result of the changes in the mode shapes of the plate which occurred after the attachment of the driver system. To correctly interpret the sound power-spectra a model of the driver system is required. A complete driver model was not built.

8 Recommendations for Further Work

The work developed in this dissertation has been oriented towards the construction of prediction methods for the sound radiated from a guitar soundboard. Further work may take one of two paths, the first being an extension of the mechanical-acoustical model and the second a study of how the radiated sound spectra translates into the psychological evaluation of the quality of a guitar. The mechanical model extension is not trivial and many of the simplifying assumptions used in the current effort will have to be reevaluated. The psychological acoustic study will require the testing of both guitars and human preferences; this task is required if prediction of musical instrument properties is to move into instrument design.

8.1 Extension of the Mechanical Model

In the current work a model of a guitar soundboard system has been built and evaluated. The low frequency behavior of the backing cavity and soundhole have been included. The augmented soundboard model has been used to predict the radiated acoustic power spectra from this simplified representation of a guitar. The major subsystems are shown to dominate the low frequency performance of guitars but do not completely describe the total system dynamics. Let the guitar be subdivided into seven major dynamic subsystems. Currently three of these have been modeled, the plate with its bracing system, the soundhole and the cavity. Additional subsystems could be added to the current model to develop a complete representation of a guitar. The seven

subsystems would be the plate, the soundhole, the cavity, the back, the sides or walls, the neck and the strings.

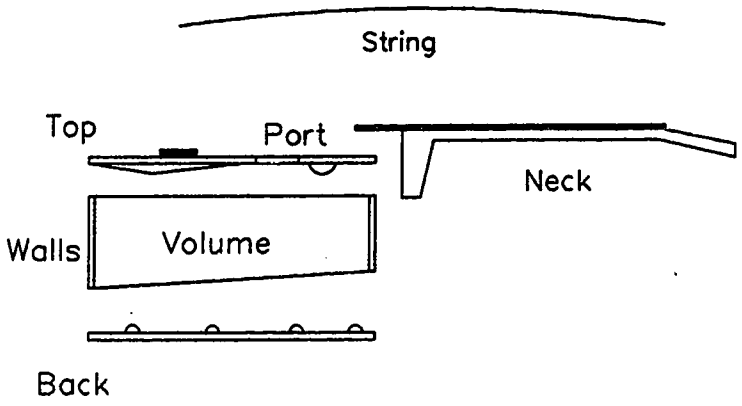

Figure 8.1 Extended Model Diagram

The system dynamics can be represented by a matrix equation relating the major subsystems and their interactions. The partitioned upper left corner of the system matrix represents the system which has been addressed in this work.

8.1)

$$\begin{bmatrix} top & M_{tv} & R_{tp} & | & R_{tb} & M_{tw} & M_{tn} & M_{ts} \\ M_{vt} & vol & M_{vp} & | & M_{vb} & M_{vw} & - & - \\ R_{pt} & M_{pv} & port & | & R_{pb} & R_{pw} & - & - \\ --- & --- & --- & -+- & --- & --- & --- & --- \\ R_{bt} & M_{bv} & R_{bp} & | & back & M_{bw} & M_{bn} & - \\ R_{wt} & M_{wv} & R_{wp} & | & M_{wb} & walls & M_{wn} & - \\ M_{nt} & - & - & | & M_{nb} & M_{nw} & neck & M_{ns} \\ M_{st} & - & - & | & - & - & M_{sn} & string \end{bmatrix} \begin{Bmatrix} a_t \\ a_v \\ a_p \\ a_b \\ a_w \\ a_n \\ a_s \end{Bmatrix} = \begin{Bmatrix} 0 \\ 0 \\ 0 \\ 0 \\ 0 \\ 0 \\ 0 \end{Bmatrix}$$

M_{ab} = Mechanical Coupling Between Elements a, b

R_{ab} = Acoustic Radiation Coupling Between Elements a, b

a_b = Amplitutes of the Assumed Modes for Element b

The soundboard plate and its bracing system has been modeled with 16 assumed modes, the modal series could be extended to refine the model. The cavity volume model has a single mode in the current model, however, a modal structure has been observed experimentally. The modeling of these interior volume modes would require an increase in the number of assumed modes for this subsystem. The port has been modeled as a slug of air moving with uniform velocity. If the complexity of the cavity model is increased, then the use of the simple port model would need to be reviewed. The port model would eventually be replaced by a model which could account for a nonuniform velocity across the soundhole. Further enhancements to the model will require the generation of new subsystem element models.

The back of the guitar interacts with the backing volume and would be a logical first addition to the guitar model. It is tempting to apply the soundboard model to the design of the back plate however this would ignore the fact that guitar backs are generally curved plates. Plate curvature would have to be added to the stiffness matrix calculations for the plate and beam models in order to predict the dynamics of the back plate and its beam structure.

The walls or sides of the instruments are curved plates which are forced along their edges by the top and back plates. Selection of an appropriate interface condition for an analytical model would require a great deal thought. Typical edge binding practices would suggest that the local angle between the top and the side remains at 90 degrees. A point collocation method may be an appropriate method to impose the top-side-back boundary condition while maintaining the assumed mode approach.

The neck of the instrument is joined to the body with a large wooden block called the heal block. The heal block is glued to the top, back and sides of the instrument coupling these three major subsystems. The neck may act as a vibration absorber at its resonances reducing or retuning top plate resonances. Player appeal is also involved in the neck, some very stiff necks are considered "cold" and "unresponsive".

The strings are the final addition to the model and with them the analytic guitar can be played in simulation. The eigenmodes of the system at the string frequencies yield information on the radiation of the instrument during the ring of the string. In addition the strings couple the neck and top plate and imposes static loads on the total structure. A string model removes the assumptions due to the introduction of a forcing driver in the modeling of forced vibration response of the guitar.

The radiation model for the top plate and port system was a discrete Rayleigh integral of a boundary with specified velocity radiating into a semi-infinite half space. The guitar is a thin shell with an interior and exterior sound field communicating through an open port. In theory the problem may be attacked using the Helmholtz radiation integral equation. The Helmholtz radiation equation in terms of the acoustic velocity potential[51] is;

8.2)

$$\int_S \left(\phi(r) \frac{\partial G(r,r_0)}{\partial n} - G(r,r_0) \frac{\partial \phi(r)}{\partial n} \right) dS = C\phi(r_0)$$

Where the Green's function for a point source is;

---

51) A. F. Seybert, T. K. Rengarajan, "The use of CHIEF to obtain solutions for acoustic radiation using boundary integral equations", J. Acoust. Soc. Am. 81(5) 1987.

8.3)

$$G(r,r_0) = e^{-jkR}/4\pi R$$

and the separation distance between the source and observer points is;

$$R = |r-r_c|$$

The velocity potential is related to the acoustic pressure by a frequency dependent scaling factor,

8.4)

$$p(r) = j\rho ck \ \phi(r)$$

The normal velocity of the surface as expressed in terms of the velocity potential is,

$$v_n(r) = \frac{\partial\phi(r)}{\partial n}$$

The constant on the right hand side of the equation is dependant on location of the source point in the space,

8.5)

$$C = 4\pi + \int_S \frac{\partial(1/R)}{\partial n} dS$$

for simple geometries the constants are;

$C = 4\pi$ Field Points

$C = 2\pi$ Surface Points (with unique tangents)

$C = 0$ Interior Points

The Greens' function and normal velocity would be specified to compute the surface pressures, the surface pressures would modify the system dynamic and the normal velocities making the solution approach iterative. Helmholtz integral evaluations have been the subject of many current studies. The guitar falls into a class of thin shell problems where one wishes to model the interior and exterior sound fields around a surface which is thin compared to a wavelength. Shell type problems are considered the most difficult class of problem to solve numerically[52].

52) A. F. Seybert, personal conversation during, Acoustic Prediction Using the Boundary Element Method Short Course, 1988.

The current approach has been to solve or propose the solution of a number of steady state representations of the guitar. The guitar sound is transient, the sound of a plucked string, therefore time domain predictions would be useful in the synthesis of guitar tone for subjective evaluation. The time dependent formulations will greatly increase the work required in the acoustic predictions but would allow for the evaluation of guitar designs, using computer music synthesis techniques, before they were built.

The extension of the guitar model is a long term project and requires a constant review and validation of the techniques based on measured data. In general predictions generated are of limited use to the guitar designer if the predictions cannot be tied to player preferences. A real time simulation approach would give the designer the ability to evaluate a guitar design before a prototype is built this capability lies in the future. The alternate approach is to try and correlate what is predictable to player preferences.

8.2 Psychological Acoustic Studies

The evaluation of the quality of a guitar is a function of the instrument's dynamics, radiation characteristics and the expectations of the listeners. An instrument which has been designed to support a soft vocal ballad may not have the volume and punch to play big band swing music, the strong bass of the dreadnought guitars used in bluegrass and country music may lack the balance to play modern jazz, the fat sound of the delta

blues guitar may muddy the quick passages of the afro-cuban-latin repertoire, ... the comparisons are endless. The point is that music and instruments have evolved together and no one instrument is likely to be judged superior in all applications. The need or desire for multiple instruments is recognized by many players of steel string guitars, if they play a wide range of music. Classical guitar players are more inclined to find a a single compromise instrument on which to play their entire repertoire.

In order to use the modeling techniques developed in this study a correlation between the predicted response and the subjective evaluation of an instrument is required. The problem is difficult and the intent of this section is to point out a possible plan of attack based on psychological acoustic testing done on the quality of classical guitars and loudspeakers.

A major project which is directly aimed at the correlation of guitar quality with spectral features is the work of Jurgen Meyer[53]. In this study 15 classical guitars were judged by 40 listeners using 6 compositions of 20 to 25 second duration, multiple randomized opportunities to listen to each guitar were given to each observer. The compositions were both monophonic and polyphonic and presented to the listeners through

---

53) Jurgen Meyer, "Quality Aspects of Guitar Tone", in Function Construction and Quality of the Guitar, edited by Erik V. Jansson, Stockholm, The Royal Swedish Academy of Music, 1983.

headphones. In Meyer's limited population of 15 classical guitars three dominant spectral peaks were noted. These three spectral peaks can be used to model the low frequency behavior of the traditional classical guitar. Meyer worked with a number of spectral features such as grouping sets of 1/3 octave band levels and overall spectrum levels. Only the results correlating radiated spectra spectral features with guitar quality are discussed here.

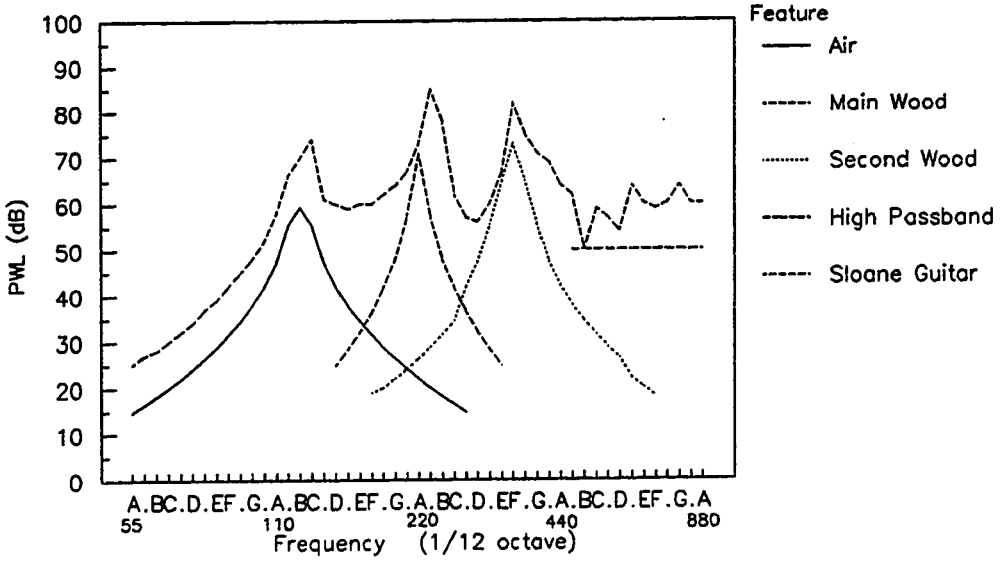

Figure 8.2 Meyer Criteria and Sloane Guitar Response

According to Meyer, the criteria for the first or air resonance is that it should have a low Q and be placed

between 95 and 112.5 Hertz. The exact placement of the resonance is not critical but should be at least 25 cents from the nearest tone played. A cent is 1/100 of a semitone.

The criteria for the second or main wood resonance is that it have a high level, lie between 184 and 242.5 Hertz. The observation that in many guitar the air and main wood resonance lie approximately an octave apart had no clear correlation on quality. The resonance should be tuned away from a speaking tone.

The second wood resonance was the best correlator with guitar quality in Meyer's study. This resonance should be placed between 390 and 440 Hertz, exact placement in this range was not a critical factor. A high peak level and high Q were desired.

Meyer's criteria are based on a number cf structurally similar guitars. In order expand the generality of Meyer's criteria a wider range of guitars would have to be tested. The quality metric would also have to be refined based on musical application and listener preference. What Meyer has stated is that peak level, resonance Q, and frequency placement are important to the nature of the sound quality of a guitar in that order.

The question of how to test guitars raises many questions which are difficult to answer. Should musicians be used to perform "live" on the test guitars? Should the listeners see the instrument? What should the

acoustic space be like? Should loudspeakers or headphones be used? How long should an individual instrument be played for the listener? If both musicians and the general public are used as observers how should there responses be averaged? What questions should be asked of the listeners and how should their responses be normalized? A long term effort has been underway at the National Research Council of Canada to answer such questions in the evaluation of loudspeakers.

Floyd Toole at the National Research Council of Canada has designed questionnaire and instructions for the evaluation of loudspeakers[54]. Part of his efforts such as the evaluation of the sound field spatial definition in a stereo setting is of little use in the study of guitars, however his efforts in describing the coloration in loudspeakers with terms like clarity, softness, fullness, and brightness are directly applicable to the study of guitars. His overall quality rating had two parts, a pleasantness and a fidelity, which may prove to be useful concepts in the description of guitar sound quality.

Toole's verbal definitions can be modified to apply to the guitar. Using these definitions tests could be conducted to help define the sound quality of guitars on a relative basis. The following definitions are those of Toole reworded to apply to the listening of guitars.

---

54) Floyd E. Toole, "Subjective Measurements of Loudspeaker Sound Quality and Listener Preference", J. Audio Eng. Soc. Vol. 33, No. 1/2, 1985.

Sound Quality Definitions (after Toole)

Clarity/Definition:
Refers to the ability to hear voices within complex arrangements. The individual notes should be distinguishable, with well defined attacks, not diffuse or muddled.

Softness:
Refers to the quality of high frequency sounds. These should be smoothly natural, neither overly subdued and mild, nor excessively hard, shrill, strident or sharp.

Fullness:
Refers to the quality of low frequency sounds and their balance between middle and high frequency sounds. A good guitar should be neither too full or too thin.

Brightness:
Refers to the balance of the high frequency sounds with respect to the middle and low frequency sounds. A good guitar should be neither too bright nor too dull.

Pleasantness:
Is an overall rating that concentrates on the lack of aggravations and annoyances in the performed music.

Fidelity:
Is the overall rating which describes how closely the tested instrument approaches your ideal of the "perfect" guitar sound.

Test formats can be constructed using a fixed point scale or magnitude estimation scheme using these conceptual criteria. Meyer's work was based on a single

quality number for each instrument from each observer. A more refined test following Toole would be more involved but may uncover some correlation between spectral features and sound quality. How does a hard, thin, bright guitar differ from a soft, full, dull guitar in their spectral shapes?

The development of an ideal listening room is discused in Toole's second paper[55] along with observations that spectral peak anomalies are more perceivable than drop outs or dips. It has also been stated that the ear will detect the area under a spectral peak. Can spectral peak level and resonance Qs be traded to achieve sound quality? In the second part of this paper[56] Toole addresses the differences in sound power response curves and on axis sound pressure response curves. In the study of guitars another observation point may be needed is that of the musicians ear. How does the instrument sound to the player and how is that related to the listening audience or recording microphone? Toole's latest paper[57] discusses the audibility and detection of resonances in loudspeakers. The resonances are viewed as modifying the timbre of the music

---

55) Floyd E. Toole, "Loudspeaker Measurement and Their Relationship to Listener Preferences: Part 1 ", J. Audio Eng. Soc. Vol. 34, No. 4, 1986.

56) Floyd E. Toole, "Loudspeaker Measurement and Their Relationship to Listener Preferences: Part 2 ", J. Audio Eng. Soc. Vol. 34, No. 5, 1986.

57) Floyd E. Toole, Sean E. Olive, "The Modification of Timbre by Resonances: Perception and Measurement", J. Audio Eng. Soc. Vol. 36, No. 3, 1988.

played through the loudspeakers; an interesting perspective, in the guitar strong resonances are used to define timbres. The impact of resonances on the time domain response of the loudspeaker is also introduced. Mr Toole's efforts warrant continual review in light of perception and quality testing of guitars.

The testing of guitars to understand the relationship between guitar sound quality and spectral response is a difficult and time consuming project. The correlation of design criteria and sound quality being the large task. Future success in mechanical modeling of musical instruments is dependent on the development of quality correlation data and the study of timbre.

9 Summary and Conclusions

> Information is not knowledge.
> Knowledge is not wisdom.
> Wisdom is not Truth.
> Truth is not beauty.
> Beauty is not love.
> Love is not music.
> Music is THE BEST.

Frank Zappa, Joe's Garage, Act III, Scene fifteen.

9.1 Summary

The subject of this work is the mechanical design of guitars without regard to the subjective evaluation of the tonal quality of the completed instrument. A complete study of the subjective evaluation of instruments along with the identification of mechanical-acoustical properties which define the desirability of design changes is yet to be made. Until the correlations between tonal characteristics and mechanical design are established, the simple model proposed here is adequate to explore design changes in guitar soundboards.

Major trends in the dynamics of guitar soundboards can be predicted with a Rayleigh-Ritz model of a simply supported orthotropic plate reinforced with simple beams. The model is useful in examining the major differences between bracing system, soundhole size and backing-cavity volume. Bracing systems have been observed both experimentally and analytically to dominate the dynamics of conventional guitar soundboards. The uncertainties of the predictions lie more with the determination of material properties of the woods used in the soundboard than in the analytic limitations of

the model. The calculated sound power spectra, based on a small array of piston sources in an infinite baffle, predicts the basic character of the experimentally determined sound power spectrum shapes.

9.2 Background

This work is an extension of the ideas presented by John Schelleng in his benchmark paper[58] "The Violin as a Circuit". In this 1963 paper, John Schelleng proposed an equivalent circuit model for the violin. Schelleng's general model included a soundboard with many resonances, a simple backing cavity and a radiation estimate based on the net volume velocity of the system. A simplified two degree-of-freedom model was discussed in detail exploring the cavity-soundboard interaction. The simplified equivalent circuit with the single top mode and a simple backing cavity has been the principal model used in the literature in describing the acoustics of the guitar. In the current work the soundboard model is restored to a multi-resonant form by modeling the guitar soundboard as a braced plate using a Rayleigh-Ritz technique.

---

58) John Schelleng, "The Violin as a Circuit", J. Acoust. Soc. Am. 35(3) 1963.

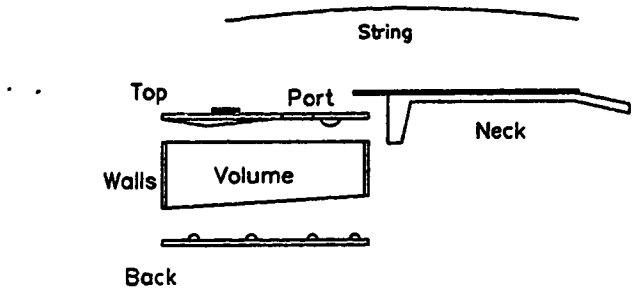

Figure 9.1 Exploded Guitar Model Diagram

The system dynamics can be represented by a matrix equation relating the major subsystems and their interactions.

9.1)

$$\begin{bmatrix} top & M_{tv} & R_{tp} & | & R_{tb} & M_{tw} & M_{tn} & M_{ts} \\ M_{vt} & vol & M_{vp} & | & M_{vb} & M_{vw} & - & - \\ R_{pt} & M_{pv} & port & | & R_{pb} & R_{pw} & - & - \\ --- & --- & --- & -+- & --- & --- & --- & --- \\ R_{bt} & M_{bv} & R_{bp} & | & back & M_{bw} & M_{bn} & - \\ R_{wt} & M_{wv} & R_{wp} & | & M_{wb} & walls & M_{wn} & - \\ M_{nt} & - & - & | & M_{nb} & M_{nw} & neck & M_{ns} \\ M_{st} & - & - & | & - & - & M_{sn} & string \end{bmatrix} \begin{Bmatrix} a_t \\ a_v \\ a_p \\ a_b \\ a_w \\ a_n \\ a_s \end{Bmatrix} = \begin{Bmatrix} 0 \\ 0 \\ 0 \\ 0 \\ 0 \\ 0 \\ 0 \end{Bmatrix}$$

M_{ab} = Mechanical Coupling Between Elements a, b

R_{ab} = Acoustic Radiation Coupling Between Elements a, b

a_b = Amplitutes of the Assumed Modes for Element b

This study follows the Schelleng model, concentrating on the elements in the upper left corner of the system matrix. These elements are 1) the soundboard and its bracing system, 2) the backing cavity and 3) the sound-hole or port.

In the last few years a number of papers have used the simplified Schelleng model to explore the acoustics of the guitar. Caldersmith[59], Christensen[60], and Firth[61] have all examined guitars and modeled them using a two-degree-of-freedom model.

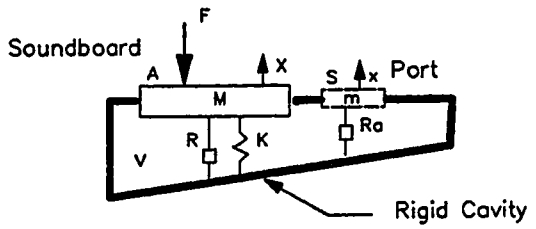

Figure 9.2 Schelleng's String-Instrument Model

---

59) Graham Caldersmith, "Guitar as a Reflex Enclosure", J. Acoust. Soc. Am. 63(5) 1978.

60) Ove Christensen, Bo B. Vistisen, "Simple Model for Low-Frequency Guitar Function", J. Acoust. Soc. Am. 68(3) 1980.

61) Ian M. Firth, "Physics of the Guitar at the Helmholtz and First Top-Plate Resonances", J. Acoust. Soc. Am. 61(2) 1977.

The studies of guitars using this model are limited to the low-frequency behavior of the instrument, typically below 200 Hz. The system is governed by the following equations.

9.2)

$$M\ddot{X} + R\dot{X} + KX = A\Delta P + F$$

$$m\ddot{x} + R_a\dot{x} = S\Delta P$$

The lumped parameters are shown by their corresponding system elements in the above figure.

The cavity is assumed to be much smaller than an acoustic wavelength and therefore the pressure in the cavity is directly related to the change in cavity volume,

9.3)

$$\Delta P = -\frac{\rho c^2}{V}(AX + Sx)$$

ρ = density of air

c = speed of sound

The pressure equation and the force-balance equations can be written as a three-by-three matrix,

9.4)

$$\begin{bmatrix} K - \omega^2 M + i\omega R & -A & 0 \\ \frac{\rho c^2}{V}A & 1 & \frac{\rho c^2}{V}S \\ 0 & -S & -\omega^2 m + i\omega R_a \end{bmatrix} \begin{Bmatrix} X \\ \Delta P \\ x \end{Bmatrix} = \begin{Bmatrix} F \\ 0 \\ 0 \end{Bmatrix}$$

ω = radian frequency

The radiation model associated with the simplified Schelleng model is that of a simple source with a source strength based on the net volume velocity of the source.

9.5)

$$P_a = \frac{\omega^2 \rho (AX + Sx)}{4\pi |r|}$$

This simplified Schelleng model will estimate the first two resonant frequencies of an instrument and its radiation characteristics. The first two resonances of a typical guitar lie at approximately 100 and 200 Hz.

9.3 Structural-Acoustic Model

In this model the Schelleng simplified model has been expanded to include 1) a number of soundboard modes and 2) the first-order effects of the radiation loading.

The structural-acoustic model is intended to represent the low-to-mid frequency behavior of a guitar (80-800 Hz). The Rayleigh-Ritz technique is used to model the soundboard as a simply supported, orthotropic, thin plate of uniform thickness reinforced by a beam substructure. The difference between the cavity back pressure and the radiation pressure is applied to the plate in dynamics calculations. Point forces are used to represent the strings and drive the model. The simplified Schelleng model is expanded to include the extra degrees-of-freedom needed to represent soundboard modes.

9.6)

$$\begin{bmatrix} [K]-\omega^2[M] & -\int\int w dy dx & 0 \\ C_{net}\int\int w dy dx & 1 & C_{net}\pi r^2 \\ 0 & -\pi r^2 & -\omega^2 m_{port}+i\omega r_{port} \end{bmatrix} \begin{Bmatrix} a_j \\ \Delta P \\ x \end{Bmatrix} = \begin{Bmatrix} f \\ 0 \\ 0 \end{Bmatrix}$$

The mass and stiffness elements of the Schelleng matrix become sub-matricies in the expanded model. The elements of these matrices are the effective mass and stiffness properties of the assumed mode shapes. These elements have contributions from both the soundboard plate and its underlying braces.

9.7)

$$k_{i,j} = k_{i,j}^{plate} + \sum_{nb=1}^{braces} k_{i,j,nb}^{brace}$$

$$m_{i,j} = m_{i,j}^{plate} + \sum_{nb=1}^{braces} m_{i,j,nb}^{brace}$$

The soundboard plate model is that of an orthotropic, uniform-thickness plate. The plate stiffness and mass-matrix elements are computed as follows,

9.8)

$$k^{p}_{i,j} = \int_{-L}^{L}\int_{-B(x)}^{B(x)} w_i \{ D_x \frac{\partial^4 w_j}{\partial x^4}$$

$$+2D_{xy}\frac{\partial^4 w_j}{\partial x^2 \partial y^2} + D_y \frac{\partial^4 w_j}{\partial y^4} \} \, dydx$$

$$m^{p}_{i,j} = \int_{-L}^{L}\int_{-B(x)}^{B(x)} w_i \rho h w_j dydx$$

w_i = assumed deflection shape

D_x = bending stiffness along the grain

D_y = bending stiffness across the grain

D_{xy} = torsional stiffness

h = plate thickness

ρ = plate material density

The stiffness term can be expressed as the sum of three integrals each depending on only a single material constant. The bending stiffness moduli are determined from experimental data. Material damping can be modeled using a complex bending stiffness.

The braces are modeled using simple beam theory using the along-the-grain properties of the wood. The beam has a fixed base width at the plate interface, the height and cross section shape are allowed to vary along the length of the brace. The brace runs along a

straight line with the end points being anywhere on the plate surface. The terms of the stiffness and mass matrices are computed as follows,

9.9)

$$k^b_{i,j} = \int_0^l w_i \frac{d^2}{ds^2}\left[EI(s) \frac{d^2 w_j}{ds^2} \right] ds$$

$$m^b_{i,j} = \int_0^l w_i \rho A(s) w_j ds$$

I = Moment of Inertia

A = Cross sectional area

s = Coordinate along the beam

The expression for the stiffness can be integrated by parts to simplify the numerical calculations. The beam matrix elements are added to the plate mass and stiffness matrices to produce braced-plate models.

In the Rayleigh-Ritz technique the ratio of the potential energy to the kinetic energy of the modeled system is minimized relative to the unknown coefficients of the assumed mode series. The assumed solution has known spatial functions and unknown coefficients.

9.10)

$$w(x,y) = \sum_{j=1}^{n} a_j \cdot w_j(x,y)$$

The assumed mode shape must meet the geometric boundary conditions. In the case of a simply supported plate the deflection at the edge of the plate is constrained to be zero.

Consider a function which describes the upper boundary of an axisymmetric plate in terms of a coordinate system with its origin at the geometric center of the plate. Using this function a suitable assumed displacement mode function has the form;

9.11)

$$w_i(x,y) = \cos\left[\frac{n\pi x}{2L} + \frac{\pi(n-1)}{2}\right] \cdot \cos\left[\frac{m\pi y}{2B(x)} + \frac{\pi(m-1)}{2}\right]$$

$2L$ = Plate length

$B(x)$ = Boundary curve

n,m = Integers 1,2,3...

The assumed mode shape is built from a mapping of the mode shapes of a simply supported rectangular plate. The mode shapes of the rectangular plate are mapped by adjusting the "width" of the rectangular plate in the second trigonometric term. The function requires that the nodal lines always lie inside the plate boundary. The actual mode shapes of the plates will be built up from these assumed mode shapes.

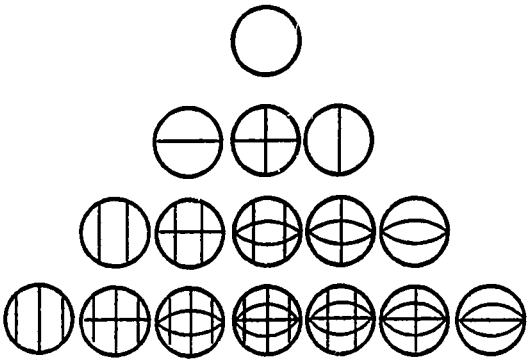

Figure 9.3 The First 16 Assumed Modes of a Circular Plate

To complete the assumed mode function an expression for the boundary curve must be established. A series of Chebyshev polynomials are used to represent the boundary curve.

9.12)

$$B(x) = \sum_{n=1}^{N_{max}} c_n T_n(x)$$

where,

$$T_n(x) = \cos(n \cdot \cos^{-1}(x))$$

The coefficients of the boundary series function are obtained using a curve-fitting procedure.

The braced plate of the guitar soundboard is backed by a ported enclosure. The port or soundhole is modeled as a rigid piston and the cavity as a simple gas spring as in the Schelleng model. The effective mass of the soundhole air-slug has been determined experimentally.

9.13)

$$m_{port} = \pi r^2 \rho (h + 2.7r)$$

$$r_{port} = \pi r^2 \rho c (kr)^2$$

The cavity model is based on the adiabatic compression of a confined gas where the change in pressure in the cavity is proportional to the change of volume of the cavity.

9.14)

$$P = -\frac{\rho c}{Vol}\left\{\int_{-L}^{L}\int_{-B(x)}^{B(x)} w(x,y)dydx \;+\; \pi r^2 z_p\right\} = C_{box}\Delta V$$

The basic radiation-loading function is that of a simple source with the area of the soundboard.

9.15)

$$P = \frac{i\omega \cdot \rho c}{\pi r_p^2}\left[\frac{(kr_p)^2}{1+(kr_p)^2} + i\frac{kr_p}{1+(kr_p)^2}\right] \cdot \Delta V = C_{rad} \cdot \Delta V$$

The cavity and radiation pressures are added algebraically to give the net pressure acting on the plate.

9.16)

$$C_{net} = C_{box} + C_{rad}$$

The driving force for the model is a simple constant force generator located at a point on the plate. The drive point locations are intended to represent the string bridge contact points. The weighting functions must be applied to the point loads to convert them into the matrix formulation.

9.17)

$$f = \int_{-L}^{L} \int_{-B(x)}^{B(x)} w_i F_{st} \delta(x - x_0)\delta(y - y_0) \; dy dx$$

$$= F_{st} \; w_i(x_0, y_0)$$

The forced response problem is solved in 1/12 octave or semitone intervals from 55 to 880 Hz. The matrix pressure terms and port terms are frequency dependent requiring the inversion of this system matrix for each frequency of interest.

Acoustic power is calculated from the displacement functions obtained using this procedure. The radiated power is then calculated by;

9.18)

$$Power = \begin{Bmatrix} v_1 \\ v_2 \\ \cdot \\ v_n \end{Bmatrix}^T \begin{bmatrix} Z_{11} & Z_{12} & \cdots & Z_{1n} \\ Z_{21} & Z_{22} & \cdots & Z_{2n} \\ Z_{n1} & \cdots & \cdots & Z_{nn} \end{bmatrix} \begin{Bmatrix} v_1 \\ v_2 \\ \cdot \\ v_n \end{Bmatrix}$$

where the volume velocity is computed by,

$$v_p = \frac{i\omega}{\pi a^2}\int w dA_p$$

the piston self impedance is[62],

$$Z_{pp} = \rho c \pi a^2\left[1 - \frac{J_1(2ka)}{ka} + i\frac{H_1(2ka)}{ka}\right]$$

$J_1(2ka)$= Bessel function

$H_1(2ka)$= Struve function

a= piston radius

$k = \frac{\omega}{a}$= wave number

and the piston cross impedance is[63],

$$Z_{pq} = \rho c \pi a^2 \frac{(ka)^2}{2}\left[\frac{\sin(kd)}{kd} + i\frac{\cos(kd)}{kd}\right]\left\langle\frac{v_p}{v_q}\right\rangle$$

d= distance between the centers of pistons p and q

v_p= velocity of piston p

v_q= velocity of piston q

---

62) Douglas D. Reynolds, Engineering Principles of Acoustics, Boston: Allyn and Bacon, Inc. 1981.

63) R. L. Pritchard, "Mutual Acoustic Impedance between Radiators in an Infinite Rigid Plane" J. Acoust. Soc. Am. 32(6) 1960.

The piston size has been selected to match the size of the soundhole of the guitar, typically a four-inch diameter. The piston size is small relative to the acoustic wavelength throughout the modeling range.

9.4 Guitar-Model Prediction Studies

The guitar model enables the study of many soundboard structural design details. The examples presented in this section are of Dreadnought guitar designs similar to the one used to experimentally verify the computational model. The modern Dreadnought guitar pattern has been built with a large number of bracing patterns. Three of these bracing systems will be examined, 1) the Gibson-low-X system, 2) the Manzer-A-brace system, and 3) the Martin-slant-brace system.

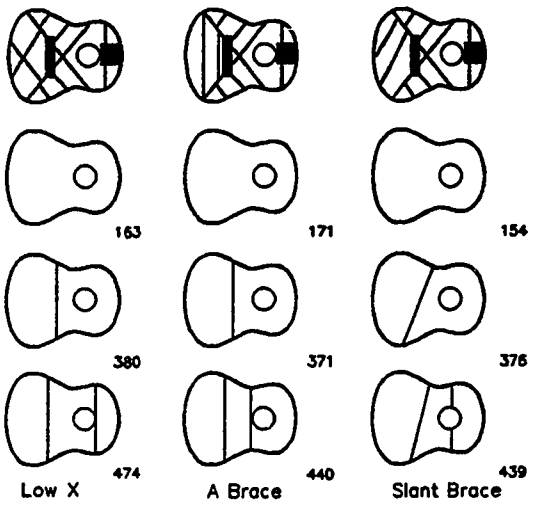

Figure 9.4 Dreadnought Bracing Patterns
Mode Shapes and Resonant Frequencies

In these models the major part of the bracing pattern is held constant differing only in the placement of the lower-bout secondary braces. The main X-brace, the upper-bout transverse brace, the fingerboard overlay, the bridge, neck, and small braces running from the X-brace to the sides of the top are constant. In each case the soundboard resonance has been raised approximately an octave above the fundamental plate resonance of 81.7 Hz.

The radiated power spectrum for each top driven at the A-string with a .1 newton force is generated to examine

the differences between the designs. The soundhole diameter was 4 inches and the box volume was 16 liters for all models.

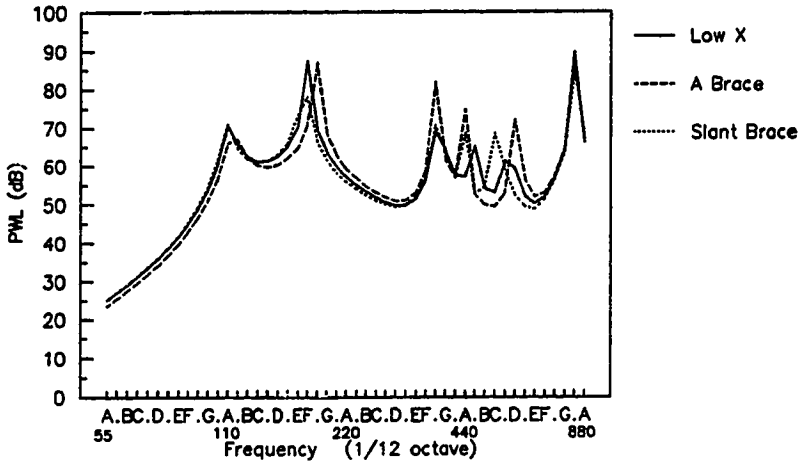

Figure 9.5 Dreadnought Bracing Patterns
Acoustic Power Spectra

The first three peaks in the radiated power spectra fall on top of one another with variances in their maximum levels. The area where the spectra differ significantly is above 400 Hz. The differences in the spectra in this frequency range is a reflection of the structural differences in the secondary lower-bout braces.

The backing cavity is known to couple the first two modes of the guitar from previous work by Schelleng and others. The effects on the higher order modes can be studied with the current model. The Manzer A-braced

soundboard was modeled with three backing cavities corresponding to guitars with 5 cm (2 inch), 10 cm (4 inch), and 15 cm (6 inch) sides.

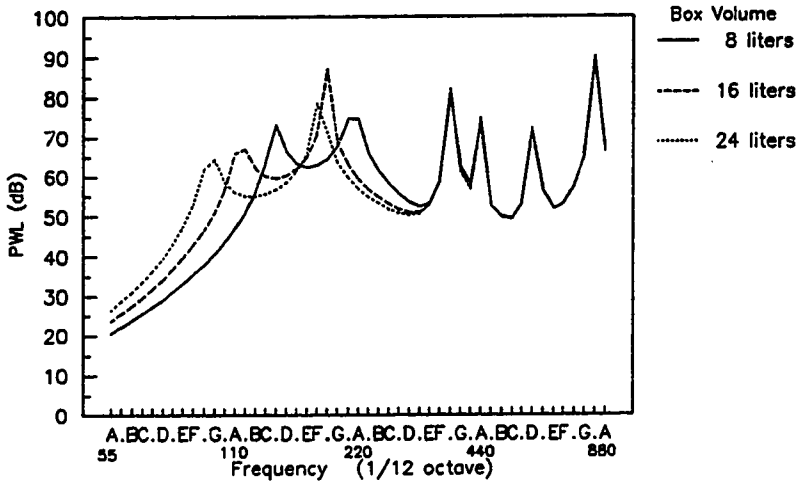

Figure 9.6 Dreadnought Backing Volume Sensitivity

There is a strong influence on the first two modes of the system with little alteration of the high frequency behavior. The air mode has dropped with increasing box volume from 139, to 114, to 98 Hz. The main plate mode followed in kind from 215, to 185, to 175 Hz. The eigenvalue solution for the plate in vacuo was 171 Hz indicating that an increase of the box volume will not lower the plate resonance much more.

The guitar-soundboard models require knowledge of the bending modulus and density of the woods used to construct the instrument. The preliminary design of a

guitar would require the use of "generic" material properties. In this next exercise a guitar soundboard bracing system is modeled with a number of different wood materials. The baseline material properties are those evaluated in the current experimental program. Additional material properties for the woods are those presented in a paper by Graham Caldersmith[64]. Martin-style Dreadnought soundboard model has been used for the study.

---

64) Graham Caldersmith, "Vibrations of Orthotropic Rectangular Plates." Acustica 56. 1984.

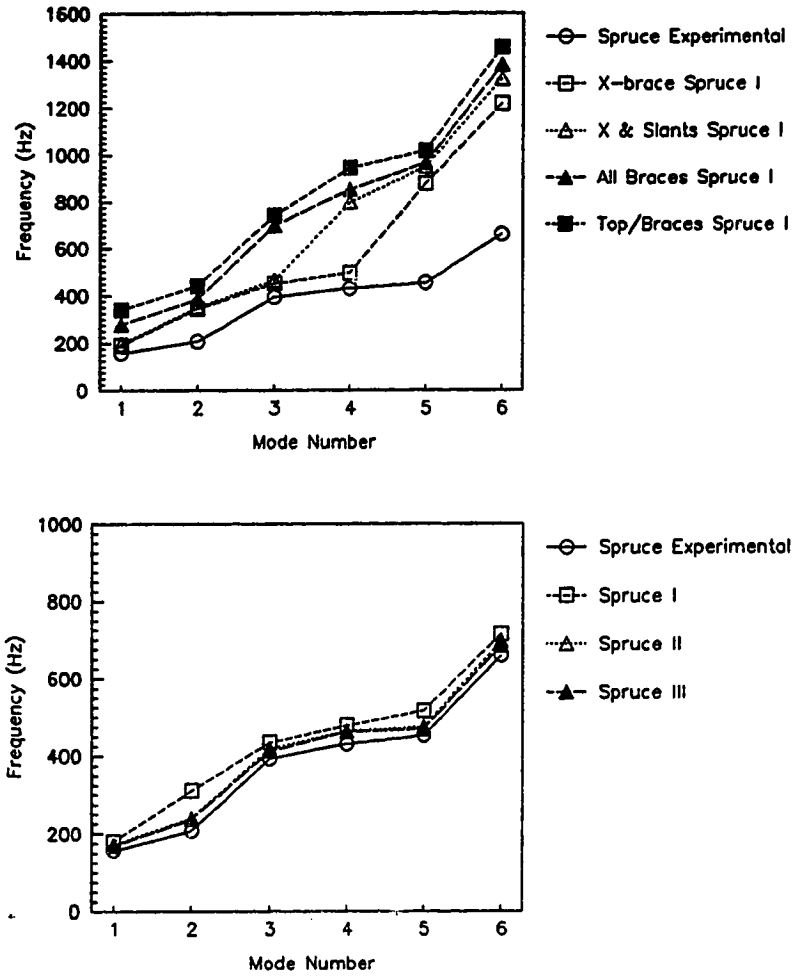

Figure 9.7 Influence of Material Properties on Plate Mode Predictions

Dramatic changes in the natural frequencies are encountered when the bracing materials under the guitar plate are replaced with a stiffer Spruce material. The ratio of the along-the-grain modulus between the baseline experimental spruce and Spruce I is approximately 1:3. A comparison of the predictions of a guitar modeled with the Spruce I material and the experimental material indicates the expected variance in the placement of the soundboard resonances when generic material properties are used. If only the soundboard plate material is changed and the bracing material remains constant, then the shifts in the resonant frequencies are not as dramatic. The frequency shifts indicate that the dynamics of the soundboard are dominated by the bracing system and not the plate material in this configuration.

9.5 Preliminary Experimental Studies

A number of preliminary experimental investigations were made before a guitar was constructed to evaluate the computational model. The first of these attempted to define the range of validity of the simple backing-cavity model. The second set of investigations was aimed at gaining some experience with guitar-shaped plates before undertaking the more complex task of building a guitar soundboard.

9.5.1 Cavity and Port Experiments

The port has been modeled as a mass slug of air, the equivalent mass of which has been determined experimentally. The natural frequency of the Helmholtz Resonator[65] is;

9.19)

$$f_H = \frac{1}{2\pi}\sqrt{\frac{(\rho c^2/V)S^2}{\rho l_{eq} S}} = \frac{c}{2\pi}\sqrt{\frac{S}{V l_{eq}}}$$

where,

V = Cavity Volume

S = Soundhole Area $= \pi a^2$

a = Soundhole Radius

$l_{eq} = l + \beta a$ = Equivalent Neck Length

l = Neck Length

β = End Correction Factor

The equivalent length of the neck includes a correction factor which is a function of the neck termination. A correction factor for the guitar can be established by varying the geometric length of the neck and measuring the change in Helmholtz frequency.

Cardboard tubes were placed in the soundhole of a Dreadnought guitar increasing the neck length of the

---

65) Leo L. Beranek. Acoustics. New York: McGraw-Hill: 1954.

Helmholtz resonator. The tubes were mounted in two configurations, in the first the tubes were internal to the body of the guitar and in the second the tubes were above the plane of the soundboard. The body depth of the guitar under the soundhole was 110 mm.

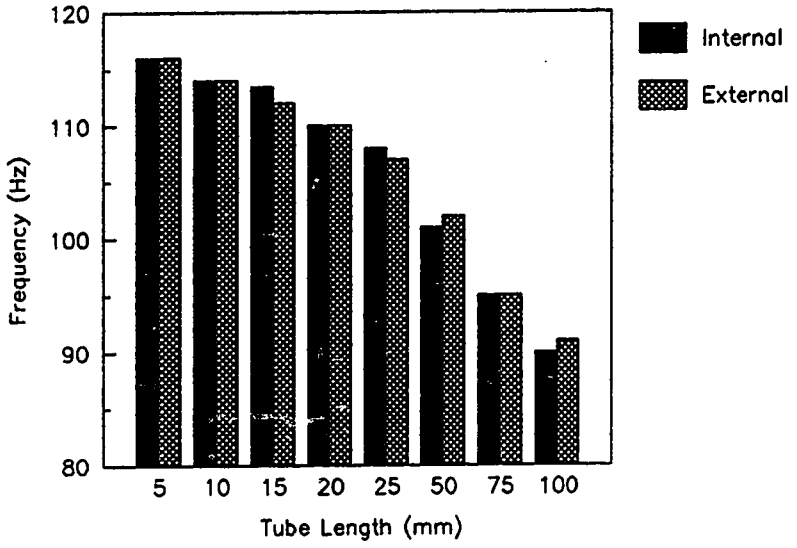

Figure 9.8 Dreadnought Helmholtz Tube Length Study

Note that the measured frequencies in these experiments show little difference between the internal and external tube configurations. From the data collected from a Dreadnought guitar using eight tube lengths in both the internal and external configurations an average end correction factor has been computed. The measured end

correction is 2.7. This value is larger than the computed classical Helmholtz end correction factor of 1.7 for infinite baffled plates.

The assumption that the pressure is uniform across the backing cavity in the frequency range of interest was examined experimentally. A rectangular space, with dimensions similar to those of a guitar box, was used to estimate the acoustic resonances of the guitar cavity[66].

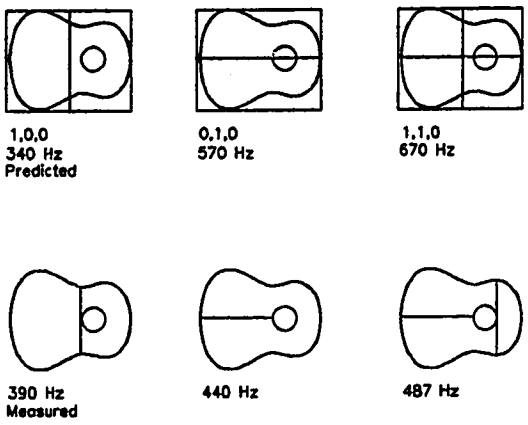

Figure 9.9 Dreadnought Cavity Acoustic Mode Shapes and Resonant Frequencies

66) Philip M. Morse. Vibration and Sound. New York: McGraw-Hill: 1948.

A six-microphone array was used to map out the acoustic modes. The mode shapes are two dimensional in form in the frequency range of interest from 55 to 880 Hertz. The cavity no longer behaves as a simple stiffness above 390 Hertz.

9.5.2 Plate Experiments

Plates were constructed and mounted on particle-board frames in order to study the effects of the plate shape on the plate resonances. Mode shapes of the rectangular and guitar-shaped plates were observed using the Chladni pattern technique. Chladni patterns are created by exciting a plate covered with a light weight powder. As the plate vibrates at one of its natural frequencies, the power migrates to the nodal lines of the excited mode. The "powder" which has been found to be the easiest to work with is poppy seeds. The modes which had a net volume displacement were easier to excite than the symmetric "zero" volume-displacement modes though both were measured and documented.

The Chladni patterns were used to trace the evolution of the plate's mode shapes through a number of geometric changes using foam-core-board.

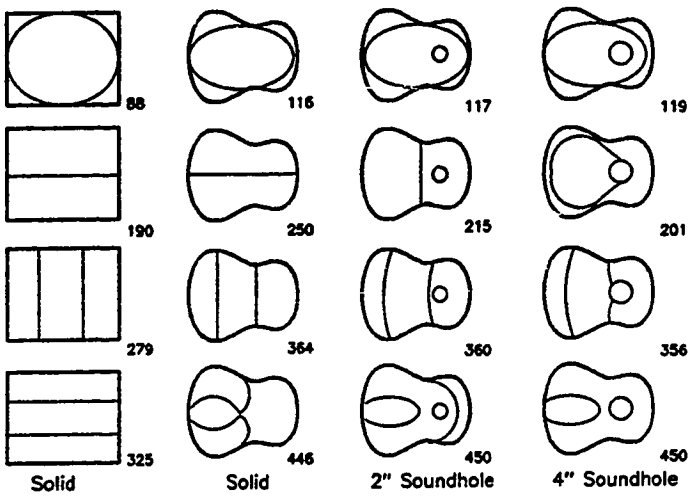

Figure 9.10 Foam Core Plate Evolution
Mode Shapes and Resonant Frequencies

The mode shapes of the rectangular plate are mirrored in the guitar-shaped plates in plates with isentropic material properties . The second mode is interesting in its sensitivity to the plate geometry while remaining modes are essentially unchanged in both mode shape and frequency.

9.6 Soundboard Experiments and Predictions

To evaluate the performance of the computational model a Martin-style Dreadnought guitar was built. The soundboard was built up on the particle-board fixture and later transferred to a set of conventional rosewood sides for completion of the guitar box. At 25 steps in

the assembly processes Chladni patterns were photographed. The fundamentals for the first 11 assembly steps are plotted against the predictions below. This data was taken on a wooden frame fixture.

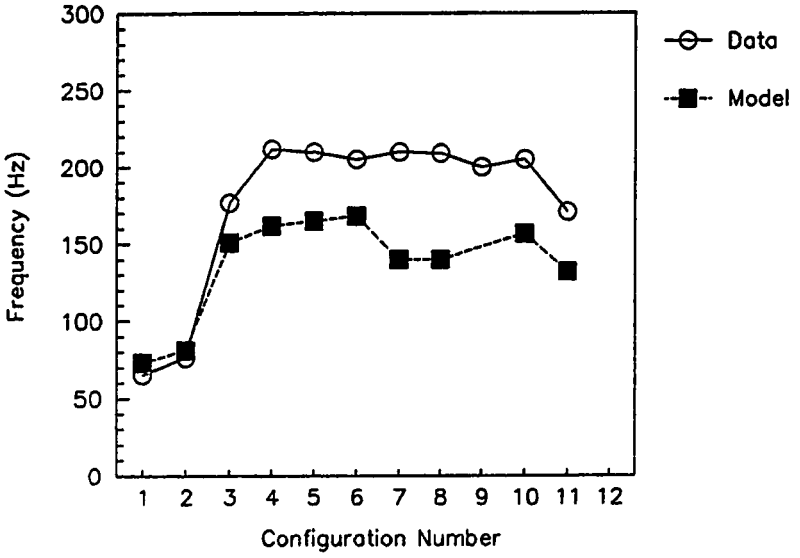

Figure 9.11 Fundamental Plate-Frequency Prediction

The first configuration is that of spruce plate. The final configuration is for a fully braced guitar top with the braces carved into their final shapes. The prediction model and the data track each other very well. There is an offset between the predictions which may be due to either the uncertainties in the material properties or to over simplification in the modeling of

the fixture's boundary conditions. The higher-order modes are also predicted with the analytical model and compare favorably with experimental data.

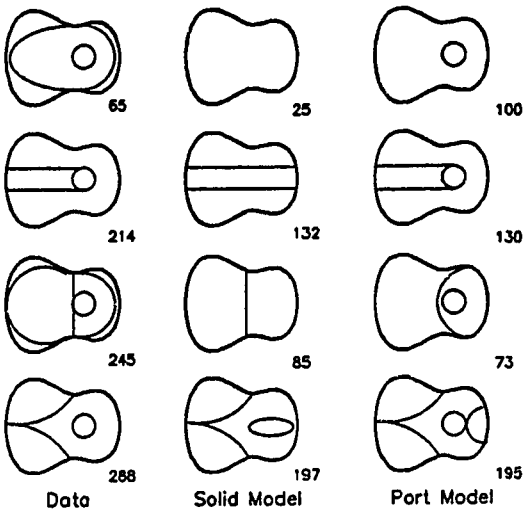

Figure 9.12 Simply Supported Bare Plate Predictions Mode Shapes and Resonant Frequencies

The Chladni patterns of the 3 mm spruce soundboard are compared to the computational model. The model is exercised with and without the soundhole. The material properties used in the model have been determined experimentally. The mode shapes and frequencies track well for the first, second and fourth resonances. The frequency of the third mode is not predicted with the same accuracy.

The bending energies of the braces are dependant on the location of the neutral axis of the brace. Two modeling options are; 1) the neutral axis can be located at the centroid of the beam, and 2) the neutral axis can be located at the plate-beam interface. These two options were compared against the Chladni patterns of the modes of the soundboard with a complete set of braces. The braces have rectangular cross sections and uniform height.

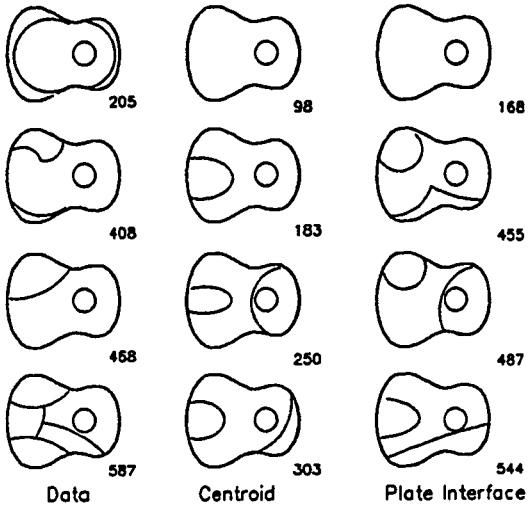

Figure 9.13 Simply Supported Braced Plate Predictions
Mode Shapes and Resonant Frequencies

The analytical model that predicts the measured results most consistently is the one with the braces modeled as

moving about the plate-brace interface. A comparison of the first and third columns of figures are similar in both frequency and mode shape.

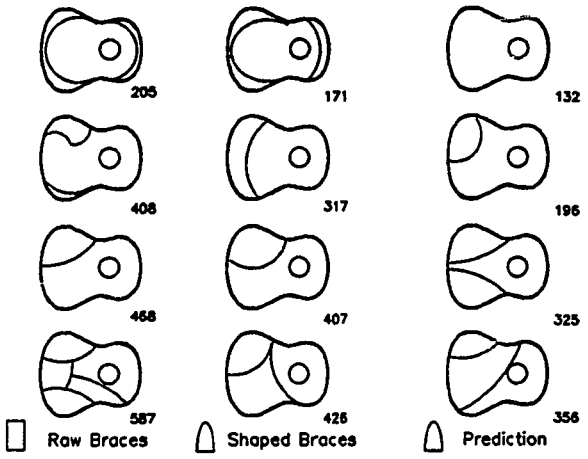

Figure 9.14 Simply Supported Carved Brace Plate Mode Shapes and Resonant Frequencies

The influence on the cross-sectional shape of the braces on mode shape is studied by carving the braces into the traditional semi-ellipitical shape and reevaluating the model predictions. The first two columns are the data before and after the braces are carved the third is a prediction for the carved brace configuration. The predictions follow the same trends as the data.

In the final assembly the soundboard with an ebony bridge was mounted on rosewood sides and a nomex honey-

comb back. The air mode is observed for the first time in these experiments upon completing the backing cavity.

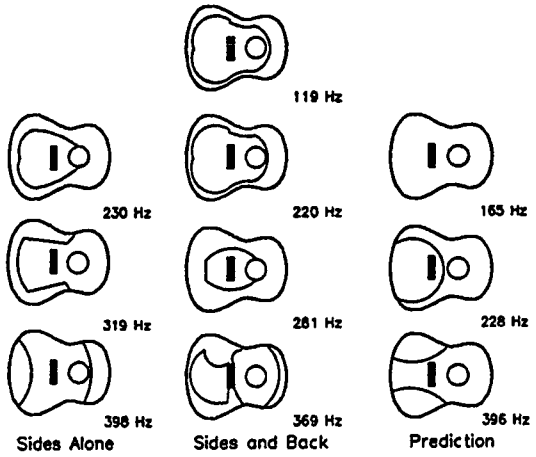

Figure 9.15 Final Assembly Data and Predictions
Mode Shapes and Resonant Frequencies

The soundboard modes with the soundboard mounted on the guitar sides are not modeled as well as those on the test fixture were. The increased complexity of the boundary conditions is the most likely source for these differences.

To complete the experimental evaluation of the guitar box a sound power measurement was made. The prediction of the acoustic response of the guitar is based on a point-force source. In the experiment a small shaker was used to drive the guitar. The driver changed the modal structure of the top plate.

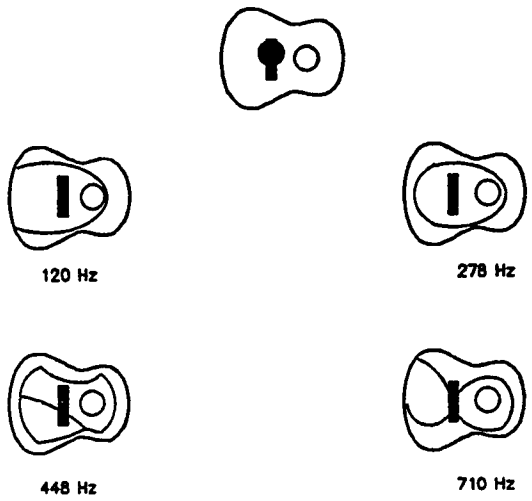

Figure 9.16 Driver Influence on Plate Modes
Mode Shapes and Resonant Frequencies

The modal changes were modeled by assuming the driver acted like a mass load on the soundboard. The acoustic power-spectrum predictions for both the mass loaded and unmodified soundboards and the experimental results are presented below.

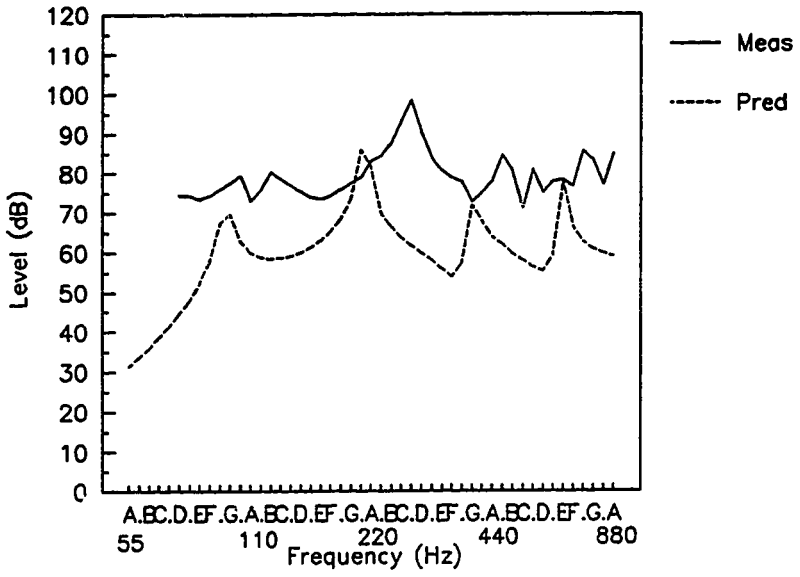

Figure 9.17 Acoustic Power-Spectrum Comparison

The model of the soundboard predicts the basic spectrum shape shifted down approximately four semitones. Recalling that the soundboard models consistently under predicted the resonant frequencies of the system it can be tentatively concluded that the model is an accurate representation of the radiation characteristics of the guitar soundboard.

9.7 Conclusion

A Rayleigh-Ritz model of a guitar soundboard has been built and experientially verified. The model is suitable for determining differences in the radiated sound for differences in plate shape, plate thickness,

soundhole size, backing-cavity volume, brace cross-section, brace tapers, and material properties of the top and braces. In this study 25 plate configurations were tested to document 150 mode shapes and over 100 computer plate models were analyzed. Estimates of the sound power levels radiated by guitars driven by a point load have been made using a planar piston array model. The acoustic confirmation experiments have required the modeling of the driver system. The acoustic sound-power level prediction matched the experimental trends. Uncertainties in the determination of the material properties of the woods used in the experimental phase was a major source of error in the prediction work.

This study has not addressed the problem of determining the relative merits of the modeled guitars. The best current assessment of guitar sound quality can be stated by a generalized version of Beranek's Law for loudspeaker design: The best-sounding musical instrument is the one designed, built or otherwise selected by a person who believes he has designed, built or selected the best-sounding musical instrument.

10 List of References

10.1 Computer Software

Dongarra, J. J. Moler, C. B. Bunch, J. R. Stewart, G. W. Linpack User's Guide. Philadelphia: SIAM 1979.

Press, William H. Flannery, Brian P. Teukolsky, Saul A. Vettering, William T. Numerical Recipes, The Art of Scientific Computing. New York: Cambridge University Press, 1986.

Smith, B. T. Boyle, J. M. Dongarra, J. J. Garbow, B. S. Ikebe, Y. Klema, V. C. Moler, C. B. Matrix Eigensystem Routines, EISPACK Guide. second edition vol 6 of Lecture Notes in Computer Science, New York: Springer-Verlag 1976.

10.2 Dynamics and Acoustics

Beranek, Leo L. Acoustics. New York: McGraw-Hill Company, Inc. 1954.

Blevins, Robert D. Formulas for Natural Frequency and Mode Shape. New York: Van Nortrand Reinhold Company 1979.

Desiderati, Frank W. Laura, Patricio A. "Vibrations of Rib-Stiffened Elliptical and Circular Plates." J. Acous. Soc Am. 48(1) part 1 1970.

Gander, Mark R. "Dynamic Linearity and Power Compression in Moving Coil Loudspeakers." J. Audio Eng. Soc. 34(9) 1986.

Kinsler, Lawrence E., and Frey, Austin R. Fundamentals of Acoustics. New York: John Wiley & Sons, Inc. 1962.

Leissa, Authur W. Vibration of Plates. Washington D. C.: Nasa SP-120, 1969.

Meirovitch, Leonard. Analytical Methods in Vibrations. London: The Macmillion Company. 1967.

Morse, Philip M. Vibration and Sound. American Institute of Physics. New York: 1976.

Nashif, Ahid D. Jones, David I. G. Henderson, John P. Vibration Damping. New York: John Wiley & Sons, 1985.

Olsen, Harry F. Elements of Acoustical Engineering. Princeton, N. J. D. Van Nostrand Company, Inc., 1955.

Pritchard, R. L. "Mutual Acoustic Impedance between Radiators in an Infinite Rigid Plane." J. Acous. Soc. Am. 44(5) 1960.

Reynolds, Douglas D. Engineering Principles of Acoustics. Boston: Allyn and Bacon, Inc. 1981.

Seybert, A. F. Rengarajan T. K. "The Use of CHIEF to Obtain Solutions for Acoustic Radiation Using Boundary Integral Equations." J. Acous. Soc Am. 81(3) 1987.

10.3 Experimental Techniques

American National Standard. Methods for the Determination of Sound Power Levels of Small Sources in Reverberation Rooms. ANSI S1.21-1972 New York, 1972.

American National Standard. Precision Methods for the Determination of Sound Power Levels of Broad-Band Noise Sources in Reverberation Rooms. ANSI S1.31-1980 New York, 1980.

American National Standard. Engineering Methods for the Determination of Sound Power Levels for Essentially Free-Field Conditions Over a Reflecting Plane. ANSI S1.34-1980 New York, 1980.

American National Standard. Precision Methods for the Determination of Sound Power Levels of Noise Sources in Anechoic and Hemi-Anechoic Rooms. ANSI S1.35-1979 New York, 1979.

American National Standard. Survey Methods for the Determination of Sound Power Levels of Noise Sources. ANSI S1.36-1979 New York, 1979.

Peterson, Arnold P. G., and Ervin E. Gross, Jr. Handbook of Noise Measurement. Concord, Mass.: General Radio Company, 1974.

10.4 Guitar Analytics

Boullosa, Ricardo R. "The Use of Transient Excitation For Guitar Frequency Response Testing." Catgut Acoust. Soc. Newsletter #36 1981.

Boehm, Tomira. Miklaszewski, Kacper. Blutner, Freidrich. Meinel, Eberhard. "Estimation of Guitar Sound Quality", Archiwum Akustyki (Archives of Acoustics) 11(3) 1986.

Caldersmith, Graham. "Guitar as a Reflex Enclosure." J. Acoust. Soc. Am. 63(5) 1978.

Caldersmith, Graham. "Low Range Guitar Function and Design." Catgut Acoust. Soc. Newsletter #27 1977.

Caldersmith, Graham. "The Guitar Frequency Response." J. of Guitar Acoustics 6 1982.

Caldersmith, Graham. "Physics at the Workbench of the Luthier." Catgut Acoust. Soc. Newsletter #35 1981.

Caldersmith, Graham. "Plate Fundamental Coupling and its Musical Importance." Catgut Acoust. Soc. Newsletter #36 1981.

Childers, Richard L. "An Analytical Expression for the Shape of a Guitar." Catgut Acous. Soc. Newsletter #41 1984.

Christensen, Ove. Vistisen, Bo B. "Simple Model for Low-Frequency Guitar Function." J. Acoust. Soc. Am. 68(3) 1980.

Christensen, Ove. "Quantitative Models for Low Frequency Guitar Function." J. of Guitar Acoustics 6 1982.

Christensen, Ove. "The Response of Played Guitars at Middle Frequencies." Acustica 53 1983.

Christensen, Ove. "An Oscillator Model for Analysis of Guitar Sound Pressure Response." Acustica 54 1984.

Dickens, Fred T. "Tuning of Guitar Plates." Catgut Acoust. Soc. Newsletter #26 1976.

Dickens, Fred T. "Inertance of the Guitar Sound Hole." Catgut Acoust. Soc. Newsletter #29 1978.

Firth, Ian M. "Physics of the Guitar at the Helmholtz and First Top-Plate Resonances." J. Acoust. Soc. Am. 61(2) 1977.

Hartman, Robert Carl. Guitars and Mandolins in America. Hoffmann Estates, IL: Maurer & Co. 1984.

Jansson, E. V. "A Study of Acoustical and Hologram Interferometric Measurements of the Top Plate Vibrations of a Guitar." Acustica 25 1971.

Kruger, Walter. "Findings In the Manipulation of Guitar-Top Plates." Catgut Acoust. Soc. Newsletter #38 1982.

Marty, S. M. "Assessment of Innovations in the Construction of the Classical Guitar." J. Catgut Acoust. Soc. #47 1987.

Meyer, Jurgen. "Quality Aspects of Guitar Tone." in Function, Construction and Quality of the Guitar. edited by Erik V. Jansson. Stockholm: The Royal Swedish Academy of Music 1983.

Richardson, Bernard E. "The Influence of Strutting on the Top-Plate Modes of a Guitar." Catgut Acoust. Soc. Newsletter #40 1983.

Richardson, B. E. Roberts, G. W. "The Adjustment of Mode Frequencies in Guitars: A Study by Means of Holographic Interferometry and Finite Element Analysis." Proceedings of the Stockholm Music Acoustics Conference July 28 to August 1, 1983 Vol II 1985.

Rossing, Thomas D. Popp, John. Polstein, David. "Acoustic Response of Guitars", Proceedings of the Stockholm Music Acoustics Conference July 28 to August 1, 1983 Vol II 1985.

10.5 Guitar Construction

Brosnac, Donald. The Steel String Guitar. Its Construction, Origin and Design. Los Angeles: Panjandrum Press. 1980.

Evans, Tom. Evans, Mary Anne. Guitars. Music. History. Construction and Players From the Renaissance to Rock. New York: Facts on File Press. 1977.

Jahnel, Franz. Manual Of Guitar Technology. Frankfurt am Main: Verlag Das Musikinstrument. 1981.

Laskin, William "Grit". "Building A Steel String Guitar." Fine Woodworking #67 1987.

Laskin, William "Grit". "Guitar Body Construction." Fine Woodworking #69 1988.

McLeod, Donald. Welford, Robert. The Classical Guitar Design & Construction. Wood-Ridge New Jersey: The Dryad Press. 1975.

Overholtzer, Arthur E. Classical Guitar Making. Chico Cal.: Lawrence A Brock pub. 1975.

Sloane, Irving. Classical Guitar Construction. New York: E. P. Dutton & Co. 1966.

Williams, Jim. A Guitar Maker's Manual. Dudly N. S. W.: Guitarcraft. 1987.

Young, David Russell. The Steel String Guitar: Construction & Repair. Radnor Penn.: Chilton Book Company. 1975.

10.6 Strings

Davis, Evan Brugh. "Design Guide for Steel-Core Bronze-Wound Musical Instrument Strings." Catgut Acoust. Soc. Newsletter #38 1982.

Hanson, Mark. Hood, Phil. "The Ultimate String Test." Frets 9(2) issue #102 1987.

Morse, Philip M. Vibration and Sound. American Institute of Physics. New York: 1976.

10.7 Violin

Hutchins, Carleen M. "A History of Violin Research." J. Acoust. Soc. Am. 73(5) 1983.

Jansson, E. Bork, I. Meyer, J. "Investigations into the Acoustical Properties of the Violin." Acustica 62(1) 1986.

Marshell, Kenneth D. "Modal Analysis of a Violin." J. Acoust. Soc. Am. 77(2) 1985.

Meyer, Jurgen. "Directivity of the Bowed String Instruments and Its Effect on Orchestral Sound in Concert Halls." J. Acoust. Soc. Am. 51(6) part 2 1972.

Schelleng, John C. "The Violin as a Circuit." J. Acoust. Soc. Am. 35(3) 1963.

Schelleng, John C. "On Polarity of Resonance." Catgut Acoust. Soc. Newsletter #10 1968.

Schelleng, John C. "Acoustical Effects of Violin Varnish." J. Acoust. Soc. Am. 44(5) 1968.

Weinreich, Gabriel. Arnold, Eric B. "Method for Measuring Acoustic Radiation Fields." J. Acoust. Soc. Am. 68(2) 1980.

10.8 Woods

Caldersmith, G. W. "Vibrations of Orthotropic Rectangular Plates." Acustica 56 1984.

Caldersmith, Graham. "Vibration Theory and Wood Properties." J. Catgut Acoust. Soc. #42 1984.

Haines, Daniel W. "On Musical Instrument Wood." Catgut Acoust. Soc. Newsletter #31 1979.

Hoadly, R. Bruce. Understanding Wood. Newtown Conn.: The Taunton Press. Inc. 1981.

Holtz, D. "On Some Important Properties of Non-Modified Coniferous and Leaved Woods in View of Mechanical and Acoustic Data in Piano Soundboards." Archiwum Akustyki (Archives of Acoustics) 9(1) 1974.

Holtz, D. "Investigations on a Possible Substitution of Resonant Wood in Plates of Musical Instruments by Synthetic Materials." Archiwum Akustyki (Archives of Acoustics) 4(4) 1979.

Lekhnitskii, S. G. Anisotropic Plates. translated by S. W. Tsai and T. Cheron. New York: Gordon and Breach Science Publishers 1967.

McIntyre, M. E. Woodhouse, J. "On Measuring Wood Properties, Part 1." J. Catgut Acoust. Soc. #42 1984.

McIntyre, M. E. Woodhouse, J. "On Measuring Wood Properties, Part 2." J. Catgut Acoust. Soc. #43 1985.

McIntyre, M. E. Woodhouse, J. "On Measuring Wood Properties, Part 3." J. Catgut Acoust. Soc. #45 1986.

Rajcan, E. "Some Differences in Physchio-Acoustic Characteristics of 'Resonant' and Standard Spruce Wood" Acustica. 48 1981.

Schelleng, John C. "Wood For Violins." Catgut Acoust. Soc. Newsletter #37 1982.

Yeh, C. T. Harte, B. J. Brown, C. B. "Damping Sources in Wood Structures." J. Sound and Vibration 19(4) 1971.

U. S. Forest Service, Wood Handbook. Washington D.C.: Government Printing Office 1974.

10.9 Psychology of Listening

Deutsch, Diana Editor. Psychology of Music. New York: Academic Press, Inc. 1982.

Toole, Floyd E. "Subjective Measurements of Loudspeaker Sound Quality and Listener Preference." J. Audio Eng. Soc. 33(1/2) 1985.

Toole, Floyd E. "Loudspeaker Measurement and Their Relationship to Listener Preferences: Part 1." J. Audio Eng. Soc. 34(4) 1986.

Toole, Floyd E. "Loudspeaker Measurement and Their Relationship to Listener Preferences: Part 2." J. Audio Eng. Soc. 34(5) 1986.

Toole, Floyd E. Olive, Sean E. "The Modification of Timbre by Resonances: Perception and Measurement." J. Audio Eng. Soc. 36(3) 1988.

Seashore, Carl E. Psychology of Music. New York: Dover Publications, Inc. reprint 1967 (1938).

11 Appendix Material Properties

11.1 Wood Properties

Wood Properties

Name	Density Kg/M^3	Modulus of Elasticty $Pa \times 10^{-9}$			Loss factor		
		Along	Cross	Shear	Along	Cross	Shear
Spruce I	460	19.6	1.01	3.36	.006	.014	.013
Spruce II	450	10.6	0.10	1.66	.007	.020	.014
Spruce III	480	10.3	0.86	1.61	.007	.017	.016
Cedar I	410	6.20	1.05	1.92	.005	.012	.011
Cedar II	410	6.35	1.24	2.02	.005	.012	.011
Mahogany	510	12.0	1.20	3.50	.007	.037	.019
Rosewood	730	13.0	2.40	5.10	.007	.013	.010
Ebony	1080	17.7	1.77	5.60	.005	.010	.010

The woods in this table reflect primary guitar building materials. The data does not reflect any one species of wood but rather generic types of woods. The spruces and cedars are top materials. Mahogany and rosewood are commonly used in the construction of the backs and sides of guitars. Rosewood and ebony are used for necks and bridges.

Spruce I is typical of the European musical instrument spruces. Spruce II is a soft spruce with a very low cross grain modulus. The third spruce type, Spruce III is a hard spruce having a modulus ratio which is similar to those generally found in other "hard" woods such as mahogany.

The cedar samples recorded in this table are typical of cedars used in guitar top construction. The range of material properties is very limited when compared to the spruce samples.

11.2 Finish Properties

Finish Properties

Name	Thickness mm	Modulus of Elasiticty Pa x 10^{-9}	Loss factor
Thin Hard	.125	3.75	.044
Thin Soft	.125	1.68	.119
Thick Hard	.25	3.75	.044
Thick Soft	.25	1.68	.119

Density = 1050 Kg/M^3

The finish data is based on experimental work varnishes. Fine violin varnishes and floor varnishes were studied and this table represents the extremes of the experimental data.

Vita

Evan Brugh Davis
Birth Date: January 15, 1955

Education
Mountain Lakes High School 1973.
Mountain Lakes, New Jersey.

B.S. Mechanical Engineering 1977.
Rutgers University, New Brunswick, New Jersey.
James J. Slade Scholar,
Topic: The Harmonic Content of an Aging Guitar String.

M.S. Mechanical Engineering 1978.
Oklahoma State University, Stillwater, Oklahoma.
Thesis: Feasibility Study on the Use of a Single Corner Microphone Position in the Determination of Sound Power Levels of Broad-Band Noise Sources in a Large Reverberation Room.

Work Experience
(1972-1976) Lydo Precision Products
Machine operator and mechanical assembly technician assembling biomedical equipment.

(1978-1983) Boeing Commercial Airplanes
Noise Staff: Analysis and prediction of noise in the passenger cabin.

(1983-1985) Honeywell Marine Systems
Transducer Design Group: Design, construction and testing of low-frequency high-power sonar transducers.

(1985-) Boeing Commercial Airplanes
Noise Staff: Transducer design for active noise control systems in the passenger cabin.